DOCTOR OF PHILOSOPHY

Bio-physical interactions over cultured mussel beds : measured and modelled chlorophyll distributions in the Menai Strait

Berx, Barbara E M

Award date:
2008

Awarding institution:
Bangor University

Bio-physical interactions over cultured mussel beds

Measured and modelled Chlorophyll distributions in the Menai Strait

Barbara E.M. Berx

Submitted in accordance with the requirements of Bangor University

for the degree of Doctor of Philosophy

February 2008

In Final Form May 2009

Research supported by Myti Mussels Ltd. and the European Social Fund

Supervisors:

Prof. J.H. Simpson

Mr. K. Mould

Abstract

This study was designed to elucidate the processes controlling the supply of phytoplankton to the commercial mussel beds in the Menai Strait which is a major centre for mussel aquaculture in the UK, accounting for approximately 50 % of the total production of *Mytilus edulis* in 2005. The Menai Strait is a shallow (mean water depth $\sim$10 m), energetic regime dominated by tidal currents of order $\sim$1 m s^{-1}. In consequence the water column remains well mixed and there is a tidally driven net transport through the Strait. Spatial and temporal surveys reveal a pronounced longitudinal gradient in Chlorophyll concentration (Chl) over the mussel beds as well as large semi-diurnal oscillations in Chl which have been shown to result from the advection of the gradient by the residual and tidal currents. In the vertical, the depletion of Chl near the bed is limited by the strong mixing and is observed only to occur around periods of slack water. Downstream (in the residual tidal advection) from the mussel beds, Chl also shows a strong oscillation over the spring-neap cycle due to the change in relative strength of mussel filtration to residual tidal advection. Observations show the range of Chl to be $\sim$ 1.7 $\mu g\, l^{-1}$ over a fortnight. Results on a seasonal time scale show a consistency between different years, and with previous longer term measurements of Chl in the Strait. The PHYBIO model is a simplified 1-D model of the ecosystem which includes tidal advection, diffusion, mussel feeding and phytoplankton production. Simulations with this model reproduce the main qualitative and quantitative features of Chl variations observed in the Strait and validate the hypothesis that these oscillations and gradients are due to the interaction of the hydrodynamics and the mussel feeding. On the longer time scale of the spring-neap cycle, the patterns predicted by the PHYBIO simulation are in good agreement with the observations. The modelling effort has been expanded to a 2-D hydrodynamic model, which uses a passive tracer to simulate the distribution of Chl in the Menai Strait. Using a semi-implicit source/sink term, the local production by phytoplankton and the localised consumption by the commercial mussel lays have been simulated. Results show a promising agreement with the outcomes from observations and the 1-D PHYBIO model. Calculations of Chlorophyll consumption and mussel production are compliant with annual production numbers from the shellfishery.

"I've got science for any occasion

Postulating theorems, formulating equations"

Sounds of Science – Beastie Boys

"Because you can't, you won't and you don't stop"

Sure Shot – Beastie Boys

Contents

List of Figures

List of Tables

List of Symbols and Abbreviations

List of Abbreviations

2-DH	two-dimensional in horizontal
2-DV	two-dimensional in vertical
3-D	three-dimensional
ADCP	Acoustic Doppler Current Profiler
AFDW	Ash-Free Dry Weight
ATP	Adenosine Triphosphate
CBL	Concentration Boundary Layer
Chl	Chlorophyll
Chl-a	Chlorophyll-a
CTD	Conductivity Temperature Depth (Profiles)
DFT	Discrete Fourier Transform
DFW	Dry Flesh Weight
EDS	Extended Deployment System
ELWS	Extreme Low Water Springs
FFT	Fast Fourier Transform
HAMELS	Harmonic Analysis MEthod of Least Squares
HPLC	High Performance Liquid Chromatography
HWS	High Water Springs
LED	Light-Emitting Diode
LISST	Laser In-Situ Scatterometer and Transmissometer
LWS	Low Water Springs

M2	Principal lunar semi-diurnal tide
M4	Lunar quarter-diurnal tide
mab	meter above bed
MNR	Marine Nature Reserve
MSL	Mean Sea Level
NADPH	Nicotinamide Adenine Dinucleotide Phosphate
Phaeo	Phaeopigments
PHYBIO	PHYsical - BIOlogical model of the Menai Strait
PS	Photosystem
QD	Quarter-Diurnal (i.e. 4 cycles per day)
S2	Principal solar semi-diurnal tide
SAC	Special Area of Conservation
SCUFA	Self-Contained Underwater Fluorescence Apparatus
SD	Semi-Diurnal (i.e. 2 cycles per day)
SSSI	Site of Special Scientific Interest
TKE	Turbulent Kinetic Energy
YD	Year Day
YSI	Yellow Springs Instrumentation

List of Symbols

A	amplitude (HAMELS)
A	cross-sectional area (PHYBIO)
α	mussel filtration parameter in PHYBIO model
α_*	mussel filtration parameter in TELEMAC-2D model
AVG	average
b	breadth
b_0	breadth at LWS
c	sound velocity
c	constant of a straight line
D	amplitude (HAMELS)
η	tidal elevation
f	frequency
F_0	reading before acidification on 10-AU
F_a	reading after acidification on 10-AU
F_m	acidification coefficient of 10-AU
γ	net phytoplankton production parameter in PHYBIO model
γ_*	net phytoplankton production parameter in TELEMAC-2D model
H_0	water depth between sea floor and MSL
H_3	water depth between MSL and LWS
K_x	linear calibration factor of 10-AU
m	slope of a straight line
Q_0	residual transport
ϕ	phase (HAMELS)
R	range
SD	Standard Deviation
t	time
U	section-mean velocity
u	horizontal velocity
v	horizontal velocity

Chapter 1

Introduction

In terms of mussel aquaculture, the Menai Strait is one of the most important regions in the British Isles. The broad scope of this research has been to elucidate the processes supplying these sessile benthic filter feeders with the necessary food for survival and growth to a marketable size. By way of introduction, this chapter presents information on the species, and its ecology, as well as the organism's main food source, phytoplankton. Previous research on the biological and physical processes driving food supply to the mussel beds is also reviewed. The aims and objectives of the research presented in this thesis will be covered at the end of Chapter 2, which presents a more detailed introduction to the Menai Strait ecosystem and reviews the relevant previous research.

1.1 The Ecology and Culture of *Mytilus edulis*

Ecology

Mussels (Figure 1.1) are sessile filter feeding bivalve molluscs. They are gregarious organisms which attach themselves to the substrate using their strong byssus threads (Hayward et al., 1996). The animal's diet is largely herbivorous, consisting of phytoplankton, although more recent research has shown they are also able to feed on small zooplankton and organic detritus (Dare, 1980; Zeldis et al., 2004; Lehane and Davenport, 2006). Studies of phytoplankton community structure in the vicinity of mussel beds have suggested *M. edulis* preferentially remove larger phytoplankton cells (Norén et al., 1999).

As can be seen in Figure 1.1, the food particles are drawn into the shell cavity through the inhalant siphon by the gills, which take the suspended particles and oxygen (for respiration) out of the water, and finally the water and waste products are expelled through the exhalant siphon (Dare, 1980). In this way, mussels may pump large volumes of water through their bodies (45-65 litres in 24 hours by a 75 mm adult, according to (Dare, 1980)), and hence, mussel beds may act as large water filters, depleting the water of food sources and other small particles. Kjørboe and Møhlenberg (1981) showed that the animal can implement some selection of its food through the production of pseudofaeces, which are undigested food particles which the organism has coated in mucus and rejected (Kjørboe and Møhlenberg, 1981). The selection process occurs above a threshold concentration (Kjørboe and Møhlenberg, 1981), and particles are rejected either due to food quantity being too high (Jørgensen, 1990), or because the quality of the particles is undesirable (Kjørboe and Møhlenberg, 1981). This selectivity means mussels can maintain a constant absorption efficiency, allowing the organism to sustain its growth at a constant level (Bayne et al., 1989).

Culture

The species *Mytilus edulis* is of commercial importance in many European countries, where mussels are generally cultured using one of four principal culture methods (Figure 1.2): suspended ("raft" and "longline") culture, bottom culture, and pole ("bouchot") culture. The suspended culture of mussels can be subdivided in two categories, that on rafts (Figure 1.2 a) and that on longlines (Figure 1.2 b). The raft culture method is mainly practised in Spain, but also has applications in Scotland, Ireland and some other countries (Spencer, 2002; Smaal, 2004). The mussels are grown on ropes suspended from floating rafts, giving them a refuge from predators (Dare, 1980). The second form of suspended cuture is the deployment of longlines. Similar to raft culture, the mussels are hung vertically on ropes suspended from a long horizontal line suspended between buoys. This culture technique is particularly popular in New Zealand, although it has more recently been introduced to Scotland, and France (Spencer, 2002; Smaal, 2004). The third method of culture is based on seeding mussel spat collected from naturally abundant locations into relatively sheltered culture beds in a reduced density to improve growth (Spencer, 2002). This technique is termed bottom culture (Figure 1.2 d) and is most commonly employed in the Netherlands and Germany, although parts of France and the UK also employ the same technique (Spencer, 2002). Generally, power dredgers are used to collect the spat or small seed mussels. The mussels are then seeded in the inter-tidal to improve shell thickness,

and are subsequently dredged, and re-layed sub-tidally for further fattening, before the final harvest for marketing (Dare, 1980). The final technique, known as pole culture (Figure 1.2 c), uses poles or stakes driven into the sea bed in shallow water regions with access at low tide (Spencer, 2002). This type of culture originated in France, and it is therefore sometimes still known as "bouchot" culture. The poles are placed in rows spaced closely together for spat collection, and further apart for on-growth (Spencer, 2002).

The advantages and disadvantages for each technique need to be compared in terms of the location, considering the species, the environmental conditions and the legislation of the region, before a conclusion can be made on the best method of cultivation. The cultivation cycle in bottom culture and pole culture may take up to 2 years (Spencer, 2002), while figures for raft culture show completion of the cycle after 1 to 1.5 years (Dare, 1980), although this difference may be partly attributed to the different species (*M. galloprovincialis*, which has a higher growth rate than *M. edulis*) and different environmental conditions in the raft culture compared to bottom and bouchot culture. Garen et al. (2004) compared mussel growth for three culture methods (longline, bouchot and bottom) on the French Atlantic coast, and concluded that longline mussels show the highest growth, and bottom culture mussels have the worst growth in this region. The best quality of mussels was obtained using the "bouchot" method, a technique which in the region is recognised under its own quality label (Garen et al., 2004). In the Menai Strait, mussels are cultured using the bottom culture method which is more fully considered in Section 2.4.

1.2 Photosynthesis and Chlorophyll

The most important nutritional food source to the mussel beds is phytoplankton: small, unicellular algae, which rely on passive transport through the water column. These autotrophic organisms use photosynthesis to convert CO_2 into more complex carbohydrate molecules. In this process, photopigments are used to capture the light energy necessary for this conversion. Some of these pigments have fluorescent properties (see Section 3.1.1) which can be brought out by illuminating the phytoplankton cells with light of a particular wave length. Fluorometers (see Section 3.1.1) use this principle, and allow us to estimate the phytoplankton biomass in the water column. Converting this biomass into Carbon fluxes into the mussel beds can then be achieved by the application of a Carbon-to-Chlorophyll ratio. This section gives a brief review of pho-

tosynthesis by phytoplankton and the associated photopigments, using material from "Aquatic Photosynthesis" by Falkowski and Raven (1997), and from articles by Krause and Weis (1991) and Maxwell and Johnson (2000).

Photosynthesis

Photosynthesis may be defined in biology as the conversion of light energy to a chemically bonded energy which is stored in the form of organic Carbon compounds. The chemical reaction for photosynthesis may be written in the form of an oxidation-reduction reaction (Equation 1.1).

$$2H_2O + CO_2 + light \xrightarrow{Pigment} (CH_2O) + H_2O + O_2 \tag{1.1}$$

In phytoplanktonic organisms, this pigment is Chlorophyll-a, which is responsible for catalysing a series of reactions, and in the process captures the light energy necessary to oxidise the water; this part of the photosynthetic process is termed the"light reaction". It describes a partial reaction (Equation 1.2) where electrons are taken from water molecules to form oxygen molecules. The other partial reaction (Equation 1.3) describes the reduction of Carbon, and is not reliant on the presence of light. This reaction is therefore also termed the "dark reaction". The two partial reactions are coupled by the formation of ATP (adenosine triphosphate) and NADPH (nicotinamide adenine dinucleotide phosphate).

$$2H_2O + light \xrightarrow{Chl-a} 4H^+ + 4e^- + O_2 \tag{1.2}$$

$$CO_2 + 4H^+ + 4e^- \longrightarrow CH_2O + H_2O \tag{1.3}$$

In unicellular phytoplankton cells, the photochemical fixing of carbohydrate molecules occurs in the chloroplasts. These are cell organelles which contain the photopigments in their thylakoid membranes. This is also the location where the light and dark reactions occur.

There are two different pathways involved in the photosynthetic mechanism; these are termed Photosystem (PS) I and PS II. These photosystems consist of antennae complexes which, located in the thylakoid membrane, contain the Chlorophyll molecules and other accessory pigments. The Chlorophyll-a molecules of PS I have an absorption peak at 700 nm, while those of PS II have an absorption peak at 680 nm. The antennae complexes absorb light, and transfer the

available energy to a complex of Chlorophyll molecules and proteins, termed the reaction centre.

The evidence for the existence of these two photosystems is termed the Kautsky effect, and consists of noticeable changes in fluorescence with time. The reason behind these time changes is that in PS II, a photon arriving at a closed reaction centre (i.e. one that has already absorbed a photon) cannot be used until it has been passed on to the electron transport chain. When a reaction centre is closed, the incoming photons are most likely to be re-emitted as fluorescence (the other option is a conversion into heat). The observed changes in fluorescence are therefore inversely related to the production of oxygen. In PS I, on the other hand, the oxidation of Chlorophyll-a molecules is not related to changes in the fluorescence.

Finally, the ATP and NADPH formed by the two photosystems during the light reaction are subsequently used in the dark reaction as an energy source for the synthesis of organic Carbon molecules from inorganic Carbon dioxide and water.

Photosynthetic pigments

As illustrated above, photosynthesis requires the light energy being absorbed by pigment molecules in the antennae complexes. Each photopigment has a specific absorption band within the light spectrum where it can absorb photons. Depending on the photosystem and the species, the pigment composition of these complexes may differ. Moreover, depending on this composition, the action spectrum (i.e. the wavelengths at which the organism is capable of harvesting the photoenergy) and the quantum yield (i.e. the ratio of the product formed per unit of absorbed light) of the photochemical reaction will change. Common to both photosystems and all photosynthetic organisms is the presence of the Chlorophyll-a molecule as a key biochemical component in the process. The presence of these pigment molecules allows for the measurement of photosynthetic organisms through the application of fluorescent techniques. The spectrum of fluorescence is different to that of the absorbed light, with the peak of the emission by fluorescence being at a longer wave length than that of the absorbed signal. Therefore, by submitting the cell to light of a fixed wave length, and measuring the re-emitted quantity of light at longer wavelengths, the fluorescence yield can measured (Maxwell and Johnson, 2000).

Carbon-to-Chlorophyll ratios

The ratio of Carbon to Chlorophyll-a in phytoplankton cells is an important factor when attempting to estimate the Carbon flux to the benthos. As explained above, the measurement

of Chlorophyll-a concentrations is relatively straightforward due to the development of fluorometers. To relate this measured Chlorophyll concentration to the Carbon flux to the benthic bivalves, however, a conversion to organic Carbon is necessary. This ratio is not strictly constant and depends on a variety of environmental cues received by the phytoplankton cell, as well as on the species (Geider et al., 1998). The Carbon to Chlorophyll ratio is related to phytoplankton growth, which may be regulated by bottom-up (i.e. the physiology and ecology of the phytoplankton) or top-down (i.e. feeding behaviour and population dynamics of zooplankton and bivalves) control (Geider et al., 1998).

It has been found that the Carbon to Chlorophyll ratio does not, however, vary randomly; rather it is related to nutrient concentrations, temperature and irradiance (Taylor et al., 1997). The ratio varies from about 12 to >200 g C g^{-1} Chl-a, with the highest values observed in nutrient-depleted conditions, with high light incidence and cold temperatures (Geider et al., 1997; Taylor et al., 1997). Various models exist to estimate the Carbon to Chlorophyll ratio, although their application seems to be mainly related to shelf sea and open ocean processes rather than coastal ecosystems (Geider et al., 1997; Taylor et al., 1997; Flynn et al., 2001). Generally, a ratio of 30 is used to convert Chlorophyll measurements over mussel beds to Carbon, which is absorbed by the animals (Grant and Bacher, 1998).

1.3 Food supply to filter feeders

1.3.1 Concentration gradients due to filter feeders

Due to their capacity to filter vast amounts of water within a short period of time, concentration gradients of Chlorophyll may be observed over mussel beds under certain conditions. These phytoplankton gradients may be on a horizontal scale, or in the vertical, when they are generally termed concentration boundary layers. This term reflects the fact that these sharp vertical gradients only occur close to the animals and thus often close to the boundary.

Vertical gradients - Concentration Boundary Layer (CBL)

Vertical concentration gradients of phytoplankton have been observed over a variety of benthic filter feeding species: coral reefs (Yahel et al., 1998), infaunal polychaete worms (Riisgård et al., 1996), and fresh-water (Ackerman et al., 2001) and marine bivalves (Wildish and Kristmanson,

1984; Fréchette and Bourget, 1985; Fréchette et al., 1989; O'Riordan et al., 1993; Butman et al., 1994; Dolmer, 2000a,b). These concentration gradients are caused by the filtration of the benthic bivalves, and although they are not necessarily observed over all mussel beds, a combination of factors is thought to be responsible for their occurrence. The most obvious factor influencing CBLs is the density of the mussel population, which will control the extent of depletion. However, the current speed is also important in the intensity of the near-bed depletion (Fréchette and Bourget, 1985), as low current velocities and their associated low levels of turbulent mixing will limit the vertical turnover of the water column, hence allowing the mussels only to access phytoplankton available in the near-bed layer. Studies by Monismith et al. (1990), O'Riordan et al. (1993) and O'Riordan et al. (1995) showed that the excurrent siphon jets can have a positive effect on supplying the bottom boundary layer with fresh phytoplankton (see Section 1.3.2).

The vertical extent of this depleted layer has been reported to be as thick as ~3 m measured above coral reefs (Ackerman et al., 2001), although over beds of *M. edulis* experiments have shown near-boundary depletion to extend less than a metre above the bottom (Wildish and Kristmanson, 1984; Fréchette and Bourget, 1985; Fréchette et al., 1989). Furthermore, it has been suggested that prolonged depletion may limit the growth rate of the bivalves, a problem particularly important for the commercial exploitation of the mussels (Fréchette and Bourget, 1985). This is particularly important in regions with low levels of turbulent mixing, and large populations of mussels, such as the Limfjorden in Denmark (Wiles et al., 2006).

In the Menai Strait, Tweddle et al. (2005) discuss the occurrence of vertical depletion over the commercial mussel beds. This research concluded that vertical depletion is likely to be very short-lived due to the dynamic regime in the channel; and that if it occurs, it would be a layer close to the mussels (Tweddle et al., 2005). Therefore, in order to observe these occasions in the field, the sampling strategy needs to cover time and spatial scales which would resolve the short time periods and the space near the mussel beds over which these events occur.

Horizontal gradients

Aside from the effects of filter feeding on the vertical water column structure, several investigators have also studied filtration effects in the horizontal plane. Studies have observed significant gradients over coral reefs in the field (Yahel et al., 1998; Fabricius and Dommisse, 2000), freshwater clams (Cohen et al., 1984), *Modiolus modiolus* in the laboratory (Wildish and Kristmanson, 1984), *M. edulis* in the laboratory (Wildish and Kristmanson, 1984) and in the field

(Norén et al., 1999; Karayücel and Karayücel, 2000; Ogilvie et al., 2000; Tweddle et al., 2005). Early observations by Wildish and Kristmanson (1984) showed significant horizontal depletion of ATP-seston (a possible proxy for phytoplankton concentration) over *M. edulis* beds in unidirectional flow in a flume, and the study therefore concluded that mussels at the leading edge of the bed would have a higher growth rate. Observations of horizontal gradients in food concentration have been made both over benthic mussels (see above), as well as within suspended mussel culture farms (Karayücel and Karayücel, 2000; Ogilvie et al., 2000; Waite et al., 2005). Observations of gradients over a large natural population of *M. edulis* in the Öresund Strait (between Malmö and Copenhagen) showed the mussels not only deplete the overall biomass of phytoplankton, they also seem to have an effect on the overall phytoplankton community structure: shifting the distribution towards smaller cells (Norén et al., 1999).

Horizontal gradients will be of particular importance in tidally driven ecosystems, where water depleted on the previous stage of the tide is advected back over the beds on reversal of the tidal currents (Tweddle et al., 2005). Especially in systems with longer residence times, this could be a more significant factor in limiting the food concentration available to the bivalves. In the Menai Strait, the effect of the large number of mussels in the North-Eastern section is noticeable through the strong along-channel gradients in food concentration (Chlorophyll) and the large oscillations which have been observed during time series measurements near the Southern edge of the commercial lays (Tweddle et al., 2005).

1.3.2 Mussels as ecological-engineers

Not only may bivalve filter feeders establish significant gradients in the food source they rely on, it has also been suggested the animals are able to modify their environment to some extent to improve their food supply. This has previously been called "ecological-engineering" (Wiles, 2007). Several mechanisms have been suggested through which the animals can achieve this.

An initial suggestion of ecosystem control by filter-feeding bivalves comes from the work by by Cloern (1982) and Officer et al. (1982) who suggested that, in South San Fransisco Bay, the large populations of mussels and clams could be responsible for limiting the occurrence of excessive phytplankton blooms under the eutrophic conditions experienced in the region.

It has also been proposed that mussels act as roughness elements in the flow, thus increasing turbulence, and therefore enhancing the supply of suspended phytoplankton to the bottom

boundary layer (Fréchette et al., 1989; Widdows et al., 2002). Field observations over beds of *Atrina zelandica* (horse mussels) showed increased drag coefficients (in the order of 0.008 to 0.010) compared to those observed over non-mussel sites (0.0055) and the typical drag coefficient applied to smooth non-cohesive beds (0.0025) (Green et al., 1998). Furthermore, van Duren et al. (2006) observed an increase in turbulent boundary layer thickness over mussel beds in a large flume.

A third mechanism, suggested by Monismith et al. (1990) and further developed by O'Riordan et al. (1993) and O'Riordan et al. (1995), is the interaction of filter feeding currents with the main flow. O'Riordan et al. (1993) studied the effect of bivalve excurrent jets on the benthic boundary layer. It is postulated that by changing the relative position of their siphons or by changing the strength of pumping relative to the flow, the bivalve, *Tapes japonica* can have a positive effect on food supply and improve its access to suspended food particles. Further work by O'Riordan et al. (1995) found that boundary layer shear and multiple jet interactions are the main sources of turbulent mixing. Therefore increasing relative velocity shear or decreasing animal density allows a better food supply to the bivalves. Increasing siphon height or increasing siphonal pumping speed only have minor effects on turbulence: the former enhances mixing, therefore reducing the refiltration of water; while the latter has different effects on turbulent mixing depending on siphon height (O'Riordan et al., 1995). Research over beds of *M. edulis* in a large flume by van Duren et al. (2006) showed that although turbulent mixing was higher due to increased bed roughness (see above), they also found that when the mussels were actively feeding, the siphonal currents enhanced mixing further. Lassen et al. (2006) showed that particularly at low flow velocities this "biomixing" (i.e. exhalent jet induced mixing) is an important source of turbulence and hence re-supplying the bottom boundary layer with food particles.

Finally, early work by Ogilvie et al. (2000) suggested that mussels suspended in longline culture can facilitate phytoplankton production as they are producers of dissolved inorganic nitrogen, a nutrient key to phytoplankton growth. Further research by Ogilvie et al. (2003) showed that enclosures enhanced with nitrogen showed a significant increase in phyoplankton, suggesting the organisms are nutrient-limited in summer. A second enclosure to which mussels had been added also showed an increase in Chlorophyll-a, suggesting the mussels have a positive effect on phytoplankton growth through supplying the nutrient-limited phytoplankton with inorganic nutrients. Thus, by stimulating phytoplankton productivity the mussels are ensuring a steady food supply, which can be seen as a form of ecological-engineering.

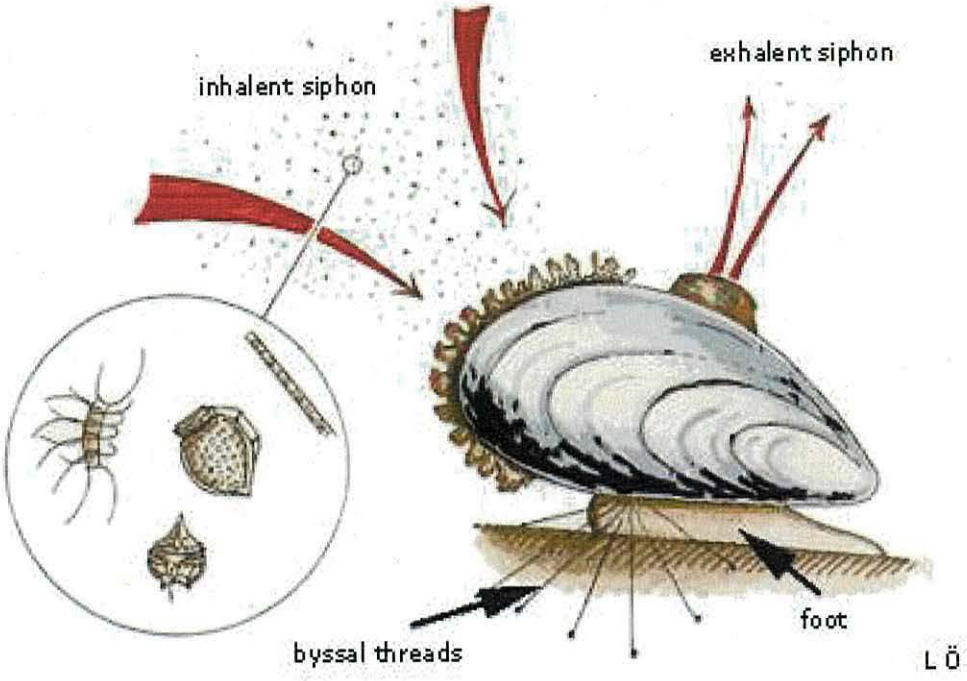

Figure 1.1: The Blue Mussel, *Mytilus edulis*, showing inhalent and exhalent siphons as well as food particles in suspension. From Tjärnö Marine Biological Laboratory.
[Source: http://www.vattenkikaren.gu.se/fakta/arter/mollusca/bivalvia/mytiedul/mytifile.html]

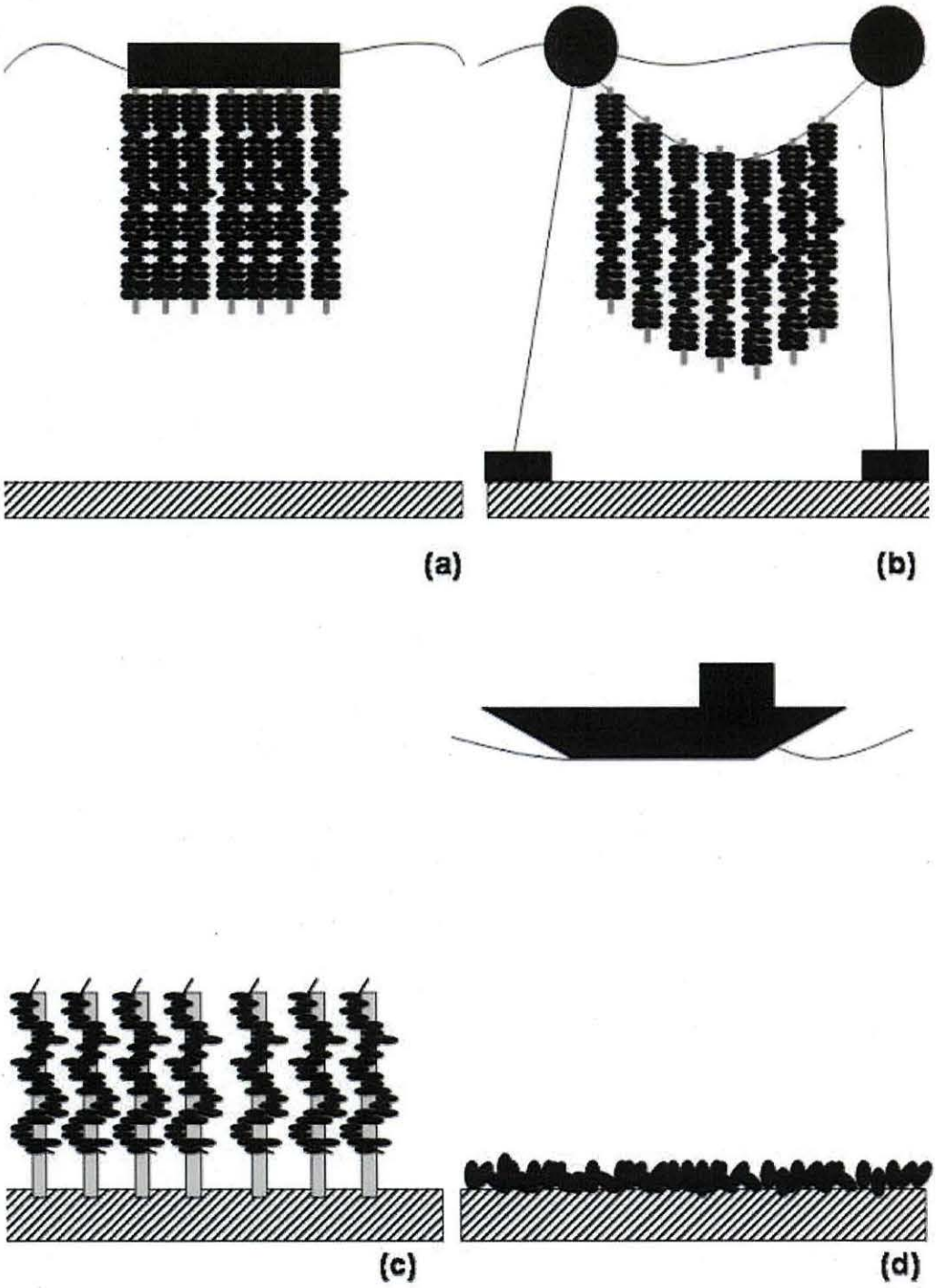

Figure 1.2: Principal culture methods of *M. edulis* (a) raft, (b) longline, (c) bouchot, and (d) bottom culture.

Chapter 2

The Menai Strait

2.1 Location and setting

Located between mainland Britain and the Isle of Anglesey, the Menai Strait (Figure 2.1) connects Liverpool Bay in the North and Caernarfon Bay to the South. The channel is approximately 20 km long, and has an average width of 800 m. In the North, the Strait is dominated by a large intertidal sand flat, called the Lavan Sands; while in the central section, between Menai Bridge and Port Dinorwic, it becomes a narrow (~300 m wide) and shallow (water depth of several metres) constriction, which is termed the "Swellies" and is known for its strong tidal currents. The maximum depth of the Strait is 22 m, while the shallow sections of the channel are just several metres deep at low water on a spring tide. There is little freshwater input into the Strait, so horizontal density gradients are generally weak (Campbell et al., 1998; Rippeth et al., 2002).

Aside from having interesting physical characteristics, the Menai Strait is also of great ecological importance due to its extensive biological assemblages. Moreover, since the mechanisation of the local slate industry, it has also become an important economic resource in a region which often suffers from high unemployment. While the tidal channel is a key factor in the succes of many recreational businesses through the opportunities it provides for diving, sailing and other watersports, the fisheries of the Menai Strait also form a big component of the local economy.

This chapter aims to introduce the physical environment of the Menai Strait, as well as the ecology of the region and the local mussel fishery. Previous research on the Strait, which is

central to our understanding of the ecosystem, will also be discussed.

2.2 Physical Environment

The Menai Strait is a dynamically energetic regime which is dominated by strong tidal currents that reach a maximum velocity of up to 2 m s^{-1} in the Swellies and near Fort Belan (the southwest entrance) (Rippeth et al., 2002). Due to the channel ebbing and flooding from both directions and due to a difference in tidal range between the two ends, the currents and elevation deviate from the simple rule of a standing wave. Because of the surface slope between the ends of the channel, there is a current component which is in phase with the elevation, as well as standing wave components at the opposing ends which are 180°out of phase with each other. These two processes lead to a combined tidal current which changes phase along the channel. As a result, the velocity and elevation do not differ in phase by 90°, as is often the case in coastal waters. Since the channel ebbs and floods at both ends, convention has it that the flood direction (i.e. positive x) is defined as a current towards the northeast, as this is when the sea level is rising for most of the time (Rippeth et al., 2002). Therefore, when the current is towards the southwest, this is termed the ebb (negative).

There is a net transport through the Strait, which has been documented by several researchers (Forbes, 1969; Simpson et al., 1971; Shuttleworth, 1979; Buckley, 2004), although Harvey (1967) was one of the first to measure this residual flow and attribute it to the difference in tidal range at the two open ends of the tidal channel. Simpson et al. (1971) obtained observations of the mean flow across a section of the channel through the measurement of the electro-magnetic field ($\sim \pm 10$ mV). They observed a net transport of $\sim$ -800 m^3 s^{-1} at mean springs, and $\sim$ -300 m^3 s^{-1} at neap tides, directed to the South West. They found this residual transport to vary with the tidal range R according to the regression relation specified in equation 2.1 (Simpson et al., 1971). Observations also showed the residual transport could be reversed during periods of strong South Westerly winds (Simpson et al., 1971).

$$Q_0 = -483.5 - 184.5(R - 3.6) - 46.4(R - 3.6)^2 \tag{2.1}$$

Further research into the dynamical balance of the Menai Strait was conducted by Campbell et al. (1998) who concluded that the surface slope and friction terms dominate the along-channel

momentum balance. Moreover, it was found that the net transport over the tidal cycle is a result of the shallow water effects and the higher frictional control of the bed during periods of low water. This net transport leads to the Menai Strait having a flushing time of 2-3 days (Campbell et al., 1998). The large sand flat of the Lavan Sands is also thought to have an important influence on the local circulation patterns, however, as studied by Buckley (2004), it does not affect the transport balance.

There have also been several measurements of flow and turbulent properties in the Menai Strait. Turbulent Kinetic Energy (TKE) and drag coefficients have been calculated by Williams (2000), Rippeth et al. (2002), Williams and Simpson (2004) and Biggs (2006). With respect to this study, the most significant of these studies was by Biggs (2006) who compared different ADCP data sets and concluded that the large scale bedforms and topography influenced the drag coefficient most significantly, while the flow direction, water depth and presence of mussel beds are of respectively decreasing importance.

The concentrations and fluxes of several water column properties, such as suspended sediment and phytoplankton concentration have also been studied over the past decades in the Menai Strait. An initial investigation of suspended matter in the Menai Strait showed the inorganic (Buchan et al., 1973) and organic (Buchan et al., 1967) suspended sediment concentration varries with tidal range, as well as during the seasons. One of the reasons for this seasonality was suggested to be the influence of the extensive mussel beds present in the Strait (Buchan et al., 1973). Nyandwi (1988) investigated the flow and suspended sediment concentration over a tidal bank in the Southwestern area of the Strait, and concluded that there is substantial sand suspension, particularly during spring tides. In the same area, Jones (1984) studied the movement of megaripples and concluded that their general migration is in a southwesterly direction, apart from during spring tide when there is an apparent reversal. More recently, Donnet (2003) conducted a comparison of optical and acoustical measurement techniques for sediment concentrations, and calculated the sediment transport in the Northeastern region of the Strait to be to the North-East. It was concluded that the large flooding and drying area of the Lavan Sands is an important influence on the sediment transport in the Menai Strait (Donnet, 2003). Further measurements of sediment concentration were obtained by Howlett (2006) who investigated the changes in turbidity over a few months in the vicinity of Menai Bridge and concluded that the signal is mainly semi-diurnal in nature and that tidal advection, rather than resuspension is the driving process. Therefore the turbidity in the Strait is mainly controlled by water velocity and

stage of the tide (Howlett, 2006). On a longer timescale, Birkett and Maggs (2001) analysed turbidity data collected between 1961 and 1999, and concluded there is a seasonal pattern in the annual cycle of turbidity. During spring and summer months (April to October) the water becomes progressively clearer, while in winter months (November to March), there is a significant increase in the turbidity (Birkett and Maggs, 2001).

There have also been several investigations into numerically modelling the flow in the Menai Strait. Early simulations by Rymell (1995) obtained good agreement with measured current velocities and elevations at high water, but less so at periods of low water, when velocities were underestimated. Moreover, the particle dispersion model was inadequately tested due to a lack of experimental data (Rymell, 1995). Bryans (2003) presented a finite difference solution of the equations of motion, which also included routines for drying banks and particle tracking. From this study it was concluded that the model formed a good representation of tidal elevation and phase in the Menai Strait, and that the inclusion of a drying bank routine only formed a minor improvement in general, although it was felt necessary in locations where the tidal flats form a large part of the channel, such as near Beaumaris (Bryans, 2003). The 2-DH numerical simulations of Marten (2006) using the Telemac model yielded promising results for the flow in the Menai Strait, with good agreement with field measurements of tidal elevation and currents. Chapter 9 further extends the hydrodynamical modelling previously done by Marten (2006) in order to simulate the distribution of Chlorophyll in the Menai Strait.

2.3 Ecological Importance

While parts of the Strait's coastline have been designated as Sites of Special Scientific Interest (SSSI) (Countryside Council for Wales, 1992), the whole area extending from the southwestern entrance to the Menai Strait to the Little Orme at Llandudno was in 1992 declared a Special Area of Conservation under the European Community Habitats Directive (92/43/EEC) (Russell, 2005). The above-mentioned SSSI's include the Lavan Sands for its waterfowl and wading birds; Dinas Dinlle for its glacial deposits; Newborough Warren for its bird community as well as geology; Foryd Bay for its sand flat organisms, overwintering waterfowl and presence of dwarf eelgrass; and the coastline stretching approximately from Trecastell Point to Llandonna and including Puffin Island for its geology, bird populations and botanical species (Countryside Council for Wales, 1992). Not only is the Menai Strait coastline of ecological importance, the

subtidal also plays host to a variety of species. Even though these species are not exclusive to the area, the extent and species diversity of the Swellies make it a unique example of bedrock communities in the UK. Moreover, there is a large sponge colony with its associated community located in the Swellies (Countryside Council for Wales, 1992). Although there have been proposals to make the Strait a Marine Nature Reserve (MNR) (Countryside Council for Wales, 1992), this has not yet materialised.

Research on the organisms living in the Menai Strait has included studies on the phytoplankton communities and the succession of species through the seasons (Jones, 1968; Strange, 1970; Al-Hasan, 1976; Blight et al., 1995), as well as studies of zooplankton populations (Castellani, 2001), sea slugs (Robinson, 1981), oysters (Frost, 1997), macro-algae and their associated communities (Musyoki, 1987), the local sponge communities (Cooper, 1976), and bird populations (Hussell, 1993; Caldow et al., 2003). In view of the importance of the Menai Strait as an SAC, Russell (2005) revisited some transects first surveyed in 1992 as part of a preliminary study for a more permanent monitoring program. Because of its status as an SAC, monitoring of the ecological diversity in the region of the Menai Strait and Conway Bay is now an obligation under European law. Russell (2005) concluded that species diversity has changed on all transects, which is thought to be related either to the changes in management of the ecosystem, or to natural variation.

The Chlorophyll concentration and distribution has also been studied by many investigators. Troëng (1994) carried out a spatial and temporal survey in the Strait of various properties including temperature, salinity and Chlorophyll-a concentration in the Menai Strait and concluded that because of the large spatial and temporal variability of these parameters in the Menai Strait, an environmental monitoring station would not necessarily be representative of the whole ecosystem. Nevertheless, in various years, several researchers have continued to monitor Chlorophyll-a concentrations using different techniques (Jones, 1968; Strange, 1970; Al-Hasan, 1976; Harker, 1997; Beadman, 2003). As part of this project, measurements of Chlorophyll have also been made and these will be compared with the above mentioned past research in Chapter 6.

The Menai Strait is not only an important environment to house all these organisms, the fact that it has these varied ecological assemblages of plants and animals, also underpins many of the recreational activities in the region. Divers particularly visiting the region are often interested in seeing these diverse subtidal communities.

2.4 The Menai Strait Mussel Fishery

Apart from the Menai Strait being an important site for ecological purposes, its large commercial mussel fishery also means it is of great economic value to the North Wales region. Although mussel cultivation has been practised in the Menai Strait since the late 1950's, there had been a strong decline by the 1980's. Since then, investment in new vessels and the adoptation of new techniques, has meant the culture of mussels has been on the rise. Now, the Menai Strait is a leading production area for the species in the entire U.K. Even though historically it has accounted for up to ~70% of the country's landings for *M. edulis*, the increase of production in other regions of the U.K. has meant its relative involvement is now smaller, contributing ~50% in 2005 (CEFAS, 2006). The industry is worth between £4 and £6 million, depending on the production and mussel price, and employs 25 people in the Bangor sector (Kim Mould, pers. comm.).

Operating out of Port Penrhyn (Bangor) since 1982, Myti Mussels Ltd. is one of the largest mussel fishing companies working within the region. They operate two vessels and farm approximately 120 Ha in the Menai Strait, in both the intertidal (Figure 2.2) and subtidal regions of the channel. The annual production levels of the fishery range from 2400 to 8000 tonnes. The company exports all its production to continental Europe, where it is further processed and sold. Between October 2004 and September 2007, the company has provided support for the research presented here through a financial contribution, as well as via hands-on involvement in the field work. Their help and support has proven invaluable in the data collection and has been key to the success of the project.

In the past, there have been several studies of the Menai Strait mussel fishery and its management. Beadman (2003) studied the effects of mussel cultivation on community structure, and concluded that the presence of cultured mussel beds reduced the community abundance and number of species present. Moreover, through the collaboration with the local fishery, this study also developed a management plan for the Menai Strait with guidelines on optimal seeding densities (Beadman, 2003). Also relevant to the mussel aquaculture in the region, Ratcliff (2001) studied the ecology of the pea crab, as well as how *M. edulis* responds to its infestation. Studies of the occurrence of the pea crab concluded that although it has detrimental effects on the condition of the mussels, the cultivated mussels have a negligible infestation rate which may be in part attributed to the cultivation technique and to the duration of the process.

Moreover, due to the Menai Strait being an area of ecological importance, the influence of the mussel fishery on other species in the region has also been extensively researched. Caldow et al. (2003) studied the effects of mussel lays on the bird population of the region and concluded that the presence of mussel cultivation was likely to be beneficial for inter-tidal feeding bird species such as the curlew, the redshank and the oystercatcher.

In more recent years, a more multi-disciplinary approach to researching mussel cultivation in the Menai Strait has been taken. In parallel with this project, biologists, physists and sedimentologists have been cooperating in a BBSRC-funded project (Grant No. D18866) which has been studying the carrying capacity of the cultured mussel beds in the Menai Strait. This multi-disciplinary approach was started by Tweddle (Tweddle, 2002; Tweddle et al., 2005) who studied the interaction of biology and physics in the Menai Strait in relation to the mussel aquaculture. Tweddle (2002) concluded that the horizontal, temporal and vertical gradients in Chlorophyll concentration in the Menai Strait are the result of the interaction of tidal advection of phytoplankton, vertical mixing and constant mussel filtration. This project aims to further develop our current understanding of the interaction of these processes.

2.5 Aims and Objectives

The main research aims of this thesis are outlined below:

- Investigate the interaction of mussel filtration and tidal advection through the collection of time series measurements of Chlorophyll concentration in the Menai Strait. Ensuring suitable spatial and time scales for the measurements, analysis of the results will allow clarification of the effect the large mussel population on the distribution of Chlorophyll, and the importance of tidal advection in the region.

- Collect along-channel measurements of Chlorophyll in the Menai Strait. Similar to the first aim, results will give further evidence as to the effect the possible interaction of physical and biological processes has on the Chlorophyll distribution in the Menai Strait.

- Develop a numerical simulation which includes all basic processes responsible for modifying the Chlorophyll distribution in the Menai Strait. Comparison with field results will show whether it is a valid hypothesis to state that the interaction of mussel filtration

and tidal advection are the main drivers in determining the Chlorophyll distribution in the Menai Strait, which have been observed in the short-term, the spatial scale and the spring-neap tidal cycle.

2.6 Sampling Strategy

In order to meet the aims outlined in section 2.5, an adequate coverage of the Chlorophyll distribution in time and space is necessary. Therefore, the sampling sites within the Menai Strait were chosen such that throughout this project, there was a good spatial coverage of the region where the commercial mussel beds are located. The sampling sites can be divided into three categories depending on their purpose: long-term monitoring sites, short-term time series and spatial surveys. The four long-term monitoring sites were located at Penmon Bay, Penmaen Swatch, Ynys Faelog and Conway Centre Dock (Figure 2.3). The time series measurements of Chlorophyll were all obtained during research cruises in the region around Bangor Pier (Figure 2.3), which is towards the Southern edge of the commercial mussel beds; and finally, the spatial surveys stretched from Puffin Island to Menai Bridge or to Fort Belan (depending on the vessel used).

Table 2.1 gives an overview of the parameters measured at these different monitoring sites for the three different strategies. The aim of all these deployments was to sample the distribution of Chlorophyll over a wide range of temporal and spatial scales, allowing conclusions to be made on the expected patterns of Chlorophyll in the Menai Strait. At all long-term monitoring stations, fluorescence and turbidity were logged, while temperature, salinity and water depth were also measured at the Conway Centre Dock and Ynys Faelog. During the time series measurements and spatial surveys, vertical profiles of fluorescence, temperature, salinity and turbidity were obtained. During the research cruises aboard the R.V. Prince Madog, Acoustic Doppler Current Profilers (ADCP) were also deployed for measurements of water velocity and elevation.

		Du	S	T	D	F	Tu	V
Long-term Monitoring	Penmon Bay	14	-	-	-	+	+	-
	Penmaen Swatch	14	-	-	-	+	+	-
	Conway Centre Dock	P	+	+	+	+	+	-
	Ynys Faelog	P	+	+	+	+	+	-
Time Series Measurements	23-25 April 2005	~4	+	+	+	+	+	+
	11-15 August 2005	~2	+	+	+	+	+	+
	3-5 May 2006	2 ×~1	+	+	+	+	+	+
Spatial Surveys	R.V. Prince Madog	<1	+	+	+	+	+	-
	Mya	<1	+	+	+	+	+	-

Table 2.1: Overview of sampling sites and instrument deployments for the three sampling strategies. Du=duration (in days, P=permanent), S=salinity, T=temperature, D= water depth, F=fluorescence, Tu=Turbidity, V=velocity.

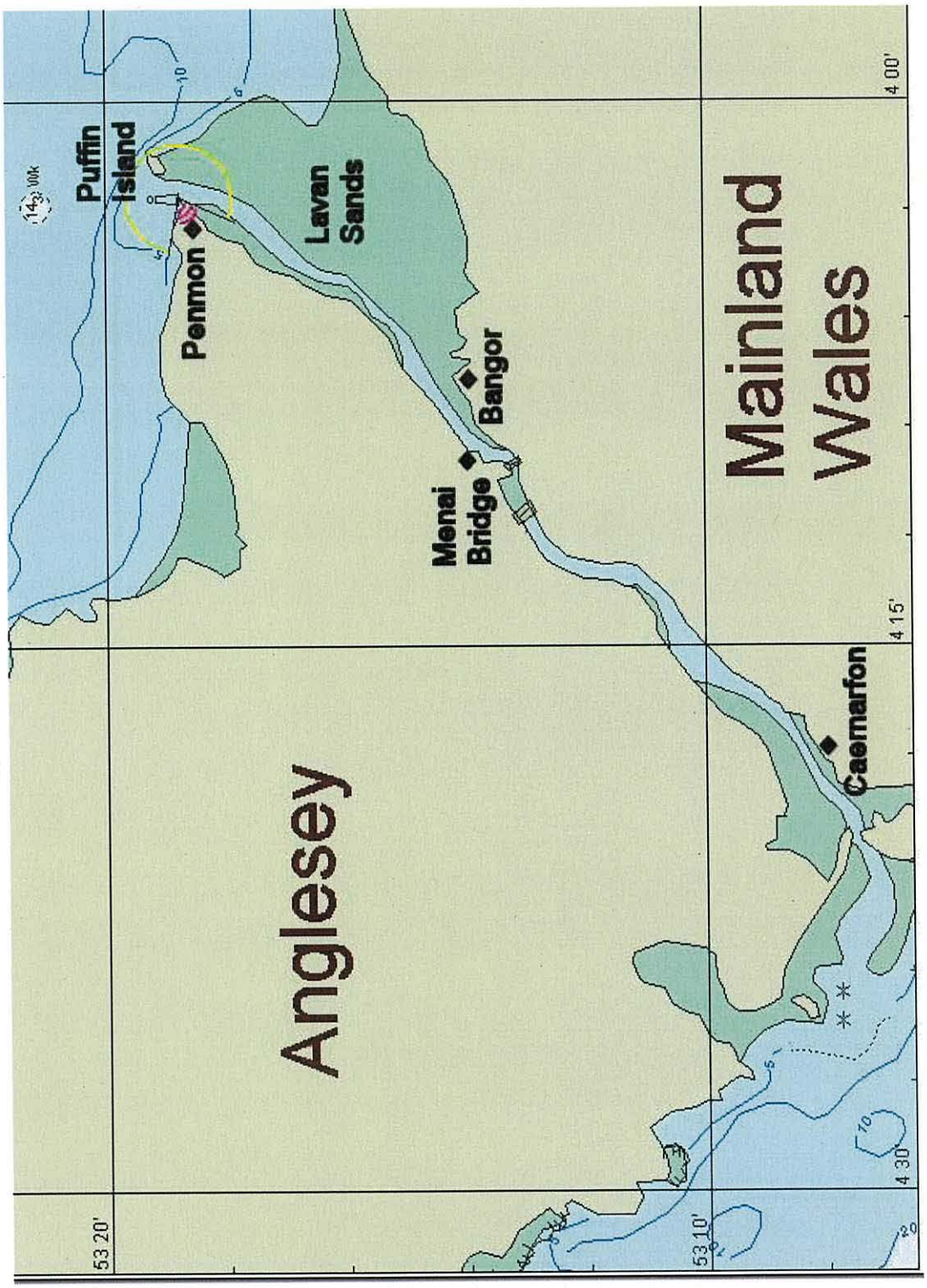

Figure 2.1: Location and setting of the Menai Strait.

Figure 2.2: Intertidal mussel beds from Bangor Pier, exposed at low water.

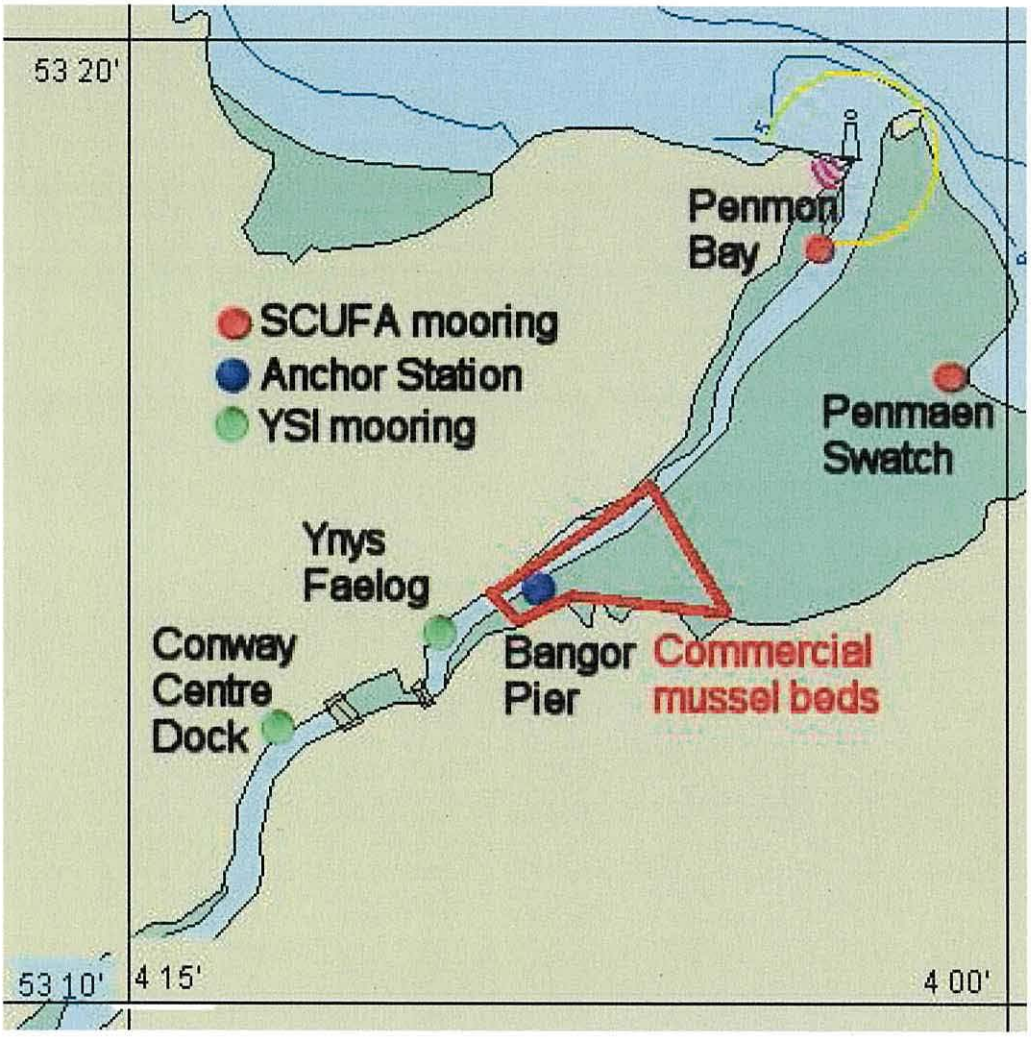

Figure 2.3: Chart of the Menai Strait, showing the locations of the various sampling sites as well as the commercial mussel beds.

Chapter 3

Instrumentation and Methodology

This chapter gives a broad overview of the various instruments deployed and the sampling sites used. As the most critical results are from Chlorophyll measurements, a more in depth discussion of fluorometers and their application will be presented. This chapter will also show how data was processed and water samples were analysed in the laboratory.

3.1 Instrumentation

3.1.1 Fluorometers

Principles of operation and instruments

Because of its fluorescent properties, Chlorophyll, one of the main photosynthetic pigments, can readily be used as an indirect measure of the phytoplankton concentration. When excited with light at a wave length in the blue region of the spectrum, Chlorophyll will fluoresce at a higher wavelength in the red region of the spectrum. Within a specific volume of water, the strength of this emitted signal is directly proportional to the concentration of Chlorophyll in the sample, and can therefore be taken as an indirect measurement of the concentration of phytoplankton. Since the 1970's, field fluorometers have been developed to use this principle to measure concentrations in the field more easily.

Despite their varying designs, all these instruments operate on the same principles and are available in submersible versions with an internal logging system and battery supply. The instrument

consists of a light source, generally a Light Emitting Diode (LED) source, which irradiates a small sample of water at a peak wavelength determined by the optical set-up of the instrument. A photodiode detector then measures the emitted fluorescent signal from the phytoplankton cells within a certain optical bandwidth, set by an interference filter. Figure 3.1 shows how this process works in general. The fluoresced light is passed through a filter to minimize the effects of scattering of light by other particles in the water column (YSI, 2006; Turner Designs, 2004).

During the field measurements presented here, two main makes of fluorometer were used: the Turner Designs Self-Contained Underwater Fluorescence Apparatus (SCUFA) and the Yellow Springs Instruments YSI-6025 fluorometer. The optical set-up of both these instruments has been outlined for comparison in Table 3.1. The SCUFA (Figure 3.2) is a fluorometer which has a 90° measurement angle between the emitted blue light (460 nm) and the measured red light (685 nm). Moreover, the instrument has internal data storage and an external power supply. In contrast, the YSI-6025 is a compact-sized fluorometer which is easily attached to a larger multi-parameter system such as the YSI6600-EDS (see below), which transmits the data via cable to a shore-based logging unit. Further setting it apart from the SCUFA, the measuring angle on the YSI-6025 is at 360°, thus the direction of the emitted and measured light are the same (Figure 3.3). This increases the possible effects of backscatter on the fluorescence readings. A further advantage of the YSI-6025 and YSI-6600 EDS is that they have a wiper system to counteract fouling. The two main advantages of the SCUFA are its ability to log turbidity simultaneous with the Chlorophyll concentration, and to correct the Chlorophyll measurement for temperature effects before storing the data. The SCUFA's main disadvantage is the instruments inability to store large quantities of data in the internal memory, which cannot yet be extended by the manufacturer. Finally, during the deployment of the SCUFA with the anti-fouling plates, minor problems were also encountered due to sediment becoming trapped in the mesh and in front of the lenses. Nevertheless, both the YSI-6025 and SCUFA proved invaluable to the collection of data from long-term monitoring sites.

Instrument Make & Model	Light Source & Wavelength	Detector & Wavelength
Turner Designs SCUFA	2 LED @ 460 nm	Photodiode @ 685 nm
YSI 6025	1 LED @ 470 nm	Photodiode @ 650-700 nm

Table 3.1: Overview of Optical Set-up of Field Fluorometers.

From the above outline of the minor differences in optical properties of each of these instruments, it can be expected that all will measure Chlorophyll concentrations slightly differently. Therefore, it is key that all instruments are calibrated against field samples, preferably measured on the same instrument, allowing for easy comparison. This has been done using the Turner Designs 10-AU fluorometer as a benchmark instrument, which has been calibrated for *in vitro* fluorescence analysis through the extraction of Chlorophyll in acetone. There are, however, additional issues with the calibration of these fluorometers which will be discussed further in the laboratory techniques and calibration sections.

Factors affecting fluorescence

The fluorescence of a water sample can be affected by a variety of different factors, and although every effort has been made to avoid interference by these factors, it becomes increasingly important to be aware of these effects and how they may alter measured Chlorophyll concentrations when comparing across longer time or length scales. There are two main types of effects on fluorescence: firstly there are the environmental effects on the phytoplankton affecting the fluorescence of Chlorophyll (sample fluorescence) and secondly, there are the environmental parameters affecting the fluorescence measured by the instrument (instrument fluorescence). Some properties have an effect on both these quantities, others only on one of them.

Sample fluorescence

The main factors affecting the fluorescence of phytoplankton cells are: the presence of other fluorescent species, the properties of the phytoplankton cells present, and the ambient temperature

and light. In contrast to the analytical techniques used in a laboratory to determine Chlorophyll concentration, *in vivo* fluorometers will measure all fluorescence within a specified bandwidth, which means there is less differentiation between the various, closely related pigments and their contribution to the fluorescent signal. This effect is only minor, and although it introduces some level of error to the measurement, it is reasonable to assume that the majority of the fluorescent signal is due to phytoplankton. A further complicating factor affecting sample fluorescence is the species composition and the properties of the cells in suspension. It has been shown that not only different species exhibit different fluorescence, differences may be detected within the same species due to cell health, cell shape, or cell size (YSI, 2006). These properties are significantly more difficult to take account of and would require the time-consuming process of visual analysis of water samples under the microscope. Finally, the fluorescence of phytoplankton cells is also affected by ambient temperature and light conditions. Experiments have shown that the fluorescence of a water sample is inversely related to the ambient temperature. It has been found that a correction of 1 to 2 % per degree Celsius is appropriate, although this response is species dependent and therefore, applying a general correction may not yield accurate field readings (Turner Designs, 2004; YSI, 2006). While the effect of temperature may be compensated for in post-processing through the application of a temperature correction, taking into account the ambient light regime is slightly more complicated and difficult to account for without additional measurements of the light field.

Instrument fluorescence

These factors include the water turbidity, the sensor fouling and the light environment. The fluorescence reading may be increased through backscatter of the light source by non-fluorescent particles, or they may be decreased due to absorption of the illuminating light. The former is possible due to imperfections of the filters which are meant to minimize illuminating light reaching the photodiode, while the latter interferes with the amount of the light source actually reaching the photosynthetic pigments. These effects of the turbidity are related to both the quantity and the composition of solids in the water sample, and will be most important in regions with high and variable turbidity readings. They can possibly be detected by the comparison of *in vivo* chlorophyll levels, turbidity measurements and extracted chlorophyll concentrations, although a compensation algorithm may be illusive. Secondly, fouling of the optical windows also affects fluorometer readings. This includes fouling by biological sources (phytoplankton, bacterial films, small animals, etc.), chemical fouling and fouling by bubbles. The latter may be

introduced during deployment or be formed by outgassing of the water column. The effects of biological fouling can be minimized through the use of anti-fouling strategies such as a wiper-system or the application of special chemicals. A relatively eco-friendly method to reduce fouling is the use of copper meshing or plating. Finally, the light environment may also affect the fluorometer measurement due to the fact that ambient light contains all wavelengths of light in the range between the ultra-violet and the infra-red bands. This means it also contains energy in the bandwidth corresponding to Chlorophyll fluorescence. Therefore, the illumination by direct sunlight may increase the measured signal by adding to the fluorescence.

3.1.2 Conductivity-Temperature-Depth (CTD) Measurements

Now common oceanographic properties to measure, conductivity, temperature and depth measurements have been obtained at each opportunity in the Menai Strait. Both during long-term time series collection as during the time series measurements aboard the research vessels, these properties have been measured, and using the UNESCO routines (UNESCO, 1981b,a, 1983) densities have been calculated. Current observation systems also allow for additional sensors to be mounted and other properties to be measured. The profiling equipment deployed from the R.V. Prince Madog, uses a Seabird 911 Plus CTD system which is complemented with a transmissometer for the measurement of suspended particulate matter, LISSTs (Laser In-Situ Scatterometer and Transmissometer) to determine particle size and distribution, and a SCUFA fluorometer (see above) for observations of Chlorophyll concentration. The whole system has been mounted on a frame containing several water bottles which can be triggered to obtain water samples at depth for the calibration of the various optical sensors. Aboard the smaller research vessel Mya, water column profiles of temperature, salinity, density, turbidity and fluorescence have been collected by hand-profiling with a Seabird SBE-19 with an additional transmissometer and seperately attached SCUFA fluorometer. During field work aboard the Mya, surface water samples have been collected using a bucket.

The measurement of these water properties at the long-term monitoring sites has been achieved through the deployment of a YSI-6600 Extended Deployment System (EDS). This advanced multi-parameter system allows for long-term monitoring of temperature, salinity and water depth, and through the addition of additional probes is capable of measuring other water properties such as pH, Chloride, dissolved Oxygen, Ammonium, Nitrate, Turbidity, Chlorophyll, and Rhodamine (YSI, 2006). The Extended Deployment System also includes a wiper sys-

tem which helps keep fouling of the instrumentation to a minimum and therefore, in theory allows for longer deployment durations without loss of data quality. The probes deployed at Ynys Faelog and the Conway Centre Dock both have the same set-up and sensors, allowing in this case specifically for the measurement of temperature, salinity, depth, turbidity and fluorescence. The instrumentation at both sites has been connected to a mains power supply and an onshore logging system to acquire and store real-time data, which is also published online at (http://straits.bangor.ac.uk). The wiper system proved useful at keeping fowling of optical surfaces to a minimum, however, measurements still proved eratic due to the effect of fouling on the protective guard mounted over the sensors, as well as due to small organisms growing in the conductivity sensor, which is not cleaned by the wiper system.

3.1.3 Acoustic Current Doppler Profilers

Within the scope of this project, Acoustic Current Doppler Profilers (ADCPs) have been used for the measurement of water column profiles of current velocity and direction, in addition to water depth. The ADCP uses the Doppler principle to determine the water velocity from particles suspended in the water column. It sends out an acoustical "ping" from 4 transducers which are orientated at an angle of 20° to the vertical. The velocities are measured at different depths by dividing the signal into discrete time steps. This method assumes these particles to passively float with the current. The particles reflect the acoustic signal and, if they are in motion, shift the frequency of the return pulse according to Doppler theory. From the return pulse received by the instrument, the along-beam velocities in each of the 4 acoustical beams can be calculated using the frequency shift (Equation 3.1).

$$\Delta u_i = \frac{\Delta f_i}{2 f_0} c \tag{3.1}$$

where u_i is the velocity along beam i, Δf_i is the frequency shift due to the Doppler effect, f_0 is the frequency emitted, and c is the sound velocity.

Using Equation 3.2 and 3.3, these can then be resolved to the horizontal velocities (Stacey et al., 1999). Using the ADCP's internal compass, these horizontal velocities can then be rotated into either North and East velocities, or more appropriate to the Menai Strait, into along-channel and across-channel flow. In addition to measuring flow velocities, the ADCP is also equipped with a pressure sensor which can be used to record the depth of the water column above the ADCP.

$$u = \frac{u_3 - u_4}{2\sin\theta} \tag{3.2}$$

$$v = \frac{u_1 - u_2}{2\sin\theta} \tag{3.3}$$

where θ is the angle of the transducer with respect to the vertical (20 °).

3.2 Overview of sampling sites

3.2.1 Long-term Monitoring

Penmon Bay

Located along the main channel, near the northern entrance to the Menai Strait, Penmon Bay (Figure 2.3) is the small embayment located near Penmon Priory on Anglesey. This measurement site is located approximately 600 metres from the Anglesey coast and is reasonably sheltered. The minimum water depth is 2 m below Chart Datum, and the maximum water depth at Spring tide is approximately 10 m. Although initially it was aimed to record Chlorophyll concentrations throughout the year at this site, this proved more difficult in practice. Figure 3.4 shows the data coverage during 2005 and 2006 at the site.

The main considerations for the mooring design at this site, as well as at the Penmaen Swatch site (see below), were that they had to be easily recovered from a small vessel and that the mooring hardware could possibly be left in place while the instrumentation was given a service. To this purpose, the moorings were a simple L-shape mooring with an anchor, weight, subsurface buoy and surface marker (Figure 3.5). A SCUFA fluorometer was mounted on a bracket which could be easily slotted into place with shackles between the bottom weight and subsurface buoy.

Due to restrictions of data logging capacity, the deployments lasted for 2-3 weeks only. After this period, the fluorometer was brought in for cleaning, downloading, and servicing before being set-up for a new deployment. Retrieval and deployment of the instrumentation was taken care of by Myti Mussels Ltd. Deployments were carried out intermittently between May 2005 and November 2006. From figure 3.4 it can be seen that winter deployments were scarce, though temporal coverage over spring and summer of 2006 was adequate.

Penmaen Swatch

Located between Port Penrhyn and Conway, the Penmaen Swatch is a slightly deeper section in the Lavan Sands, the large intertidal sand flat in the North-eastern section of the Strait. This location was chosen in order to see whether Chlorophyll patterns differed between the deep main channel section and the shallower sand flat section of the Menai Strait. Ranging between 2 and 11 m deep, the local water depth is similar to that of the mooring at Penmon Bay, although it is located slightly further from the shore ($\sim$ 3.5 km).

Mooring and instrumentation set-up at the Penmaen Swatch measurement site were the same to those at Penmon Bay (see above) and deployments and retrieval at this site were generally carried out simultaneous to those at Penmon Bay. Data cover throughout 2005 and 2006 can be seen in Figure 3.4.

Ynys Faelog

Located in the proximity of the School of Ocean Sciences in Menai Bridge (Anglesey), Ynys Faelog has proven an invaluable sampling site for much of the fieldwork conducted by the institute. It is therefore not surprising that there is a long standing record of salinity and temperature from CTD monitoring equipment located on the Extreme Low Water Spring (ELWS) tide level. In 2005, it was thought advantageous to expand the monitoring station to measure a wider variety of parameters. Due to the ease at which additional probes can be added at a later stage if necessary or when funding becomes available, a YSI-6600 EDS system was acquired for the site. In addition to salinity, temperature and depth sensors, the system was also fitted with optical sensors for turbidity (YSI-6136) and fluorescence (YSI-6025). Figure 3.6 shows a schematic diagram of the mooring set-up and location at Ynys Faelog.

This monitoring station is being maintained in cooperation with the Countryside Council for Wales, and the data is made available through a website (http://straits.bangor.ac.uk). This website also presents real-time data from two local weather stations, located at Caernarfon Airport and on the top of the Westbury Mount building in Menai Bridge. This allows local residents to check weather and sea conditions within the Strait for recreational purposes, as well as gives them an idea of the type of research the School of Ocean Sciences does. Data coverage is near-continuous, and has been shown in Figure 3.4.

Conway Centre Dock

At the start of 2006, a second YSI-6600-EDS unit was purchased with the help of the Countryside Council of Wales in order to expand the spatial coverage of the observations in the Strait. Locating the mooring near ELWS at the Conway Centre Dock was thought to be an ideal position due to the convenience of shore power and a safe, dry location for the logging equipment (hence bearing much similarity to the set-up at Ynys Faelog). The mooring location relative to the shore and the slightly different mooring design for the Conway Centre Dock can be seen in Figure 3.7.

Due to the inability to network the logging system to the University of Wales, Bangor computing network, Mr. G. Worley developed a logging box which could phone in its data through a mobile telephone network. Similar to the system at Ynys Faelog, this data was also displayed in real-time online on the above mentioned website. The data coverage for 2006 for this site can also been seen in Figure 3.4. Due to problems with getting this set-up to work, and the intermittancy of the telephone link, the data for this station is sparser.

3.2.2 Time Series Measurements

Time series measurements of the Chlorophyll distribution in the Menai Strait were obtained during 3 research cruises aboard the R.V. Prince Madog. Two cruises (April 2005 and May 2006) were carried out as part of the School of Ocean Sciences postgraduate teaching curriculum, which meant Masters-students were brought on and taken off over the course of the cruise and given a chance to gain some sea-going experience. The third cruise (August 2005) was part of the BBSRC-funded project (Grant No. D18866) which also studied the commercial mussel beds. During these anchor stations, the R.V. Prince Madog was anchored for and aft in the vicinity of Bangor Pier, close to Southern edge of the commercial mussel beds for the duration of the time series measurements.

Every 30 minutes, water column profiles using the ship's profiling equipment were made and water samples of surface and bottom water obtained. These samples were filtered for Suspended Particulate Matter and Chlorophyll analysis for calibration of the optical sensors. Further to profiles of water column properties, permanently submerged instrumentation was also deployed close to the anchor location to collect continuous measurements of the velocity profile & water

elevation (1.2 MHz ADCP), Chlorophyll concentration (SCUFA), and particle size distribution & suspended matter concentration (LISST, only August 2005 and May 2006). During the field measurements obtained in August 2005 and May 2006, vertical structure of Chlorophyll concentration was also measured through the deployment of two fluorometers: one close to the bed, the other nearer the surface. Appendix A gives further information for each of these cruises on the sampling strategy, the instrumentation deployed, and their locations. Figure A.3 shows the mooring design in August 2005, while Figure A.5 shows that of May 2006. The near-surface SCUFA fluorometer was defective during the latter cruise, and therefore no continuous measurements of the vertical structure of Chlorophyll have been made.

3.2.3 Spatial Surveys

In order to establish the spatial distribution of Chlorophyll in the Menai Strait, several along-channel surveys were conducted over the course of this project. The main limitation to these surveys has been the channel's constriction between the Menai Suspension and Brittania bridges, the Swellies. In order for the R.V. Prince Madog to safely sail South through this section of the Strait, spring tides at Liverpool need to be higher than 9 m, an occasion which rarely coincides with a free time slot in the ship's schedule. However, during the research cruises of August 2005 and May 2006 (data not presented), longitudinal sections in the Northern part of the Strait were also collected. During these sections, data was collected continuously through the ship's flow-through system, while in 2005 on the steam from Puffin to Menai Bridge, vertical profiles were made using the profiling instrumentation. Water samples from both vertical water sampling and the flow-through system were taken for calibration of the optical sensors.

The only complete transect of the Strait was conducted with the help of Mr. Gwynne Parry-Jones aboard the smaller surveying vessel, Mya, in August 2006. During this fieldwork, regular CTD profiles were made to estimate salinity, temperature and turbidity, while an attached SCUFA fluorometer allowed for fluorescence measurements. Water samples were collected for calibration of the optical equipment.

Further information on spatial survey locations and instrumentation deployed may be found in Appendix B.

3.3 Laboratory sample analysis

Even though the use of instrumentation allows for the easy acquisition of high-resolution data, it does pose problems of calibration and verification of the measured properties against actual values. After the initial calibration of the sensors, temperature and salinity measurements are sufficiently stable, and require little to no verification or further calibration. However, as optical sensors have more variables which can affect the measured concentrations, calibration against *in situ* samples is key. The following section aims to deal with the calibration of fluorometers, as these are the main optical sensors used in the field work, and therefore the laboratory analysis of Chlorophyll samples. The complications arising from the calibration and cross-comparison of the different manufacturers will also be discussed.

Sampling and filtering of sea water samples

During field work, the sea water samples have generally been taken using a bucket (collecting surface water) or using the water bottles mounted on the rosette sampler aboard the R.V. Prince Madog. Samples are then filtered immediately or temporarily stored in translucent plastic bottles before filtration.

The filter (Whatman ® 47 mm diameter glass microfibre filter, pore size F 0.7μm) is placed onto the manifold, a measured quantity (minimum 500 ml) of water is then poured onto it, and a vacuum pump is used to suck the water through the filter, leaving the suspended matter too large for the pore size behind on the filter. The holders are rinsed with some distilled water to make sure no particles stick to its side and no salts are left on the filter (although this is only of minor importance for Chlorophyll analysis). While working with filters, contact with the skin and other surfaces must be avoided at all cost.

The filter is then prepared for storage: it is folded double, placed on a piece of aluminium foil, which is folded close and labelled, and is then placed in a freezer. The analysis for Chlorophyll is conducted through the extraction of the filters in 90% acetone. This method has been in practice for over two decades, and is recognised as one of the most straightforward methods of measuring Chlorophyll in the laboratory (Parsons et al., 1984). The methodology outlined below holds to that of previous researchers closely, although there are minor differences.

Extractive analysis of Chlorophyll samples

After being defrosted, the filters are unwrapped, rolled into a small cigar shape and placed in a 10 ml tube, which is filled with a known quantity of 90% Acetone (generally 10 ml); and these are then left overnight in the fridge for the extraction process to take place.

In the morning, the samples are taken from the fridge and left to gain room temperature. Subsequently, the filters are removed from the tubes, which are then allowed to settle. The laboratory fluorometer used is a Turner Designs 10-AU which has been fitted with optical kit 10-037R for the analysis of Chlorophyll using the extractive (*in vitro*) method. This instrument needs to be switched on thirty minutes before starting the measurements to warm up the light source. Once the fluorometer is ready, the sample is poured into a glass cuvette which is placed in the instrument. After taking the initial measurement, a few drops of 10% HCl are added to acidify the solution and a second reading is taken.

The combination of the two readings allows for a correction to be applied for the significant contribution of Phaeopigments to the measurement of Chlorophyll-a. This method has been derived from Parsons et al. (1984), Baker and Wolff (1987) and Knap et al. (1996). Equation 3.4 and 3.5 show the calculations necessary to find the Chlorophyll-a concentration ([Chl-a]) and Phaeopigment concentration ([Phaeo]). These concentrations will both be expressed in $\mu g\ l^{-1}$ as long as the unacidified and acidified readings have also been expressed in these units.

$$[Chl-a] = \left(\frac{F_m}{F_m - 1}\right) \times (F_0 - F_a) \times K_x \times \left(\frac{vol_{ex}}{vol_{filt}}\right) \tag{3.4}$$

$$[Phaeo] = \left(\frac{F_m}{F_m - 1}\right) \times [(F_m \times F_a) - F_0] \times K_x \times \left(\frac{vol_{ex}}{vol_{filt}}\right) \tag{3.5}$$

where F_m is the acidification coefficient found during calibration of the 10-AU, F_0 is the reading before acidification, F_a is the reading after acidification, K_x is the linear calibration factor which is also found during calibration of the 10-AU, vol_{ex} is the extraction volume, and vol_{filt} is the sample volume filtered.

Two of the above-mentioned coefficients are found during the calibration of the 10-AU fluorometer against a pure Chlorophyll-a standard, and it is strongly suggested that this calibration is carried out for each data series. However, due to many different researchers using the 10-AU fluorometer, the calibration has been limited to being done every couple of years, and in

between the instrument drift is measured using a secondary solid standard. The re-calibration of the 10-AU has been carried out on two occasions of relevance to the results presented. The resulting values of the coefficients F_m and K_x can be seen in Table 3.2 below.

Date	F_m	K_x
12-06-2002	1.905	0.9973
06-09-2005	1.884	1.0099

Table 3.2: Overview of calibration coefficients for Turner Designs 10-AU bench fluorometer.

Verification of laboratory techniques

The analysis of filters for Chlorophyll-a using the extractive method is varried, with different researchers using different techniques, volumes filtered etc. When first becoming involved with this research, it seemed that there were no official reasons as to why these protocols used certain guidelines, and different researchers methods had also gone unquestioned. To this end, some time was spent in verifying the errors introduced from the use of different gloves, touching filters with gloved hands, or with bare hands, as well as spending some effort checking if sample volume and storage prior to filtration made a significant difference to the results.

Filter handling techniques

Five different treatments for handling filters were compared, using only blank filters papers. The filters were made slightly wet with a small quantity of distilled water. The first technique involved following strict protocol of not touching the filter with anything except for a pair of forceps (control experiment), the second and third treatment looked at the effects of touching the filter with latex or vinyl gloves, the fourth method involved extracting acetone overnight in empty tubes and the final treatment looked into the effects of skin contact by having different colleagues touch the filters with their bare hands. When asking fellow researchers if the use of these different types of gloves could add error to the analysis of laboratory samples, there was no clear unifying answer. For this reason, the effects of touching the filters with gloves were tested. Similarly, the extraction of empty tubes overnight allowed to verify that there is no significant influence on the tube's material on the fluorescent signal. Finally, filters were also analysed for skin contact as when at sea, this is the most likely source of error due to the

added complications of attempting the use of precision instruments and protocol on an unstable platform. Results of the analysis of 10 samples for each filter treatment showed that there is no statistically significant difference between the methods of handling filters with only forceps, latex or vinyl gloves. There was also no significant contribution to sample fluorescence by the sample tubes used. Contact with the skin does however create a fluorescence signal which is significantly different from zero. However, when using the above conversion to Chlorophyll-a and Phaeophytin and assuming that the addition to the fluorescence signal is independent of the volume filtered, then there would be an addition of the order of magnitude 10^{-3} to the calculated concentration (taking a typical volume of 500 ml). Filtering larger volumes would further minimize the relative contribution and error.

Filter volume

Depending on the experimental set-up, the volume capable of being collected may differ and limited boat space or storage could mean smaller quantities need to be filtered. The storage of samples in the cold and dark could also be limited by the experimental design. Generally, guidelines suggest a minimum of 500 ml of water to be filtered through the filter, preferably without storing the sample first. Storage guidelines recommend storing the samples in the dark and refrigerating them for a minimal amount of time. Within the scope of this project, samples were generally stored in the open for several hours in white plastic bottles, or rarely were they stored in a refrigerator, before being filtered. To investigate whether this deviation from protocol made any significant difference to the end result, 5 different treatments were analysed using laboratory cultures of *Tetraselmis* algae and filtered seawater. Using an Eppendorf © pipette, 1 ml of culture was added per 500ml of filtered UV-treated seawater in a white plastic bottle, and the sample was inverted in order to mix the algae with the seawater. Depending on the treatment, the sample was stored on the counter in the laboratory, in the fridge or immediately filtered. For analysis of the Chlorophyll concentration, a measured volume of sample was filtered through the filter. If the sample had been stored, the sample was inverted again to resuspend all the settled algae before measuring the filtered volume.

The five methods compared were the filtration of 1000 ml immediately, that of 500 ml immediately, that of 500 ml after storage for 5 hours in the fridge, that of 500 ml after storage for 5 hours on the counter in daylight conditions and that of 100 ml using the Sweenex Syringe set-up. This laboratory experiment showed there was no statistically significant difference in

the mean Chlorophyll, Chlorophyll-a or Phaeopigment concentration measured in a sample size of 10 samples for these five methods. Therefore, it is possible to conclude that neither the storage methods used or filter volumes chosen during the field and laboratory work introduce a significant error to the measurement.

Fluorometer calibration

Laboratory fluorometer

The calibration of the Turner Designs 10-AU laboratory fluorometer has been carried out on two occasions of relevance to this research (June 2002 and September 2005). Since the last re-calibration, the instrument drift was monitored with a solid standard, to ensure no significant deviations occurred.

The laboratory fluorometer works on the principle of a two-point calibration: the first point being a blank sample, and taking a known standard solution as the second point. This standard solution is made up by dissolving a known quantity of pure Chlorophyll-a in a known volume of 90% acetone. The absorbance of this standard is then read at wavelengths of 430 nm, 668.5 nm and 750 nm on a Schimadzu Spectrophotometer before and after acidification in order to measure the Chlorophyll-a concentration of this solution. This standard is then used to calibrate the bench fluorometer giving it a range between zero and twice the concentration of the standard solution.

In order to find the linear calibration factor, K_x, and acidification factor, F_m, an additional 7 dilutions of the standard solution are made up, and read on the 10-AU fluorometer before and after acidification with 10% HCl. K_x is then the slope of the unacidified fluorometric reading against the Chlorophyll-a concentration calculated spectrophotometrically. F_m is obtained by averaging the ratio of unacidified and acidified readings of the dilutions. The values of F_m and K_x obtained during the two different calibrations of the bench instrument can be found in Table 3.2. Finally, some attention should be given to the notation and terminology of these coefficients: K_x is sometimes referred to as the door factor, the fluorescence response factor or F_s; F_m is also referred to as the acidification coefficient or r. However, throughout this thesis, the notation of K_x and F_m for the linear calibration factor and acidification factor, respectively, will be strictly adhered to.

Field fluorometers

The calibration of field fluorometer readings against the actual concentrations measured on the 10-AU bench fluorometer can prove difficult at the best of times, however the main problem arises through the fact that the field fluorometers have the inability to distinguish between Chlorophyll-a and Phaeopigments due to the overlap in wavelength bands they operate in. Hence, both substances will be measured in the fluorescence reading stored. Even on the bench instrument, the only method of making a distinction between these two substances is through acidification of the sample. It is therefore thought that on shorter deployment durations and with a good resolution of water samples throughout the time series, calibration of instrument fluorescence against Chlorophyll-a could prove reliable. In the long term, however, the ratio of Chlorophyll-a to Phaeopigments changes with species composition and phytoplankton health, and therefore using samples spaced far in time or space, or using a calibration made for a specific deployment could prove erroneous when attempting to reconstruct longer time series. During the field work, it moreover proved difficult to collect an adequate number of samples to calibrate the field fluorometers (especially those located in more hard to reach places such as Penmon Bay and Penmaen Swatch).

For the reasons outlined above, a variety of different calibration curves have been calculated depending on what was thought to provide the most accurate answer for the phytoplankton concentration. For short term deployments with the necessary samples, calibration has been done to concentration in Chlorophyll-a. For the mooring data from Penmaen Swatch and Penmon Bay, calibration has been done for measurements made with laboratory cultures. Finally, the fluorometers deployed at Conway Centre Dock and Ynys Faelog were calibrated with a two-point calibration (distilled water and known concentration cultured algae) prior to deployment. Calibration of the fluorometer at Ynys Faelog against field samples during its deployment revealed a calibration equation close to a one-to-one relationship, therefore no further correction on the data was done. The fluorometer at the Conway Centre Dock could not be calibrated against field measurements, although it was assumed it would be under similar conditions to that at Ynys Faelog, and therefore no further correction was made to the data. An overview of the calibration coefficients for the calibration equation (Equation 3.6) has been given in Table 3.3.

$$[10 - AU] = m \times [FF] + c \tag{3.6}$$

where [10-AU] is the concentration measured by the 10-AU laboratory fluorometer in $\mu g\ l^{-1}$, [FF] is the fluorescence (as concentration or voltage) measured by the field fluorometer, and m and c are the slope and constant of the regression analysis, respectively (given in Table 3.3, page 41).

Statistical analysis (using a General Linear Model (GLM) with covariates in Minitab ®) of the linear calibration relationships given in Table 3.3 has revealed that for the CTD calibrations (April 2005 and August 2005 R.V. Prince Madog) neither the difference in slope or intercept of these equations were statistically significant (F=1.32 with p=0.20 for slope and F=-0.38 with p=0.71 for intercept). GLM analysis of three different deployments of the SN639 SCUFA fluorometer, however, has shown that significant differences in the slope of the calibration can occur (F=4.45 with p=0.02); with the laboratory calibration being most different from the others. Comparison of three calibrations using the same method and same type of instruments (all 3 SCUFAs) has shown that the equations can differ significantly between instruments (F=17.83 with $p \leq 0.001$). These statistical analyses demonstrate that it should not be assumed that calibrating one will be sufficient for identical instruments. Moreover, even the same instrument may be subject to a different calibration equation depending on the environmental conditions. However, within the scope of this project, at times it has been inevitable to gloss over these issues and apply calibration equations outside of their regular scope.

3.4 Data analysis techniques

There are two main data analysis techniques which have been used in the analysis of field measurements of Chlorophyll concentration in the Menai Strait. For the smoothing of data and removing spikes, two seperate techniques have been used: the first is a novel technique which has takes the mode of the distribution, the second technique uses the standard deviation of the data to smooth out spikes in the Chlorophyll concentration. For the signal processing, harmonic analysis has been used to fit waves of tidal frequency to the observations, while Fourier analysis has been applied to find prevalant frequencies. Below these techniques are discussed in more detail.

Calibration Reference Name	Units of [FF]	Number of Observations	Slope (m) ± SE	Constant (c) ± SE	R^2
Long-term SN615	$\mu g\, l^{-1}$	11	1.07 ± 0.12	1.55 ± 1.33	0.902
Long-term SN639	$\mu g\, l^{-1}$	11	2.59 ± 0.22	0.61 ± 1.11	0.938
Long-term SN693	$\mu g\, l^{-1}$	11	1.41 ± 0.11	0.80 ± 0.96	0.951
April 2005 R.V. Prince Madog P	volts	11	155.15 ± 45.12	-1.57 ± 1.20	0.568
April 2005 SN639	$\mu g\, l^{-1}$	9	2.59 ± 0.66	-1.78 ± 1.14	0.689
August 2005 R.V. Prince Madog P	volts	17	100.46 ± 17.45	-1.14 ± 0.49	0.688
August 2005 R.V. Prince Madog FT	$\mu g\, l^{-1}$	19	9.64 ± 1.70	-1.19 ± 0.54	0.655
August 2005 SN639	$\mu g\, l^{-1}$	18	0.86 ± 0.09	-0.05 ± 0.17	0.860
August 2005 Aquatracka	$\mu g\, l^{-1}$	17	2.30 ± 0.19	0.15 ± 0.13	0.907
May 2006 R.V. Prince Madog P	volts	–	20.69	0.25	0.580
August 2006 Mya SN615	$\mu g\, l^{-1}$	–	0.46	0.66	0.737

Table 3.3: Coefficients for calibration equation (Equation 3.6) for the different instruments and their different deployments where appropriate. P = profiling, FT = flow-through.

3.4.1 Smoothing data and removing spikes

The majority of issues encountered with fluorometer data has been the fact the data can be highly variable. Much of this variability does not seem to be actual variation in the water column concentration, but rather momentary interference in the fluorescence reading. Different ways to deal with this variability have been investigated, and eventually, the two smoothing methods outlined below were found to be the best solution without compromising the actual changes in water column concentration in the data.

Smoothing using a Modal Filter

For a given data window (generally a 30-minute window, although for daily averaging YSI-data a 24-hour window has also been used), a histogram of the values is calculated in bins of 0.3 μg l^{-1}. The mode of the distribution is found, and the average of the two second most common bins is taken to be the smoothed concentration at this instance. It was found that taking the most frequent bin led to a skew towards the higher values in the smoothing. Although this form of smoothing data proved successful for longer time windows, it was thought for smoothing on smaller time scales it would be unsuitable.

Smoothing using Standard Deviation (StDev-filter)

This smoothing method applies the idea underlying the 95% Confidence Interval in statistics. Using a specified data window (generally 30 minutes for smoothing SCUFA data), the mean (AVG) and standard deviation (SD) of the data contained within the window are calculated. If the value is outside $AVG_{window} \pm SD_{window}$, it is discarded. Further to this smoothing, a second pass at the data is made excluding any data outside the interval specified by the average value of the whole data set and its standard deviation by $AVG_{data} \pm 1.5 \times SD_{data}$. Figure 3.8 shows an example of raw SCUFA data, obtained in August at Penmaen Swatch which has been subjected to this filter using a window of 14 values (equal to 28 minutes).

3.4.2 Signal Processing

Harmonic Analysis Method of Least Squares (HAMELS)

Harmonic analysis allows to extract amplitudes and phases at specific frequencies from a data record. It is particularly used for extracting the amplitudes and phases of the tidal constituents in oceanographic measurements. These amplitudes and phases can be obtained statistically through fitting the harmonics using a least squares approach. The data series $x(t_n)$ can be expanded according to Equation 3.7 to include the contribution of M possible constituents. $x_r(t_n)$ is the residual signal which may include other harmonics, although none of the M harmonics fitted (Emery and Thomson, 2001).

$$x(t_n) = \bar{x} + \sum_{i=1}^{M} D_i \sin(2\pi f_i t_n + \phi_i) + x_r(t_n) \tag{3.7}$$

where $\bar{x}$ is the mean of the data series, and D_i, f_i & ϕ_i are the constituent's amplitude, frequency and phase respectively.

Equation 3.7 can then be expanded so the harmonic is expressed in a cosine and sine component (Equation 3.8) (Emery and Thomson, 2001). By calculating $\cos(2\pi f_i t_n)$ and $\sin(2\pi f_i t_n)$, the values of A_i and B_i can be found using least-squares analysis. Using Equations 3.9 and 3.10, the values of the constituent's amplitude D_i and phase ϕ_i can be calculated (Emery and Thomson, 2001).

$$x(t_n) = \bar{x} + \sum_{i=1}^{M} [A_i \cos(2\pi f_i t_n) + B_i \sin(2\pi f_i t_n)] + x_r(t_n) \tag{3.8}$$

$$D_i = (A_i^2 + B_i^2)^{1/2} \tag{3.9}$$

$$\phi_i = tan^{-1}(A_i/B_i) \tag{3.10}$$

The advantages of this technique are that a continuous or evenly spaced record is unnecessary, and that using matrix algebra in MATLAB ® , the coefficients A_i and B_i are easily solved for.

When calculating the phase of the oscillation, the origin of time becomes important. For the data sets where phase differences were calculated, it was made sure that the start of both variables was the same moment in time. When comparing phase differences, the original reference time

is then unimportant. For analyses where the absolute phase was compared, the time variable was adjusted so for all datasets the HAMELS analysis was from the same starting time, hence all phases were relative to the same reference time.

Fourier Analysis using Fast Fourier Transform (FFT)

Fourier analysis seperates a wave into sinusoid waves of different frequencies, which when summed represent the original wave. This makes it in some respects similar to HAMELS. However, in Fourier analysis, the frequencies which are resolved in the original data are defined by the record length, T. The longest period wave represented in the series is $\frac{1}{T}$. The frequency of the highest harmonic is defined by the record length, and the number of data points N. This frequency, also termed the Nyquist frequency, is equal to $\frac{N}{2}\frac{2\pi}{T}$. All frequencies in between are integer multiples of the lowest harmonic. Therefore, unlike with harmonic analysis, where waves of a user-defined frequency are fitted to the data, the harmonics fitted through Fourier analysis are predefined by the length of the record, and the number of values. A further disadvantage of using Fourier analysis is that a continuous and evenly spaced record is necessary for successful analysis. The main advantage of using Fourier analysis is the possibility to with reasonable ease fit a large number of harmonics to the data set (a total of $\frac{N}{2}$).

Within the MATLAB ® software package, the signal processing toolbox includes a Fast Fourier Transform (FFT) routine, which is a less computationally intensive method of Fourier analysis, while still retaining the accuracy of the Discrete Fourier Transform (DFT) (Emery and Thomson, 2001). More information on the FFT can be found in the MATLAB ® help files and Emery and Thomson (2001).

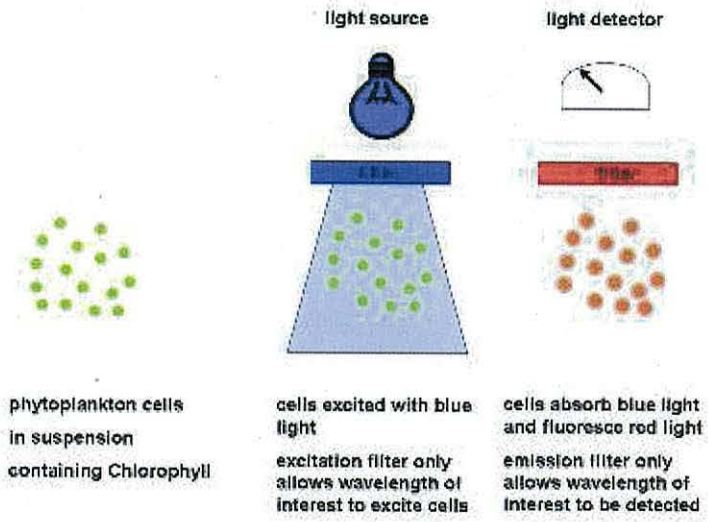

Figure 3.1: General principles of fluorescence measured through fluorometer (adapted from Turner Designs Ltd.)

Figure 3.2: Turner Designs SCUFA submersible fluorometer.

(a)

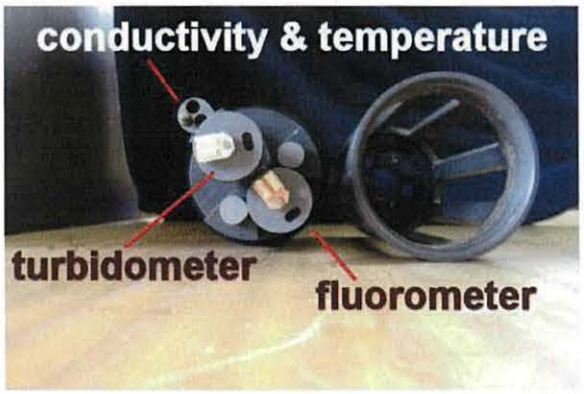

(b)

Figure 3.3: YSI multiparameter system (a) with probe guard for deployment, and (b) showing temperature and conductivity probes, YSI-6025 Fluorometer and YSI-6136 Turbidometer

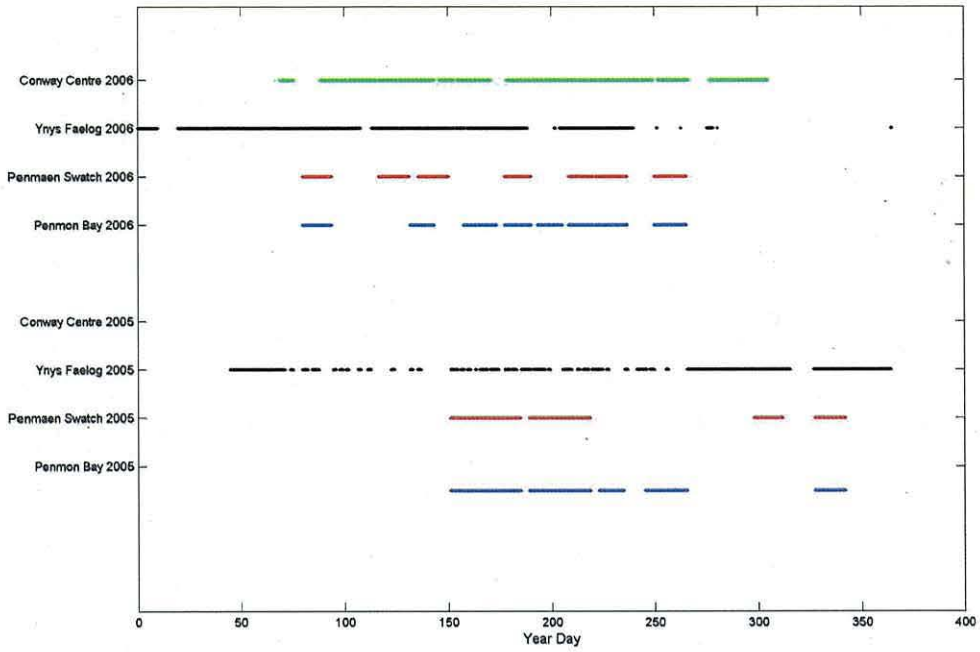

Figure 3.4: Annual coverage at long-term monitoring sites for 2005 and 2006.

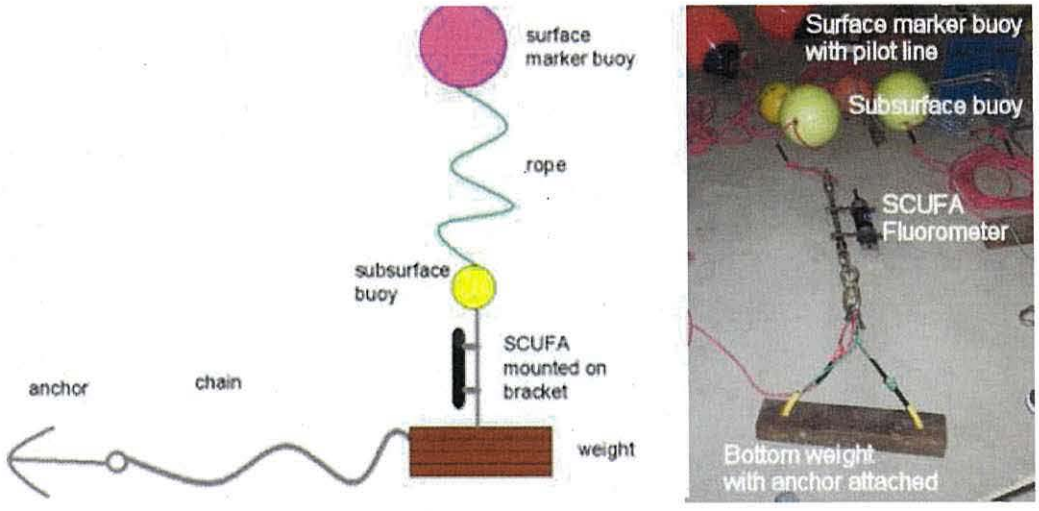

Figure 3.5: Schematic diagram and photograph of Penmon Bay and Penmaen Swatch moorings.

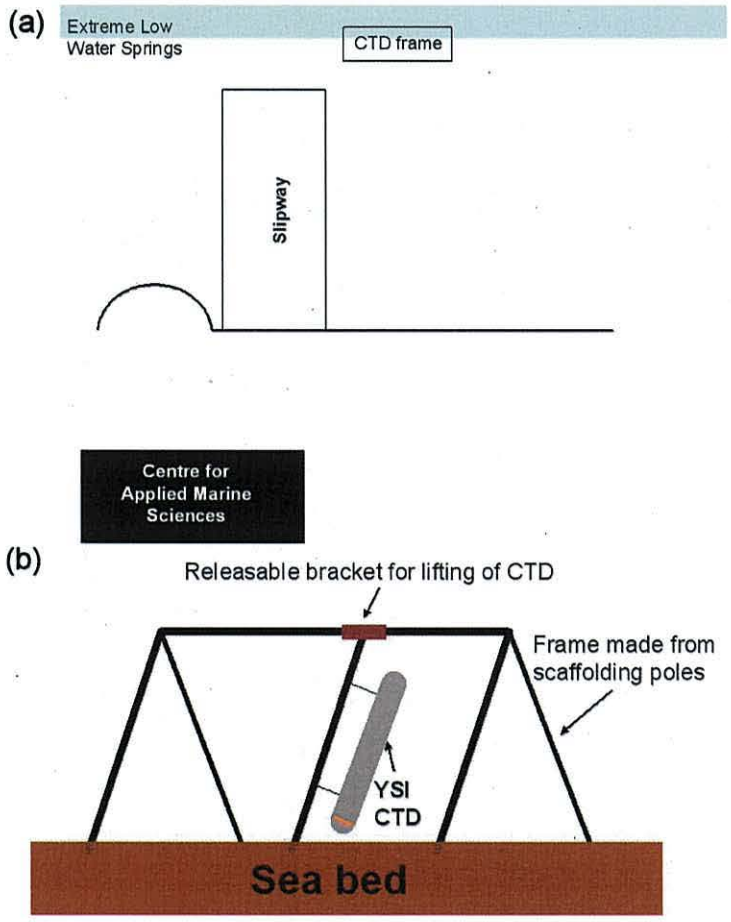

Figure 3.6: Mooring design and location at Ynys Faelog. Not to scale.

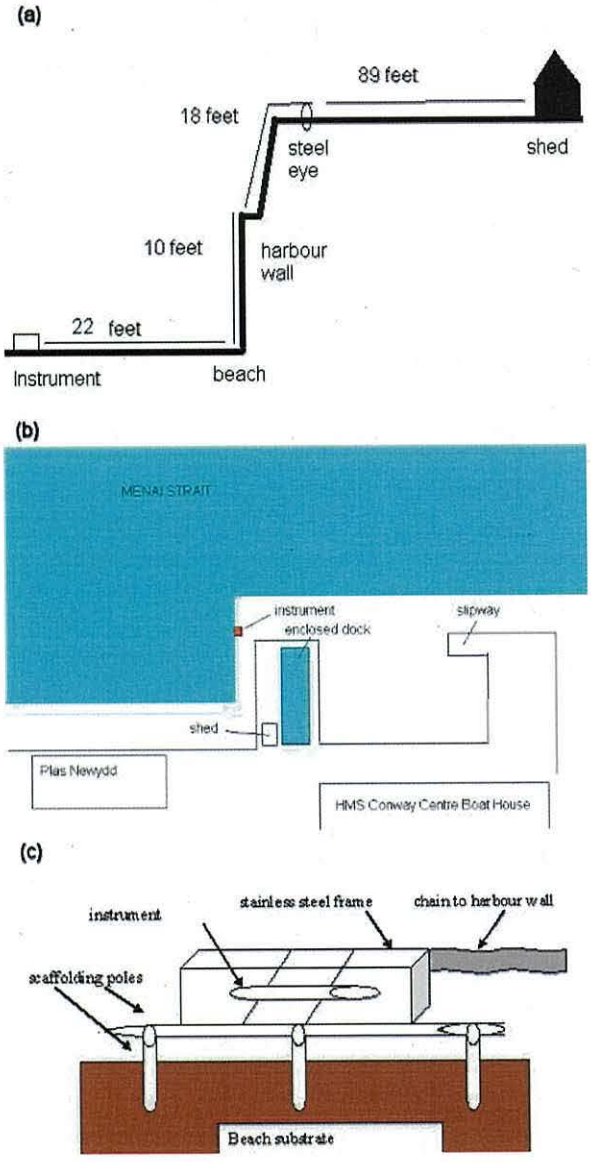

Figure 3.7: Mooring design and location Conway Centre Dock. Not to scale.

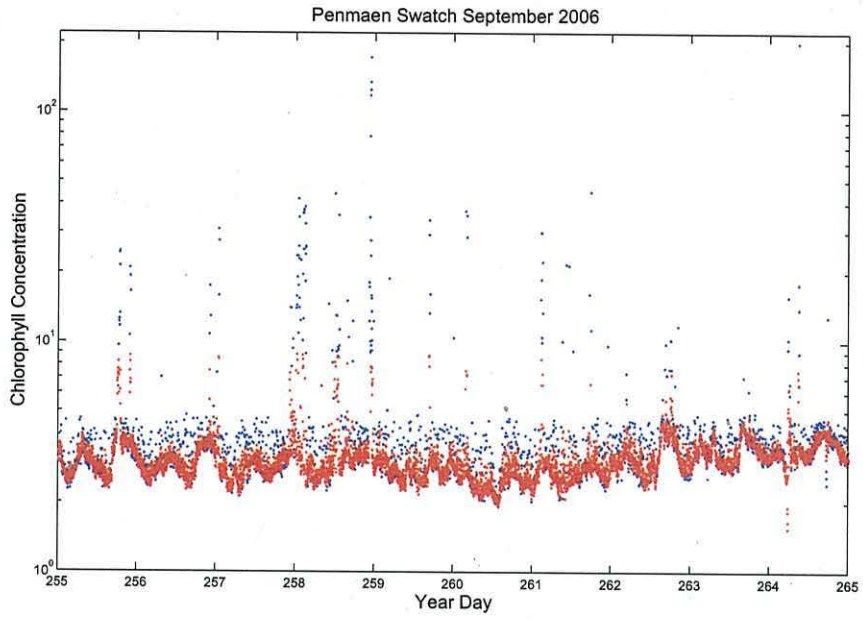

Figure 3.8: Raw (blue) and smoothed (red) Chlorophyll data ($\mu g\ l^{-1}$) from SCUFA deployment at Penmaen Swatch in September 2006, using a StDev-filter.

Chapter 4

Short-term and Spatial Patterns of Chlorophyll

4.1 Introduction and Methodology

As previously discussed, the presence of large quantities of mussels in the Menai Strait produces a strong horizontal gradient in phytoplankton concentration. This gradient can be observed both during point-measurements over a period of time, and during spatial surveys in the along-channel direction of the strait. In previous measurements, it could be seen that phytoplankton-rich water is advected past the mussel beds on the ebb stage of the tide; while during flood tides, the Chlorophyll concentration of the water is lower due to the mussels having filtered out much of the suspended phytoplankton. This interaction of tidal advection and mussel filtration in the Strait therefore creates strong oscillations in the Chlorophyll signal at a single location. As these changes are associated with the semi-diurnal tide, they can be observed during field campaigns of relatively short duration ($\sim$ days).

The measurements presented within this chapter have been made during various research cruises in the Strait (see Section 3.2.2), each lasting several days in order to observe the changes in phytoplankton concentration over the semi-diurnal tidal cycle. The data presented comes from two teaching cruises in the Menai Strait (April 21-26 2005 and May 3-5 2006), where various Masters-students had a chance to gain some hands-on experience, and from one BBSRC-funded research cruise (August 11-15 2005). During these field measurements, Chlorophyll concentra-

tion was regularly determined over the depth of the water column (through profiles every 30 minutes) as well as continuously at depth (through deployment of a submersible fluorometer) and with discrete water sampling (through filtration for laboratory analysis). The latter of these measurements allows for the calibration of the deployed fluorometers. Section 3.2.2 presents the data collection during these research cruises in greater depth, while more details on the laboratory analysis and data processing can be found in Sections 3.3 and 3.4, respectively. All the Chlorophyll measurements presented have been calibrated against *in situ* measurements, and details of these calibrations can also be found in Section 3.3.

There have also been several opportunities to measure the spatial distribution of Chlorophyll in the Menai Strait, through along-channel surveys conducted aboard the R.V. Prince Madog (August 11-15 2005) and the smaller survey vessel Mya (August 4th 2006). These transects offer a good complementary view of the interaction of mussel feeding and tidal advection in the Menai Strait and the associated effects on the spatial distribution of Chlorophyll. Further details on the data collection can be found in Section 3.2.3, while details of the laboratory sample analysis and data processing may be found in the above mentioned sections.

This chapter aims to discuss these patterns in Chlorophyll which may be observed on a short time scale. Through the presentation of results recently collected in the Menai Strait, the existing understanding of the interaction of tidal advection and mussel filtration will be expanded. These results have already in part been published by Simpson et al. (2007)[1]. In Chapter 8, the field results presented here will also be used for the validation of the PHYBIO model (see Chapter 7).

4.2 Time series Observations of Chlorophyll Distribution

There is a strong, clear semi-diurnal pattern observable in the data made during anchor stations in the Menai Strait. Figures 4.1, 4.2 and 4.3 show the Chlorophyll concentration near the Southern edge of the mussel beds (vicinity of Bangor Pier) on three seperate occasions when measurements were made from the anchored R.V. Prince Madog. Measurements of salinity, temperature, density, suspended sediment concentration and particle size were also made during the three research cruises. For completion, these results, as well as the velocity observations

[1] Text written by J. Simpson, analysis of data & model and response to review & corrections by B. Berx (corresponding author), and help with laboratory analysis from C. Saurel and J. Gascoigne, who also organised the field work aboard the R.V. Prince Madog

from the ADCP have been presented in Appendix C.

For each research cruise, as well as the Chlorophyll distribution, the depthmean along-channel velocity and elevation from the ADCP measurements are shown in Figures 4.1, 4.2 and 4.3. As these measurements are not always at the same location, with the ADCP being deployed on a mooring which is generally closer to the navigation channel, the total water depth varies between the ship-based measurements and those from the ADCP. It can be seen that on the ebb tide, the concentration of Chlorophyll is higher than during the flood tide, which is due to the mussel filtration clearing the water column of phytoplankton (Figures 4.1, 4.2 and 4.3). This strong semi-diurnal oscillation is particularly obvious in the data collected in April 2005 (Figure 4.1) and August 2005 (Figure 4.2). The measured Chlorophyll concentration profiles from May 2006 (Figure 4.3) show this oscillation less convincingly, although the general pattern can still be discerned.

It can also be seen that the vertical distribution of Chlorophyll is homogenous for the majority of the tidal cycle. During all three cruises, there was hardly any density stratification at any stage of the tide in the Menai Strait (see Appendix C), indicating that the water column is well mixed by the strong tidal currents. The strength of mussel feeding could, however, bring about a vertical gradient in Chlorophyll due to the mussels filtering out the Chlorophyll near the bed. If the fresh supply of food from the overlying water is insufficient, this could lead to a layer close to the bed being deplete of Chlorophyll. This effect would therefore be most pronounced during periods when the tidal currents are weakest and mixing is minimal, i.e. around slack water. Looking at Figures 4.1, 4.2 and 4.3, however, if anything, in the Menai Strait there seems to be a higher concentration near the bed around times of slack water. This could be an indication that the settling of particles from the water column to the bed occurs, resuppling the bottom boundary layer with food particles for the mussels. However, it should also be noted that due to safety considerations, the CTD-profiling unit can not be lowered closer than approximately 0.5-1 m above the bed, therefore missing out the most important part of the water column, seeing that this process of vertical depletion probably occurs within 0.5 mab.

Comparison of the three (Figures 4.1, 4.2 and 4.3) also shows the seasonality of the Chlorophyll concentration in the Menai Strait. In April, the concentration of phytoplankton is at its highest due to optimal conditions for the bloom. Immediately following the spring bloom, conditions are less favourable and the concentrations will therefore be lower. Concentrations of phytoplankton are again slightly higher in August in the run-up to the smaller autumn bloom. A

further discussion of the seasonal cycle in Chlorophyll may be found in Chapter 6.

The strong oscillations in Chlorophyll concentration can be more readily observed when analysing the data from the permanently submerged fluorometers, which were deployed during the same three research cruises. Figure 4.4 shows a strong semi-diurnal oscillation in all three data sets. However, it can also be seen that there is a strong signal at a quarter-diurnal frequency, which is less obvious in the depth profiles of Chlorophyll concentration. Using HAMELS analysis (see Section 3.4.2), the signals can be extracted at these specific frequencies and their relative strength and phasing can be compared. Moreover, the same procedure can be carried out on the elevation data from the ADCP measurements, which allows us to compare the relative phasing of the elevation and Chlorophyll concentration. Due to the short duration of each time series, it is difficult to discriminate between the M2 and S2 tidal frequencies, and therefore, a general Semi-Diurnal (SD) and its equivalent Quarter-Diurnal (QD) frequency are used. Comparison of the results in Table 4.1 shows that there is a consistency in the phase difference between the Elevation and Chlorophyll Concentration at the semi-diurnal frequency. Furthermore, it can be seen that the phytoplankton concentation lags consistently by $\sim 75°$ behind the elevation signal at the SD frequency.

		A_0	A_{SD}	ϕ_{SD}	A_{QD}	ϕ_{QD}	R^2	DF
04/'05	η (m)	-0.02	3.193	90°	0.238	160°	0.973	390
	C (μg l^{-1})	2.64	0.681	12°	0.318	45°	0.531	390
08/'05	η (m)	0.03	2.206	90°	0.104	140°	0.997	218
	C (μg l^{-1})	1.52	0.324	17°	0.375	74°	0.755	218
05/'06	η (m)	8.5	2.043	90°	0.112	166°	0.960	434
	C (μg l^{-1})	11.5	2.177	12°	0.365	-37°	0.470	492

Table 4.1: HAMELS analysis for amplitudes (A) and phase leads (ϕ) of Elevation (η) and Chlorophyll concentration (C) at a semi-diurnal period (SD; ω= 0.503 rad h^{-1}) and quarter-diurnal period (QD; ω= 0.2515 rad h^{-1}). R^2 is given as an indication of goodness of fit. Degrees of Freedom (DF) are equal to n-5, where n is the number of observations.

4.3 Horizontal Distribution of Chlorophyll

Two data sets on the longitudinal gradients of Chlorophyll in the Menai Strait were acquired. In August 2005, several repeat sections between Puffin Island and Menai Bridge were obtained from the R.V. Prince Madog, and in August 2006, the use of the smaller survey vessel Mya meant the distribution of phytoplankton over the total length of the Strait could be sampled.

Figure 4.5 shows the Chlorophyll concentration in the Northern section of the Menai Strait (Puffin to Menai Bridge) measured in August 2005 on 6 separate occasions and at different stages of the tide. It can be seen as the tide changes, the gradient is advected back and forth past the mussel beds: during the ebb tide, the gradient is pushed further into the Strait (Figure 4.5 c, d & f); while at the flood stage of the tide, the concentration gradient is advected northward (Figure 4.5 a, b & e). Analysis of the concentrations measured by the flow-through system aboard the R.V. Prince Madog in August 2005 (Figure 4.6), showed a statistically significant difference in the gradient ($p=0.03$) between periods of ebb and flood flow. A possible explanation for these changes in gradient is through the stretching of the water column, as demonstrated in Figure 4.7. Further estimates of the horizontal Chlorophyll gradient have been made using the data of submerged moorings in August 2005 (SCUFA at Penmon Bay and Aquatracka at Bangor Pier) and May 2006 (SCUFA's at Penmaen Swatch and Bangor Pier). The horizontal gradient of Chlorophyll calculated by taking the difference in tidally averaged Chlorophyll concentration between the two locations, and the distance was equal to 8.7×10^{-4} $\mu g\, l^{-1}\ m^{-1}$ in August 2005, and 3.5×10^{-4} $\mu g\, l^{-1}\ m^{-1}$ in May 2006. Although these gradients differ by a factor of 2, they are similar in magnitude. Differences between them could be due to the different seasons in which the data was collected.

Figure 4.8 shows the horizontal distribution of phytoplankton over the total length of the channel in August 2006. Comparison of Figures 4.5 and 4.8 shows that even though the initial concentration at Puffin Lighthouse is different, the same pattern can be observed, with the strongest gradient in Chlorophyll overlying the mussel beds.

An easier method of comparison is to normalise the measured Chlorophyll concentration at any location (Chl_i) using the concentration at Puffin Island (Chl_0). Figure 4.9 shows the normalised (depth-mean) Chlorophyll concentration ($=\frac{Chl_i}{Chl_0}$) measured by Tweddle et al. (2005), as well as in the horizontal sections mentioned above. There is a striking agreement between years, and there is also good similarity between different seasons. The stronger horizontal gradient observed by

Tweddle et al. (2005) in spring 2002 could be due a higher filtration effort from the mussels, related to optimum conditions for growth.

4.4 Vertical water column structure

During the August 2005 research cruise, a permanently submerged mooring (see Appendix A) was deployed from the R.V. Prince Madog with two fluorometers sampling Chlorophyll concentration every 30 seconds. One instrument was located near the bed (AquaTracka ~0.33 mab), while the other recorded concentrations higher in the water column (SCUFA ~2.50 mab). The continuous deployment of these fluorometers meant the vertical structure of the Chlorophyll distribution in the water column could be observed.

Figure 4.10 shows the depletion value calculated from observations made in August 2005, where negative values indicate a lower Chlorophyll concentration near the bed than higher up the water column. Using the definition of Tweddle et al. (2005) where depletion events are defined as being two standard deviations below the mean difference, four depletion events can be observed in August 2005 (Figure 4.10). As expected, these occur at times of low currents, and hence when tidal mixing is almost non-existent. It is at these occasions that insufficient replenishment of the near-bed layer occurs and therefore mussel filtration depletes the Chlorophyll concentration. As can be seen in Figure 4.10, these occurrences of vertical depletion are short-lived and may not be sampled if the interval between observations is too long. Moreover, this process also occurs on a small vertical scale, and may not always be represented in the observations if the vertical sampling scale is too coarse.

4.5 Summary

Observations of the Chlorophyll distribution on relatively shorter time scales show:

- There is a strong horizontal gradient in Chlorophyll concentration which can be observed in time series measurements, as well as during spatial surveys of the tidal channel.
- The time series measurements of Chlorophyll show a consistent phase lag with respect to the elevation between different seasons and different years of ~75°.

- The horizontal gradient in Chlorophyll calculated from fluorometer observations is equal to $\sim 8.7 \times 10^{-4}$ μg l^{-1} m^{-1} in August 2005 and $\sim 3.5 \times 10^{-4}$ μg l^{-1} m^{-1} in May 2006.

- Observations of the horizontal distribution of Chlorophyll through the R.V. Prince Madog's Flow-Through System have shown a different gradient to occur at ebb and flood stages of the tide. A possible explanation for this occurrence can be found in the stretching of the gradient when the water column is more shallow.

- Observations of the vertical Chlorophyll distribution show the depletion of phytoplankton in the near-bed layer on several occasions. These events are short-lived in time and occur on a small vertical spatial scale

In conclusion, it can be said that these observations show convincing evidence that the measured patterns are the result of a combination of tidal advection, mussel filtration and vertical mixing. The data presented here will also be used for the validation of the PHYBIO-model (Chapter 8).

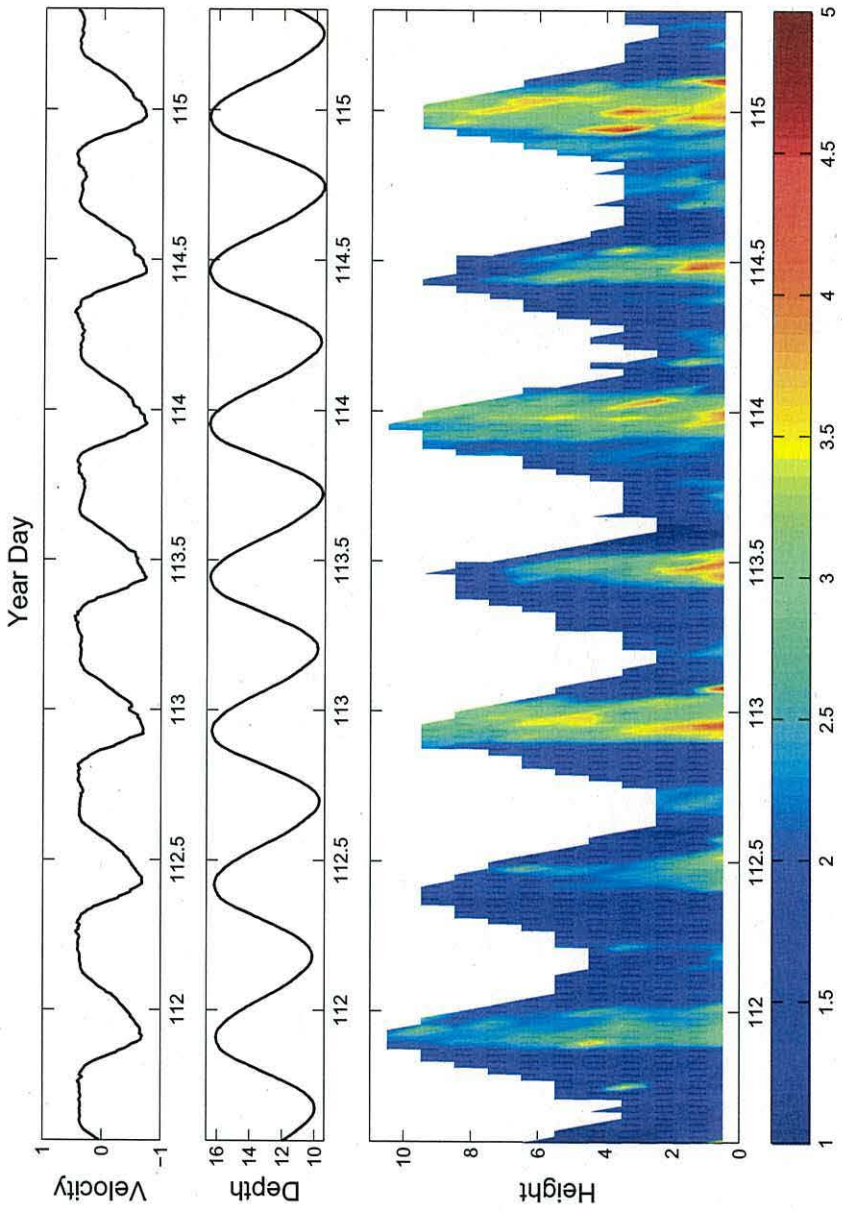

Figure 4.1: Chlorophyll depth profiles (interpolated shading) in April 2005. Top: Depth-mean along-channel velocity (m s^{-1}) from nearby ADCP; Centre: Tidal elevation (m) from nearby ADCP; Bottom: Chlorophyll concentration ($\mu g\, l^{-1}$) profiles from aboard the R.V. Prince Madog.

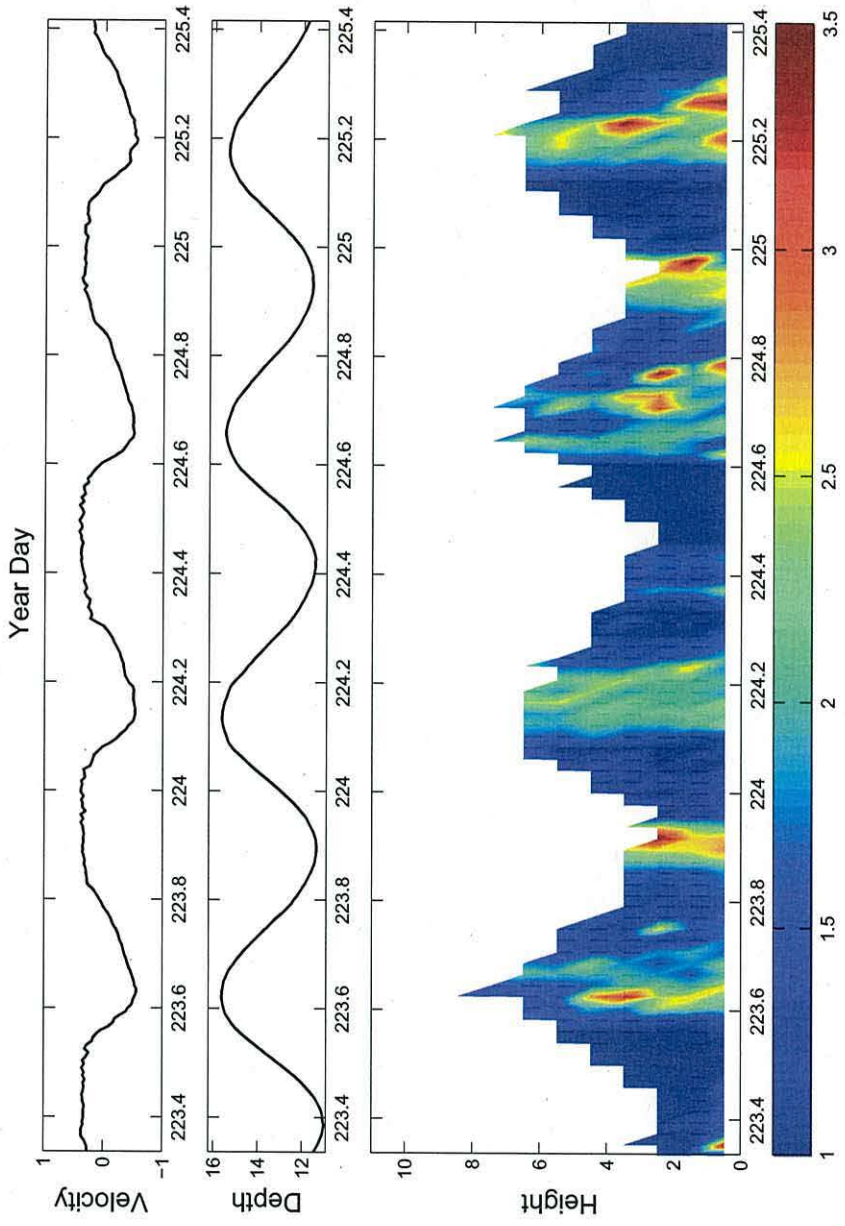

Figure 4.2: Chlorophyll depth profiles (interpolated shading) in August 2005. Top: Depth-mean along-channel velocity (m s^{-1}) from nearby ADCP; Centre: Tidal elevation (m) from nearby ADCP; Bottom: Chlorophyll concentration (μg l^{-1}) profiles from aboard the R.V. Prince Madog.

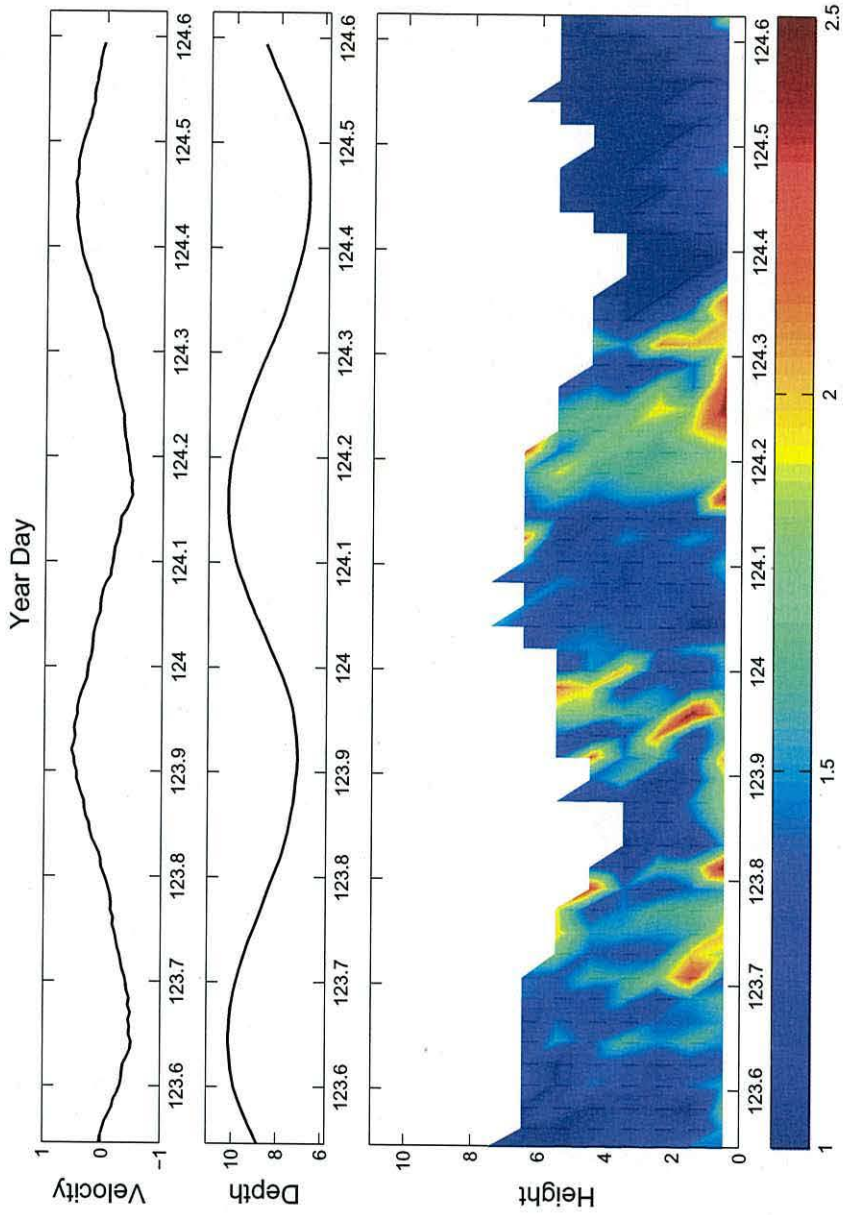

Figure 4.3: Chlorophyll depth profiles (interpolated shading) in May 2006. Top: Depth-mean along-channel velocity (m s^{-1}) from nearby ADCP; Centre: Tidal elevation (m) from nearby ADCP; Bottom: Chlorophyll concentration ($\mu g\ l^{-1}$) profiles from aboard the R.V. Prince Madog.

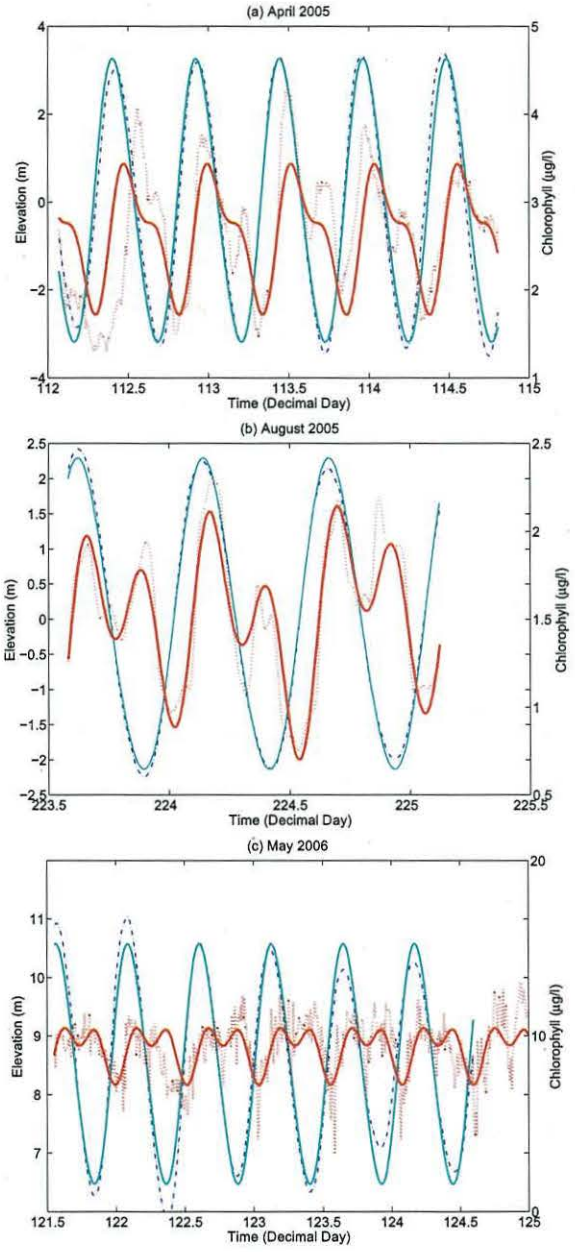

Figure 4.4: Time series of Elevation (m) (blue) and Chlorophyll (μg l^{-1}) (red) for (a) April 2005, (b) August 2005, and (c) May 2006. Raw data (dash) and HAMELS fit (solid) for semi- and quarter-diurnal constituent.

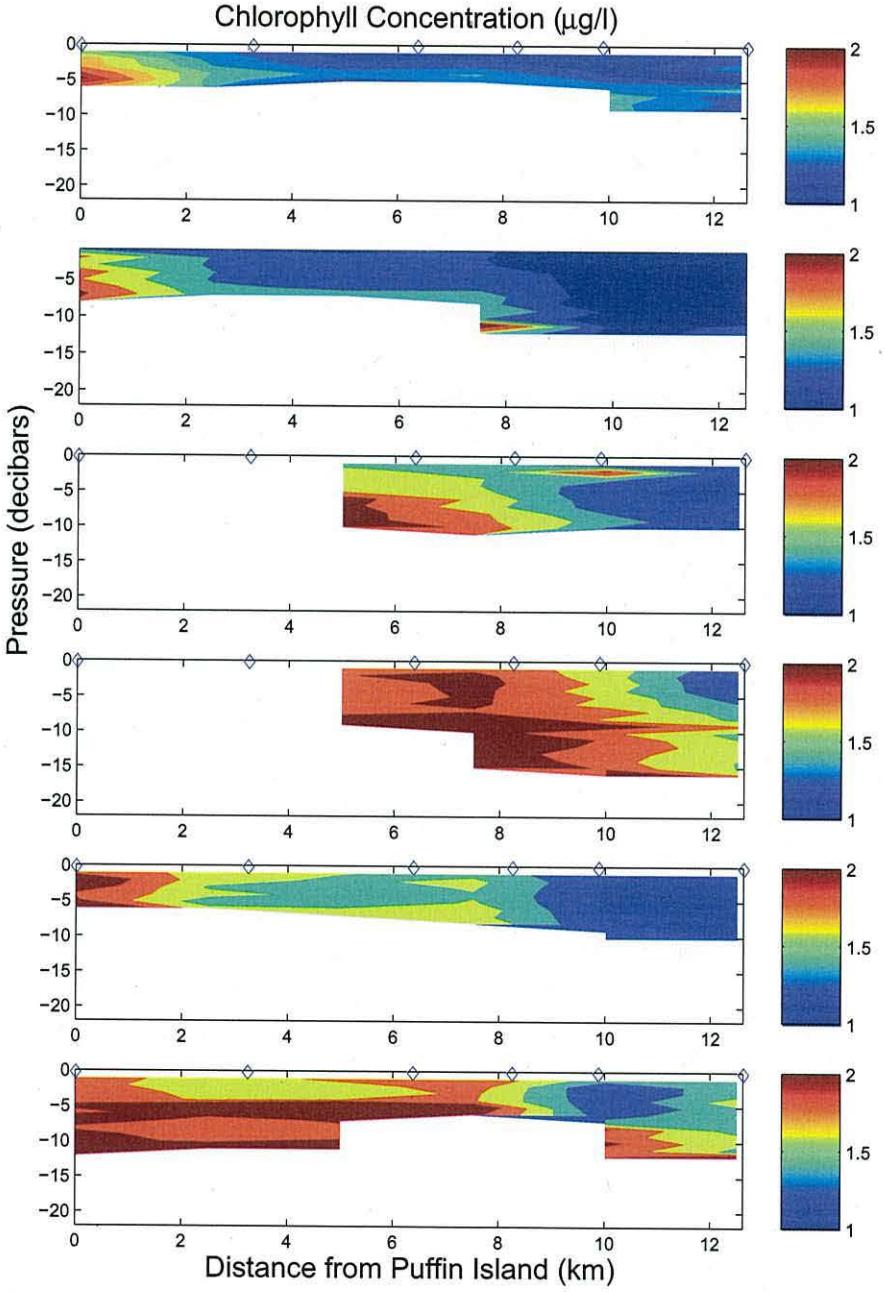

Figure 4.5: Contoured sections (interpolated shading) of Chlorophyll (μg l^{-1}) during 6 transects made aboard the R.V. Prince Madog in August 2005.

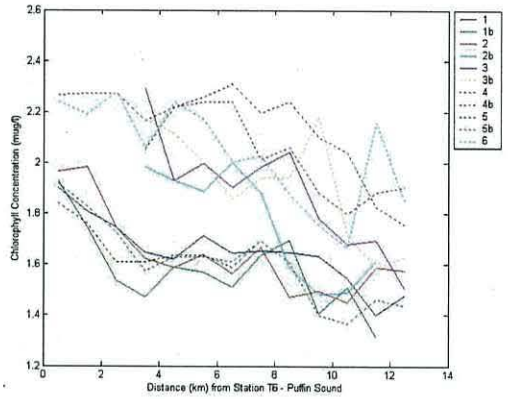

Figure 4.6: Horizontal Chlorophyll distribution (μg l^{-1}) measured by flow-through from the R.V. Prince Madog in the Menai Strait in August 2005. 1-6 Transect number (see Figure 4.5), the b signifies the return leg Menai-Bridge to Puffin Island.

Figure 4.7: Schematic diagram showing probable mechanism behind different gradients depending on stage of the tide.

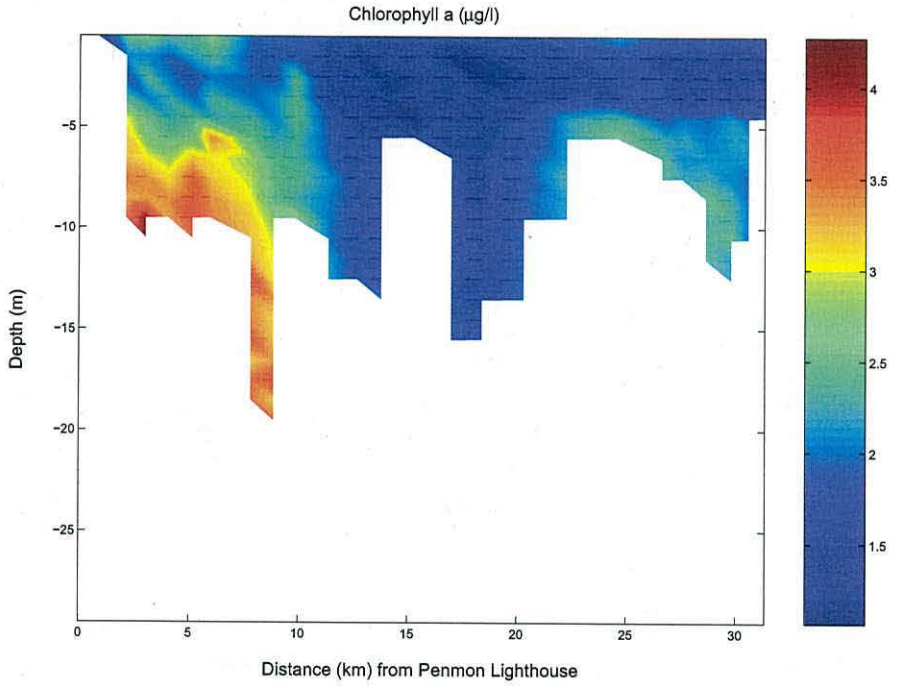

Figure 4.8: Depth profiles of Chlorophyll ($\mu g\ l^{-1}$) during transects made aboard the Mya in August 2006.

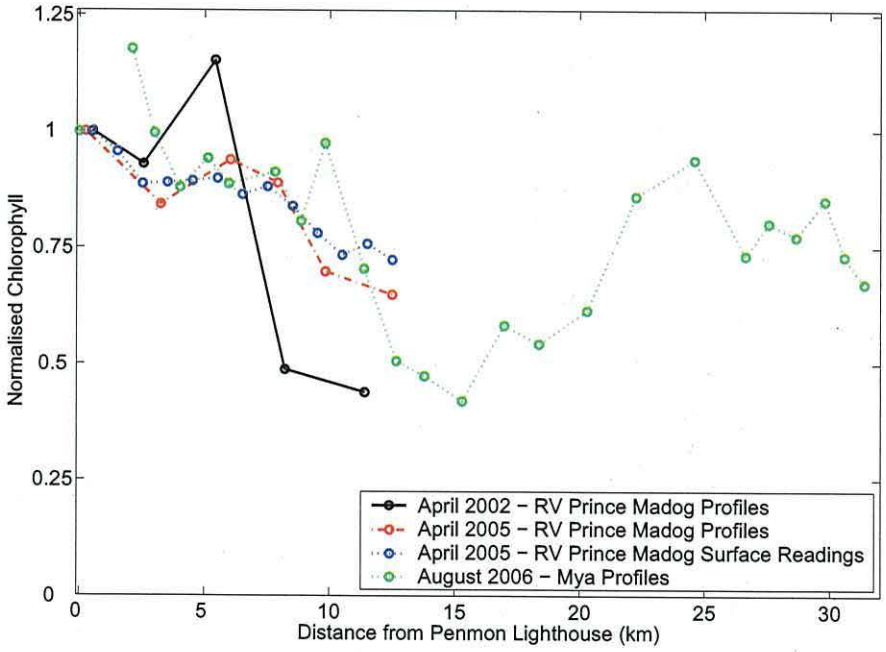

Figure 4.9: Comparison of normalized depthmean Chlorophyll concentration during 4 different along-channel surveys in the Menai Strait.

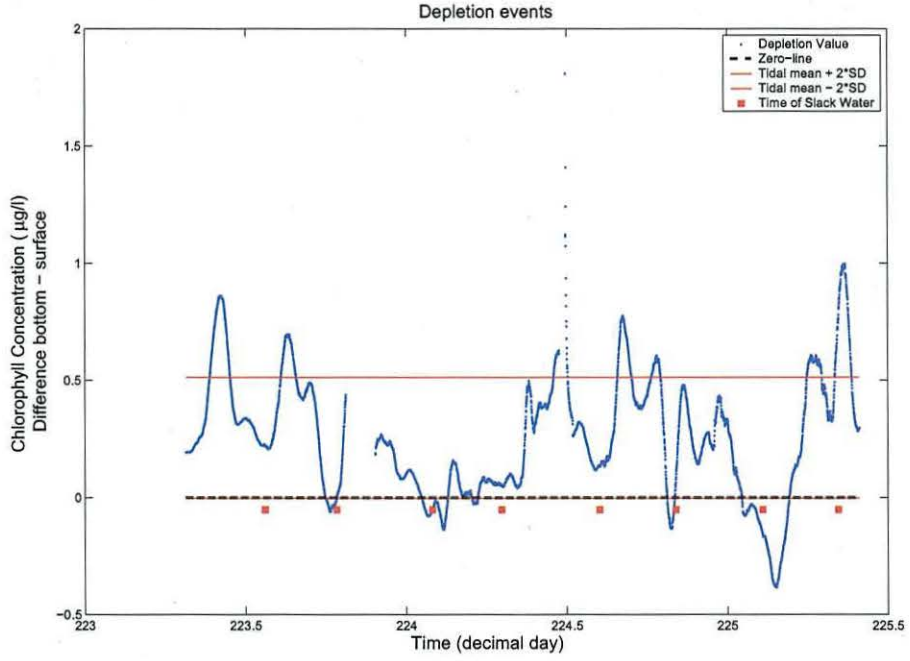

Figure 4.10: Observations of Chlorophyll depletion near Bangor Pier in August 2005, showing times of slack water from ADCP depthmean current measurements.

Chapter 5

Spring-Neap oscillations in Chlorophyll concentration

5.1 Introduction and Methodology

The observations of Chlorophyll in the Menai Strait not only cover the short-time scales of days, measurements have also been made on the medium- and long-term time scales. This chapter aims to investigate how the interaction of physical and biological processes influence the distribution of Chlorophyll in the tidal channel on medium time scales, more specifically within the period of the spring-neap cycle (14 days).

As discussed previously (see Chapter 2), there is a residual flow in the Menai Strait, transporting between 300 and 800 $m^3\ s^{-1}$ of water towards the South-West. Due to the direction of this residual transport relative to the location of the mussel beds, the effect on the Chlorophyll distribution on a spring-neap time scale will be most noticeable on the downstream side of the mussel bed. The sampling strategy has aimed to cover this region, and results from the Ynys Faelog and Conway Centre Dock sites will be presented. More information on instrumentation and site locations can be found in Sections 3.1 and 3.2, respectively. Data presented will be from YSI fluorometer measurements of Chlorophyll concentration at Ynys Faelog, and from a SCUFA which was deployed in April 2007 at Conway Centre Dock. The deployment of the latter came about through the realisation that data quality from the YSI monitoring stations was insufficient to resolve the signals at the shorter time scales, and often even at medium time scales. Although

more observations have been recorded, the analysis has been limited to these two data sets, as they showed the least interference of fouling.

5.2 Results

Figure 5.1 shows the hourly-averaged Chlorophyll concentrations recorded by the YSI monitoring station at Ynys Faelog for a 30 day period between March 1st and 31st 2006. When studying the top panel of this figure, the presence of filter feeders to the North (upstream the residual circulation) is immediately obvious, as the mean Chlorophyll concentration is lower during neap tides, when the strength of mussel feeding compared to the tidal advection is relatively larger than during spring tides. Figure 5.2 shows the measured concentration of Chlorophyll from a SCUFA deployed between April 2nd and May 1st 2007 at Conway Centre Dock. Due to small sediment becoming trapped in the anti-fouling mesh in front of the optical lenses, data past Decimal Day 112 has been discarded. Similar to results presented in Figure 5.1, the results presented in Figure 5.2 show strong oscillations in the Chlorophyll concentration, most likely due to the presence of the mussel beds near the entrance to the channel.

In order to identify which periods are most responsible for these oscillations, a Fast Fourier Transform (FFT) analysis was performed on both data sets. Figure 5.3 presents the power spectrum calculated by FFT analysis of the observations in March 2006 at Ynys Faelog. The analysis shows distinct peaks at the frequencies corresponding to the main tidal signals (M2/S2 and M4), as well as at a 7-day and 14-day period. Figure 5.4 shows the FFT analysis for the data, and similar to the data previously analysed from Ynys Faelog, there are distinct peaks in the frequency spectrum corresponding to the M4, S2/M2, 7-day and 14-day period oscillations.

In order to identify the importance of the spring-neap oscillation (i.e. with a periodicity of 14 days) and extract its amplitude and phase, a HAMELS analysis (see Section 3.4.2 for more information on this method) was performed on the 48-hour running averaged data. This meant all oscillations of shorter duration, including both the semi-diurnal and quarter-diurnal tidal oscillations and the shorter period noise, were excluded. The results of this HAMELS fit can be seen in Table 5.1 and Figures 5.5 and 5.6. For the Ynys Faelog site, 55% of the fluctuations in the data can be explained by the spring-neap period. As can be seen from Table 5.1, the Chlorophyll concentration oscillates over this 14-day period with an amplitude of $\sim 0.79\ \mu g\, l^{-1}$. From Figure 5.5, the strong spring-neap oscillation can also be observed. Therefore, at Ynys Faelog, during

a spring tide, the concentration of phytoplankton is higher than during a neap tide. As stated before, it is thought that this is most likely due to the relative change in the strength of mussel filtration and tidal advection: at neap tide, the transport of water is weaker, and therefore mussel filtration has a larger impact on the water column concentration of Chlorophyll. Several other possible reasons for this change in the Chlorophyll concentrations further South along the Menai Strait include the resuspension of previously deposited particles: the faster tidal currents are capable of bringing this material in suspension, thus increasing the Chlorophyll concentration. These particles could consist of living benthic phytoplankton, dead cells which have previously been deposited, or broken up macroalgae. Studying the phaeopigment-to-Chlorophyll *a* ratio could provide further insight into this hypothesis. Within the research undertaken for this thesis, the appropriate water samples have not been collected to analyse for this effect.

Applying the same HAMELS analysis as for the Ynys Faelog data, the fit for the Conway Centre Dock observations shows that 38% of the signal is explained by the oscillation over the spring-neap period. As can be seen from Table 5.1, the amplitude of the fortnightly oscillation is approximately 0.93 μg l^{-1}. Results shown in Figure 5.6 show that there is not only a strong spring-neap oscillation at Conway Centre Dock. There is also a stronger oscillation with a periodicity of ~7 days, which is also confirmed in the FFT analysis presented in Figure 5.4.

	Ynys Faelog	Conway Centre Dock
A	0.79	0.93
ϕ	-43.7 °	-105.3 °
A_0	3.33	10.06
R^2	0.55	0.38
DF	724	486

Table 5.1: HAMELS analysis for amplitude (A) and phase leads (ϕ) of Chlorophyll concentration at Ynys Faelog (YSI) and Conway Centre Dock (SCUFA) for spring-neap cycles (14 day period).

Comparison of the results of the HAMELS analysis of the Conway Centre Dock and Ynys Faelog data shows that there is good agreement between the two locations, despite the different periods of the year covered. Due to the phasing being calculated for the data relative to midnight on January 1st 2006, the calculated values of ϕ are directly comparable. The phase of the fortnightly oscillation does not agree completely, and the phase difference of ~62 ° translates to the oscillation at Conway Centre Dock lagging the oscillation at Ynys Faelog by 2.4 days. This lag is not unexpected as the residual tidal advection takes several days to make its way down the Menai Strait, so some lag is to be expected between the oscillations at these locations.

The amplitudes measured at the two locations are also similar, giving further support to the hypothesis that there is a strong spring-neap oscillation in the downstream direction of the mussel beds. When scaled to the baseline Chlorophyll concentration (i.e. A_0 of the HAMELS analysis) the amplitude of the spring-neap oscillation are approximately 23% and 9% for Ynys Faelog and Conway Centre Dock, respectively.

The above presented results are in agreement with the hypothesis that as the tide progresses from spring to neap, the relative strength between the residual advection and mussel feeding changes, therefore affecting the Chlorophyll concentration. At spring tides, when transport is large, the mussels have relatively less time to deplete the food supply, as the water is transported past too quickly. At neap tides, on the other hand, the strength of tidal transport is less and in relative terms to the situation at springs, they have a longer period to filter out the phytoplankton. From this, it is therefore to be expected that upstream from the mussels there will be nearly no oscillation with the spring-neap progression.

This second part of the hypothesis is, however, more difficult to confirm with the observations currently obtained. Due to fouling of instrumentation setting in after a period of just over 14 days, the deployments at the moored sites of Penmon Bay and Penmaen Swatch were limited to this period. Excluding the time between switching on the instruments and deploying them on site, leaves a data set which is too short to confidently analyse for a signal with a fortnightly periodicity. Hence, no definite conclusions can be drawn about whether advection on a fortnightly time scale influences the region upstream of the commercial mussel lays.

5.3 Summary

Observations of Chlorophyll on medium time scales can be summarized as:

- Downstream from the mussel beds a strong spring-neap oscillation in the Chlorophyll concentration may be observed. It is thought this oscillation comes about through the changing strength of the residual advection throughout this period. Hence, at times of weak residual transport, mussels are capable of accessing a better proportion of the imported Chlorophyll food source than during spring tides. Resuspension of material as the origin for this increase in Chlorophyll has not been considered within this project, although it should be considered for future investigations.

- Upstream of the mussel beds, the observations do not allow us to make any firm conclusions due to the record length being too short.
- Chapter 8 compares these field measurements with simulations of the PHYBIO model.

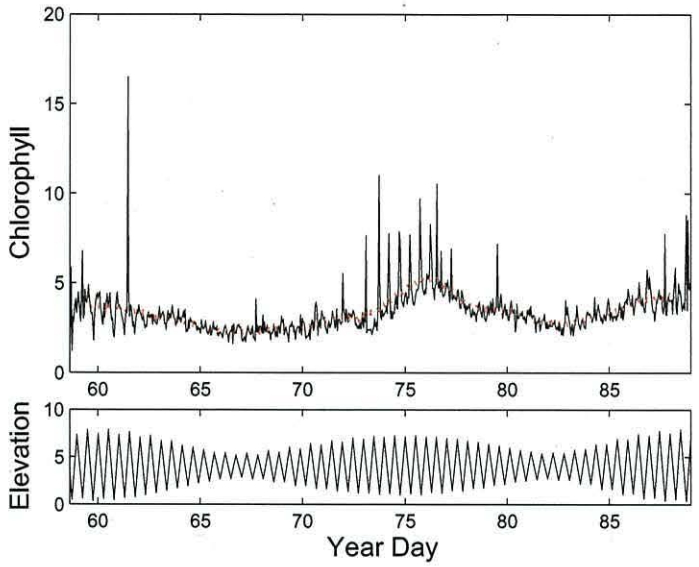

Figure 5.1: Chlorophyll concentration measured in March 2006 at Ynys Faelog using the YSI monitoring system. Top: hourly-averaged Chlorophyll concentration (black solid) and 48-h moving averaged Chlorophyll concentration (red dotted), both expressed in $\mu g\ l^{-1}$; Bottom: Tidal elevation (m) at Menai Bridge.

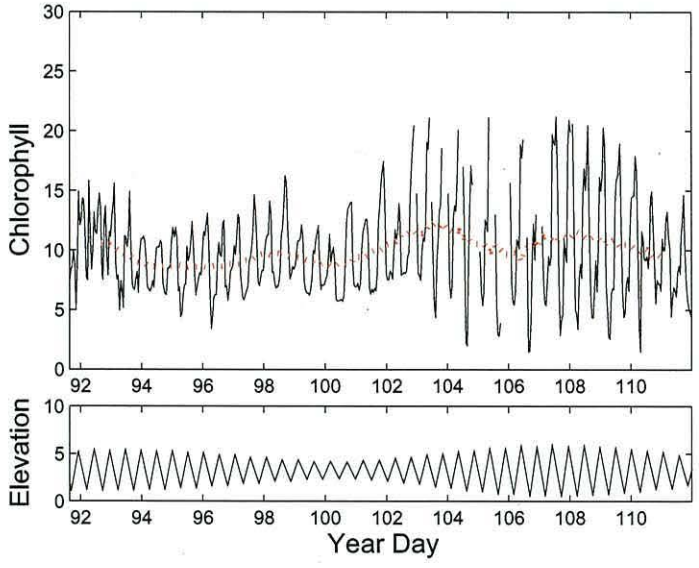

Figure 5.2: Chlorophyll concentration measured in April 2007 at Conway Centre Dock using a SCUFA fluorometer. Top: hourly-averaged Chlorophyll concentration (black solid) and 48-h moving averaged Chlorophyll concentration (red dotted), both expressed in $\mu g\ l^{-1}$; Bottom: Tidal elevation (m) at Port Dinorwic.

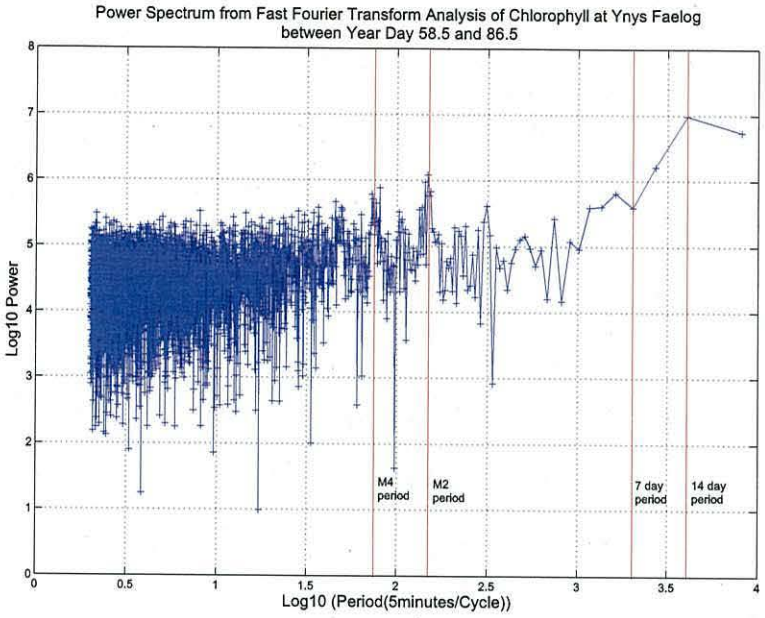

Figure 5.3: Power Spectrum from FFT analysis of Chlorophyll concentration recorded in March 2006 by the YSI-6600 at Ynys Faelog.

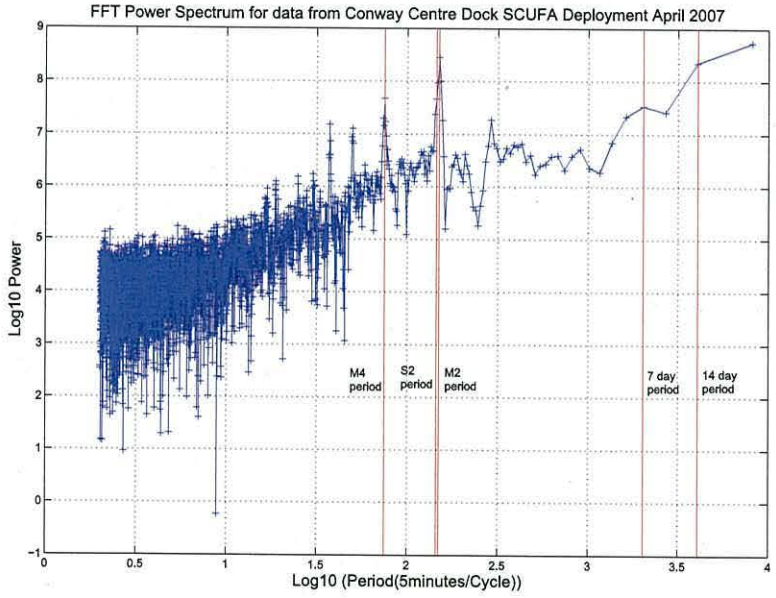

Figure 5.4: Power Spectrum from FFT analysis of Chlorophyll concentration recorded in April 2007 by SCUFA at Conway Centre Dock.

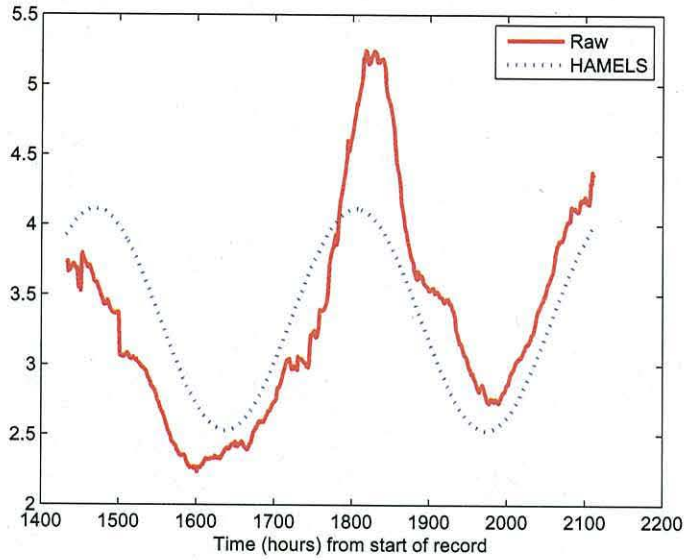

Figure 5.5: 48-h running averaged data and HAMELS fit for an oscillation with a period of 14 days for observations from a YSI-6600 deployed at Ynys Faelog in March 2006.

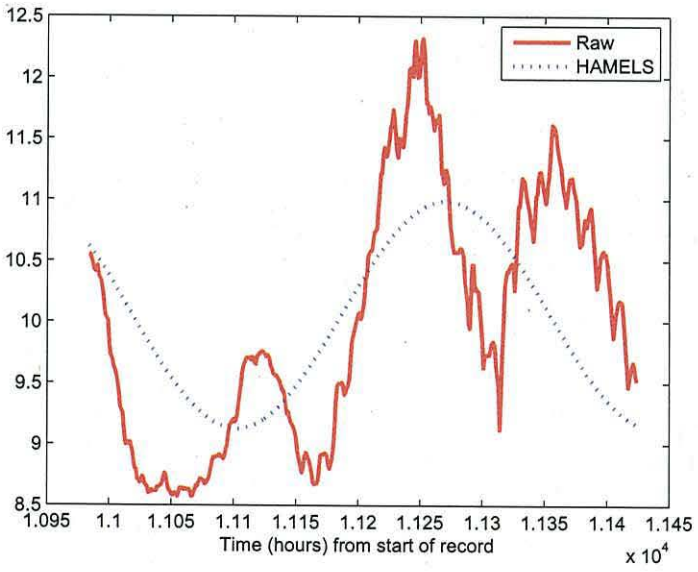

Figure 5.6: 48-h running averaged data and HAMELS fit for an oscillation with a period of 14 days for observations from a SCUFA deployed at Conway Centre Dock in April 2007.

Chapter 6

Seasonal Patterns of Chlorophyll

The seasonal cycle of Chlorophyll in the Menai Strait has previously been measured and discussed by several researchers (Jones, 1968; Strange, 1970; Harker, 1997; Beadman, 2003). This chapter brings together measurements made during 2005 and 2006 in the Menai Strait and compares them to these previous measurements. This chapter aims to highlight the consistency in the observed pattern of Chlorophyll in the Menai Strait between different years, as well as between the different measurement techniques employed.

6.1 Introduction and Methodology

The levels of phytoplankton in the Menai Strait in late autumn, winter and early spring are low due to the unfavorable conditions for phytoplankton growth. Chlorophyll concentrations are approximately 2 $\mu g\, l^{-1}$ during these periods (Al-Hasan, 1976). Depending on water temperature and light levels, the conditions for growth become optimal between March and May (Gowen et al., 2008), and result in a phytoplankton bloom, leading to a noticeable increase in Chlorophyll concentrations. This spring bloom consists of a succession of populations: in late March or April a mixed diatom bloom occurs, followed by diatom and *Phaeocystis* in May/June (Blight et al., 1995). The maximum observed concentrations around this time of favorable growth can be as high as 30 $\mu g\, l^{-1}$in Liverpool Bay (Gowen et al., 2008). This optimal growth period comes to an end when the phytoplankton have used much of the available nutrients, and in particular Silica becomes a limiting factor (Newton, 1986). Compared to the winter season, there is still a higher concentration of phytoplankton in summer, although they are not as abundant

as during the spring bloom. In early autumn, there is a renewal of nutrients through the mixing of the thermocline, and a brief smaller second bloom can be observed (Al-Hasan, 1976; Blight et al., 1995).

In the period 2005-2006, Chlorophyll concentrations were measured at 4 locations in the Menai Strait: Penmon Bay and Penmaen Swatch, near the Northern entrance to the Strait; Ynys Faelog, close to Menai Bridge; and the Conway Centre Dock, just beyond Llanfairpwllgwyngyll on the Southern side of the Swellies. The daily-average Chlorophyll concentration at Penmon Bay and Penmaen Swatch was determined by calculating a daily average of the already smoothed data (previously despiked using a StDev-filter, see Section 3.4.1), while the data of the YSI-6600 system at Ynys Faelog and the Conway Centre Dock was daily-averaged using a modal spike filter with a 24-hour window on the raw data (see Section 3.4.1). Data from when the instrument was obviously fouled have been omitted for reasons of clarity.

6.2 Results

Figure 6.1 shows the mean daily concentration of Chlorophyll in the Menai Strait at the four long-term monitoring sites chosen for this project for 2005 and 2006. It can be seen that around Year Day (YD) 110 the Chlorophyll concentration starts to increase rapidly as the on-set of the spring phytoplankton bloom occurs (Figure 6.1). The data series from Penmon Bay and Penmaen Swatch show hardly any fouling, in part thanks to the regular servicing and cleaning of the instrumentation. This was done less often for the YSI-6600 series as the self-wiping system was thought to make cleaning nearly obsolete. This, however, proved a wrong assumption, and in particular fouling on the probe guard is thought to play a strong interfering role in the measurements. In order not to confound the seasonal pattern in Chlorophyll observed in the channel, these have been omitted from the final plots.

It can be seen that the seasonal pattern in Chlorophyll distribution does indeed comply with the expected pattern previously measured in coastal shelf seas (Gowen et al., 2008). Moreover, the instrumentation does show good agreement between different years, although the onset of the spring bloom was missed in the 2005 measurements and therefore, no comment can be made on changes in its timing between the two different years.

6.3 Comparison with Previous Research

Figure 6.2 shows the seasonal cycle previously measured by Jones (1968), Strange (1970), Al-Hasan (1976), Harker (1997), Beadman (2003) and Bravo[1]. Comparison of Figures 6.1 and 6.2 shows that the pattern of the seasonal cycle of Chlorophyll is consistent between the different years. The main difference between the different years lies in the onset of the phytoplankton bloom. This is partly determined by the ambient conditions of light and water temperature. Even though the seasonal cycle of sunlight is relatively constant between years, it is the changes in meteorological conditions which are responsible for the different start times of the spring phytoplankton bloom. For example, a harsher winter or spring can shift the bloom further towards summer, while a relatively mild winter or spring may mean the phytoplankton bloom falls early in the season. Generally, it is thought the spring bloom in the Menai Strait can start anytime between late March and early May, depending on conditions.

Moreover, differences in the actual measured concentrations of Chlorophyll between the different years is most likely due to each researcher using a different technique. Jones (1968), Strange (1970) and Al-Hasan (1976) used phytoplankton cell counts to determine the phytoplankton concentration. These were converted to concentrations in $\mu g\ l^{-1}$, using the relationship found by Newton (1986) during measurements in the Menai Strait. Beadman (2003) used a tidally averaging basin and the filtration of water samples to determine the Chlorophyll concentration. Finally, Bravo used the filtration of discrete water samples and analysis using HPLC (High-Performance Liquid Chromatography), an accurate method to measure Chlorophyll-a concentrations as it separates the different chemical compounds contained in the sample through their partitioning behavior. Finally, the data collected in 2005 and 2006 come from the use of fluorometers which take measurements at intervals of a few minutes, allowing for great time resolution, but due to the possible sources of interference in these measurements, their use more than likely introduces some error in the observed Chlorophyll concentrations. Of all the above methods, those of Bravo and Beadman (2003) are likely to give the most accurate measures of Chlorophyll-a concentration.

[1] pers. comm.; data collected as part of a different PhD. research project in chemical oceanography, and kindly contributed for comparison with measurements made for this research.

6.4 Summary

In summary, it can be said that on a seasonal cycle:

- Measurements made in the period 2005-2006 show a good agreement between different years at the same site, as well as between the different sites.
- The general pattern observed in the period 2005-2006 agrees well with that observed by previous researchers in the Strait.
- The Menai Strait Chlorophyll distribution on a seasonal time scale follows closely that of temperate shelf seas, where there is a strong phytoplankton bloom in spring, an elevated Chlorophyll concentration in summer, and a small secondary bloom in autumn, with a low concentration in winter months, when conditions for growth are least favorable.

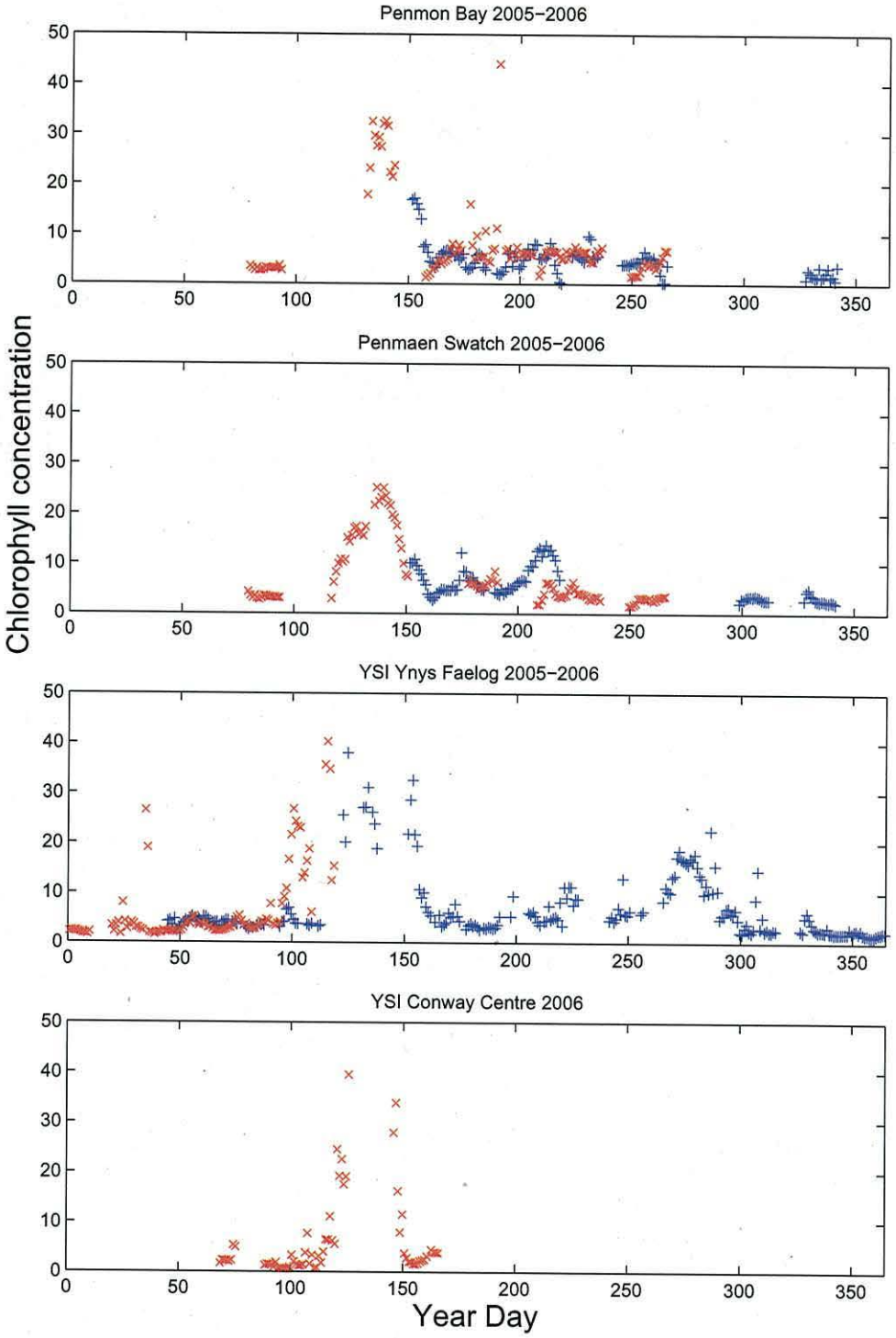

Figure 6.1: Daily-average Chlorophyll concentration (μg l^{-1}) in the Menai Strait at (a) Penmon Bay, (b) Penmaen Swatch, (c) Ynys Faelog and (d) Conway Centre Dock; in 2005 (blue +) and 2006 (red ×).

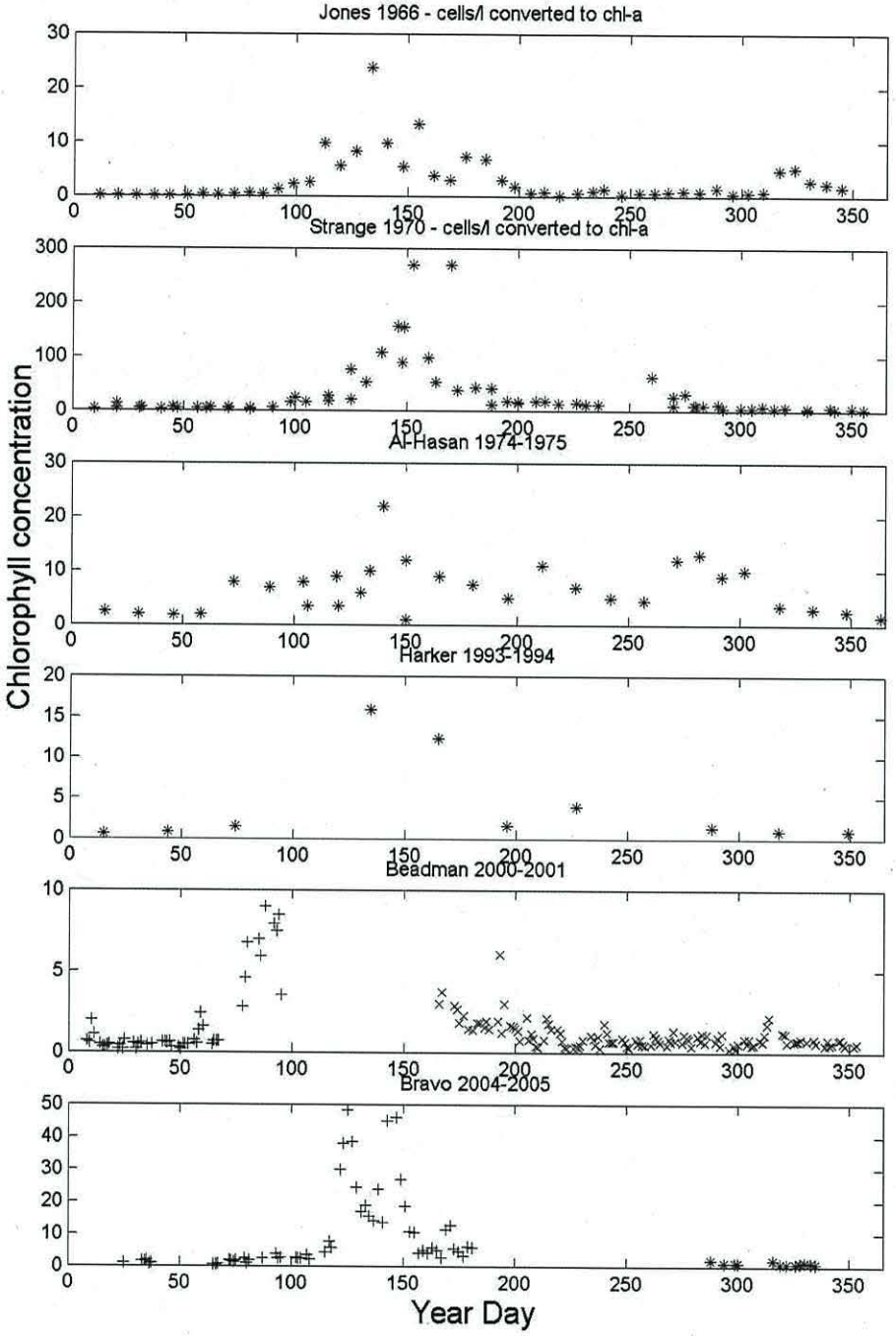

Figure 6.2: Daily-average Chlorophyll concentration (μg l^{-1}) in the Menai Strait from previous researchers Jones (1968); Strange (1970); Al-Hasan (1976); Harker (1997); Beadman (2003) and Bravo (pers. comm.).

Chapter 7

PHYBIO: Model Description and Results

This chapter introduces the numerical bio-physical model developed for research conducted on the mussel beds in the Menai Strait. The model aims to elucidate how the main physical and biological processes interact in the ecosystem, driving the observed changes in Chlorophyll distribution. The model will be described below, and some initial modelling results will be presented. Comparisons in future chapters between model results and field measurements will assume the basic model set-up and driving forces, although specific parameters will be reported where appropriate. A copy of the model code may be found in Appendix D.

Developed in MATLAB ® , PHYBIO includes physical processes such as advection and biological processes such as mussel feeding and phytoplankton production. Figure 7.1 shows the main processes thought to drive the Menai Strait ecosystem. The model simulates the changes in Chlorophyll concentration brought about through the interaction of these processes. This model is a compound hypothesis model, which includes the important physical and biological processes affecting the Chlorophyll concentration in the Menai Strait. It is thought that the inclusion of the correct theories will predict distributions which match reality, while a misrepresentation or lack of the key processes will lead to incorrect predictions.

The model is driven by the prescribed tidal elevations at the two open boundaries and the equations are solved using the finite difference method (starting from rest). An upwind differencing scheme is used to avoid computational errors in estimating the Chlorophyll concentration gra-

dient. This method uses the concentration at the upstream boundary of the grid cell to calculate the flux of Chlorophyll in each cell; in other words it introduces a bias towards the upstream direction. This type of scheme is unconditionally stable, although a disadvantage is that it may introduce numerical diffusion, which was not the case for PHYBIO (J.H. Simpson and A.J. Elliot, pers.comm.).

A further extension to the model has been made to explore the dynamics of vertical depletion of Chlorophyll above the mussel beds. In this add-on, the model has been extended to be 2-D in the vertical (2-DV) over the mussel beds in order to simulate the interaction of mussel feeding and vertical diffusion and mixing, an important process in supplying the near-bed layer with Chlorophyll.

7.1 Model Domain

A 1-D horizontal section of the Menai Strait (Figure 7.2) is simulated in the model using 30 bins which are each 1 kilometre in length. The cross-sectional area of each grid cell is computed using a trapezoidal section of variable width and depth (Figure 7.2 d). Using this changeable description of the cross-sectional area allows for the simulation to have a more realistic resemblance to the Menai Strait; including a shallow narrow section at the centre of the channel, the Swellies (Figure 7.2 a & b), and a slightly wider Northern boundary (corresponding to Lavan Sands) compared to the Southern one (Fort Belan) (Figure 7.2 a & b). Equation 7.1 and 7.2 prescribe how the cross-sectional area A and the width b are varied with the tidal elevation η.

$$A = b_0(H_0 + \eta) + \overline{cot\theta}(H_3 + \eta)^2 \tag{7.1}$$

$$b = b_0 + 2(H_3 + \eta)\overline{cot\theta} \tag{7.2}$$

where A is the area of the cross-section, and b is the width, b_0 is the channel width at Low Water Springs (LWS), H_0 is the depth at Mean Sea Level (MSL), H_3 is the difference between MSL and LWS and $\overline{cot\theta}$ is the mean of the slope angles at the sides of the channels (see Figure 7.2 d).

7.2 Physical model

7.2.1 Description

The main physical process included in the model is advection, although in the vertically extended version, vertical diffusion is also included. Equation 7.3 is the continuity of water volume, and equation 7.4 is the momentum equation.

$$b\frac{\partial \eta}{\partial t} = -\frac{\partial}{\partial x}(AU) \tag{7.3}$$

$$\frac{\partial U}{\partial t} = -U\frac{\partial U}{\partial x} - g\frac{\partial \eta}{\partial x} - \frac{kU|U|}{\bar{h}} \tag{7.4}$$

where η is the elevation, A is the cross-sectional area, U is the section mean along-channel velocity, k is the drag coefficient and $\bar{h}$ is the section mean depth ($H_0 + \eta$).

As can be seen in Equation 7.4, a quadratic drag law is used to specify the frictional resistance to the flow. The drag coefficient, k, which is used to specify this resistance has been chosen as 0.0025, which has been found to be consistent with ADCP measurements of shear stress in the Menai Strait (Rippeth et al., 2002).

7.2.2 Model results

In order to make the model a realistic simulation of the Menai Strait, the prescribed tidal elevations at the open boundaries are taken to be those of the Admiralty Tide Tables (Sherwin, 2000). As discussed in Simpson et al. (2007), the model results show general agreement with observations of the currents, elevation and transport in the Strait (Figure 7 in Simpson et al., 2007). Forcing the physical model with a spring tide (M2 + S2), shows a strongly oscillating current with maxima in the Swellies and near the SW entrance to the Strait (Fort Belan).

Within the northern section of the Menai Strait, there is a rapid phase change in tidal flow (>100°) associated with the fact that the channel is open-ended on both sides. Due to differences in the tidal amplitude at the northern and southern boundary, there is a current component in phase with the elevation, on top of the standing wave components at the opposite ends of the

channel which are out of phase by 180° with each other. The combination of these two components results in a combined tidal current which changes phase along the channel. This is the reason why the tides within the Strait deviate from the simple rule of a standing wave by which velocity and elevation differ in phase by 90°.

The physical component of PHYBIO manages to simulate the observed changes in phase accurately (Figure 7 in Simpson et al., 2007). At a distance of approximately 9 km from the Northern boundary, the model also correctly predicts the observed minimum in tidal transport (Figure 8 in Simpson et al., 2007). Moreover, the model is able to simulate correctly the residual transport (Simpson et al., 2007), which is brought about by rectification of the tide, as well as its variation as the range increases over the Spring-Neaps cycle (Figure 9 in Simpson et al., 2007). This relationship between the tidal range and the volume transport in the Menai Strait is that previously established by Simpson et al. (1971) (see Section 2.2).

7.3 Biological model

7.3.1 Description

When adding the biological component to the model, it was thought best to build up complexity as the modelling effort progressed in order not to confound which physical and biological processes are driving observed changes. To this end, several underlying assumptions have been made which need justification.

The model was initially developed as a 1-D simulation, and therefore, an initial assumption is that the vigorous tidal flows experienced in the Menai Strait sustain a fully mixed, homogenous water column for most of the tidal cycle; thus making it justified to use a vertically integrated form of the advection-diffusion equation for Chlorophyll concentration C (Equation 7.5).

$$\frac{\partial \overline{C}}{\partial t} = -U\frac{\partial \overline{C}}{\partial x} - \alpha\frac{\overline{C}}{h} + P - G \tag{7.5}$$

where $\overline{C}$ is the vertically-averaged Chlorophyll concentration, U is the section-mean velocity, h is the water depth, α is the mussel filtration parameter, P=$\lambda\overline{C}$ and G=-$\mu\overline{C}$ are the specified local rates of production (P) and grazing (G) of phytoplankton in the water column.

During model development, the filtration parameter α has been set to 0.0002 m s^{-1} over the mussel beds and kept 0 elsewhere. Even though it is a tough assumption to justify that only the commercial mussel beds eat out phytoplankton from the water column, in the relative scheme of things, they are thought to be the most important consumers of Chlorophyll in the system. Therefore it is assumed other grazers which are of minor importance, will be represented through the grazing parameter G. Furthermore, it is also assumed that the local production of phytoplankton is only a minor contribution compared to the advection of plankton from Liverpool Bay. This assumption is partly justifiable through the fact that the residence time of the passively floating phytoplankton is around 3 days in the Menai Strait, a period which is thought to be too short for significant phytoplankton production. Within the biological component of PHYBIO, the grazing and production are represented by a single parameter ($\gamma = \lambda - \mu$) based on average values of measurements of plankton metabolism by Blight et al. (1995). This net production-grazing rate γ is set to $\sim$0.2 day^{-1}.

The Chlorophyll distribution in PHYBIO is modelled using a time step of Δt=30 s forward in time and starting from a uniform initial concentration C_0, generally 2 μg l^{-1}, and using the boundary conditions of $\overline{C}$=C_0 at northern end (upstream) and $\frac{\partial \overline{C}}{\partial x}$=0 at the SW boundary (downstream). This latter assumption may be considered controversial as in reality there is input from Caernarfon Bay into the SW section of the Strait. However, seeing that this research is focused on the commercial mussel beds located in the NE sector of the Menai Strait, this is considered of minor importance.

The mussel parameter α can be considered a feeding velocity with which the mussels remove Chlorophyll from the water column. This parameter is the only tunable parameter available in the model, and through matching the modelled oscillations in Chlorophyll with the observed amplitude changes, the value has been finalised to equal 0.000301 m s^{-1} in the model. This value is, however, not completely inconsistent with reality: taking typical values of mussel density (750 mussels m^{-2}) in the Menai Strait, and mussel filtration rate (2 l h^{-2}) gives an estimate of $\alpha \sim$ 0.0004 m s^{-1}. Values of mussel filtration rate from the literature, shown in Table 7.1, are in general agreement with the final parameter value of α. As highlighted by Riisgård (2001), the measurement of filtration by *Mytilus edulis* in the laboratory is not without problem, which explains the disagreement between the measurements. The range in α from the literature lies between $\sim$ 0.0004 m s^{-1} and $\sim$ 0.0013 m s^{-1}

Reference	Filtration parameter (units)		Notes
Dare (1980)	1.9 - 2.7	lh^{-1}	75 mm adult
Grant et al. (2007)	2.4	lh^{-1}	
Riisgård (2001)	6.1	lh^{-1}	54 mm adult
Smaal and Vonck (1997)	2.2	lh^{-1}	50 mm adult, annual mean

Table 7.1: Filtration rate values from the literature.

The sensitivity of the model to the choice of α was also investigated. Figure 7.3 shows the root mean square difference (RMSD) compared to a choice of $\alpha = 3.01 \times 10^{-4}$ m s^{-1}. As can be seen, in the range 0.0002 to 0.0004 the RMSD is within a 10% change from the input concentration $C_0 = 2$ μg l^{-1}. Moreover, over the range of values found in the literature, the difference in results is within a factor of 2. A second method to visualise the model response is to use the sensitivity parameter S, defined by Haefner (2005) (Equation 7.6).

$$S = \frac{\frac{R_a - R_n}{R_n}}{\frac{P_a - P_n}{P_n}} \tag{7.6}$$

where R is the response variable in the model (in this case, Chlorophyll concentration), and P is the parameter (α); subscript a denotes the parameter model and n denotes the nominal parameter ($\alpha = 3.01 \times 10^{-4}$ m s^{-1}) (Haefner, 2005).

When calculating the value of S for different parameter values of α (Figure 7.4), it can be seen that the value of S is generally negative. This indicates that the model response is in the opposite direction to the parameter change. This is to be expected as increasing the filtration parameter α reduces the Chlorophyll concentration. If the value of S would be equal to -1, then the normalised change in model response is equal to the change in parameter. Within the range of α equal to 0.0002–0.0005 m s^{-1}, the sensitivity parameter changes by 10% in either direction (from the -0.4 value at the nominal value of α). This sensitivity analysis concludes that a factor of 2 change in the nominal parameter value shows acceptable differences in the results. Moreover, throughout the range in the filtration parameter found in the literature, the model sensitivity is minimal.

In a further extension to the model, the vertical structure above the mussel beds has been resolved (PHYBIO-2DV) in order to look at vertical depletion of Chlorophyll with minimal sac-

rifice to computational complexity. Due to the Menai Strait being such a dynamic regime, it is acceptable to assume vertical homogeneity of the water column for the majority of the tidal cycle. However, it was hypothesised that during periods of reduced flow mussel feeding may still exert a strong enough effect on the water immediately overlying the beds to bring about a vertical depletion of Chlorophyll. In order to include vertical diffusion in PHYBIO, a 1-D vertical advection-diffusion model (Equation 7.7) was embedded over grid cells containing mussels. This submodel is driven by the horizontal gradient in Chlorophyll which is taken from the 1-D horizontal model. The grid-spacing in the vertical is adjusted according to the local instantaneous water depth $\left(\Delta z = \frac{\bar{h}}{10}\right)$.

$$\frac{\partial C}{\partial t} = -U\frac{\partial C}{\partial x} + \frac{\partial}{\partial z}\left(K_z\frac{\partial C}{\partial z}\right) + P - G \tag{7.7}$$

where $\frac{\partial C}{\partial x}$, the horizontal gradient of Chlorophyll is derived from the vertically integrated advection-filtration model, and K_z is the vertical diffusivity (using Equation 7.8).

$$K_z = \kappa u_* z(1 - \frac{z}{h}) \tag{7.8}$$

where u_*=(τ/ρ) is the friction velocity (τ is the bed stress, ρ is the density), and h is the water column depth.

The above relationship is a fit derived from ADCP measurements in the Menai Strait of the eddy viscosity (Rippeth et al., 2002), and assumes that the diffusivity of scalars and momentum are equal (the Reynolds analogy).

The boundary conditions for the vertical submodel are that there is no flux at the surface, and that the flux at the bed is matched by the mussel filtration (see Equations 7.9).

$$\begin{aligned} -K\frac{\partial C}{\partial z} &= 0; & z &= h \\ -K_z\frac{\partial C}{\partial z} &= -\alpha C_b; & z &= 0 \end{aligned} \tag{7.9}$$

where α is the filtration rate and C_b is the Chlorophyll concentration in the lowest bin over the mussel bed; 0 is the bed level and h is the surface.

7.3.2 Model Results: PHYBIO-1D

Starting from a uniform distribution of Chlorophyll, a steep gradient develops rapidly, with the PHYBIO model taking only 4 tidal cycles to reach a regular cycle. This period is coincidently the residence time of the advected water particles in the residual current. The steep gradient is established by the mussel filtration from the commercial beds (located between 8 and 12km in the model domain) and it can be seen that tidal advection oscillates this gradient back and forth (Figure 7.5). This produces large oscillations of Chlorophyll in the vicinity of the mussel beds. A better method of looking at the model output can be to either look at a point in space over time, similar to an anchor station or monitoring site during the field study; or at a point in time over space, considered a longitudinal section of the Menai Strait.

Figure 7.6 shows a look at an anchor station at four different locations in the domain: the upstream boundary of the domain, the centre of the mussel beds, slightly downstream of the beds, and the downstream boundary of the domain. The left and right panels of Figure 7.6 show these for a spring (M2+S2) and neap (M2-S2) tide. Looking at the two panels in Figure 7.6, there are a few points to notice: firstly, the concentration at the downstream stations is lower than that at the upstream boundary, due to the mussels feeding on the Chlorophyll. Next, it is also noticeable that the concentrations in bins 10, 16 and 29 are lower during neap tides than during spring tides. The main reason for this being that the mussels have longer to feed on a particular parcel of water at neap tides due to the weaker tidal advection. Thirdly, it can also be seen that the amplitude of the Chlorophyll oscillation is highest over the mussel beds and becomes smaller as you move away from the mussel bed. Finally, it should also be noted that in the Chlorophyll signal over the mussel beds, the M4-component which leads to the apparent phenomenon of a double peak, is most significant during spring tides, once again an effect of the relative strength of the tidal advection. During spring tides, at the onset of ebb, Chlorophyll-rich water enters the Strait through the Northern boundary and is swiftly advected past the mussel beds, not giving the mussels much opportunity to filter out the Chlorophyll; as the tide slows down, they get better access to the water column and are able to filter out more food. However, this leads to a higher concentration of Chlorophyll to be just beyond the cultivated beds, which then on the flood is advected back over the mussels, creating the double-peak observed in the Chlorophyll signal.

As suggested above, an alternative look at model output may also be provided by looking at

longitudinal sections of the Chlorophyll concentration in the model domain. Figure 7.7 shows 4 such sections at different stages of the tide, and once again for spring and neap tides. The advection of the gradient established by the mussel feeding can be seen: as the tide floods, the steepest gradient is pushed North towards the boundary. Comparing the longitudinal sections at spring and neap tides shows that the concentration near the Southern boundary is lower at neap tides due to the mussel feeding in relative terms being stronger than the tidal advection during neap tides. This relationship is also responsible for making the Chlorophyll gradient in the domain steeper during neap tides (see Section 7.3.4).

This strong M4-component in the Chlorophyll signal is not only related to the relative strength of the mussel feeding and tidal advection, it is also a result of the mussels being organised in a commercial bed limited to part of the Northern section of the model domain. It may be expected that this M4-signal is not so obvious, if the mussels were organised in a uniform bed spanning the total length of the Menai Strait. For this simulation, the tidal amplitude at Puffin was set to 3.35 m and the initial concentration C_0 to 2 μg l^{-1}. In a first model run, the bed was 4 km long (bins 8-12) and the mussel filtration α=3.01 $\times$ 10^{-4} m s^{-1}; in a second simulation, the mussel bed was spread over all the grid cells, and the filtration parameter was matched so that the volume filtered per second over the integrated domain was equal between both runs (α=4.013 $\times$ 10^{-5} m s^{-1}). As can be seen in Figure 7.8, at the location in the centre of the mussel bed (10 km from the upstream boundary) the M4 component of the Chlorophyll distribution with a uniform spread of the mussels is much reduced. In order to compare these differences quantitatively, HAMELS was used to analyse the variability explained by the M4 component of the model only. As can be seen in Table 7.2, the M4 component explains significantly less variability ($\sim$ 3%) when the mussels are uniformly distributed throughout the model domain, compared to the restricted distribution ($\sim$ 39%) which is a more realistic representation of the mussel beds in the Menai Strait. Moreover, the amplitude of the M4 oscillation is also significantly greater when the mussels occur in a restricted area of the Menai Strait (Table 7.2). These results strongly suggest that one reason for the strong M4 oscillation in the Strait is due to the restricted nature of mussel beds in the channel.

Mussel bed Distribution	α (m s^{-1})	R^2	Amplitude M4 (μg l^{-1})
Restricted (8-12 km)	3.01×10^{-4}	0.386	0.23
Uniform (0-30 km)	4.013×10^{-5}	0.033	0.04

Table 7.2: HAMELS fitted amplitudes for the M4 constituents on modelled Chlorophyll distribution for a uniformly distributed and a restricted mussel bed. $A_{Puf}(\eta) = 3.35$ m, and C_0=2μg l^{-1}.

7.3.3 Model Results: PHYBIO-2DV

The advection-filtration model was extended to include a 2-dimensional vertical (2-DV) structure above the mussel beds, allowing for the investigation of the vertical water column structure at different stages of the tide. Figure 7.9 shows the vertical profile of Chlorophyll over the mussel beds at spring and neap tides. It can be seen in Figure 7.9 a & b, that at slack water, there is a thin layer immediately overlying the mussels where the concentration of Chlorophyll approaches 0 μg l^{-1}. The mussels are only capable to eat out most of the Chlorophyll from the immediately overlying water during the short-lived period of slack water in the tidal cycle. For the remainder of the tidal cycle, the vertical mixing is sufficient to replenish the bottom boundary layer with fresh Chlorophyll.

Comparison of the Chlorophyll distribution during the two different stages of the fortnightly cycle (Figure 7.9) shows that the duration of this local depletion in Chlorophyll is slightly more extended during neap tides, when slack water lasts longer. It can also be seen that during neap tides the vertical depletion of Chlorophyll extends higher into the water column (Figure 7.9). Nevertheless, due to the limited duration of slack water and its associated vertical depletion in Chlorophyll, it is reasonable to assume that even though there may be a lack of food for the mussels at certain stages of the tide in the Strait, the dynamical regime ensures that the effects on mussel health and growth are limited.

7.3.4 Model Results: PHYBIO-1D over fortnightly cycle

In order to simulate changes in the Chlorophyll concentration associated with the spring-neap cycle (medium time scale), the PHYBIO model was forced with the predicted elevation range

at Beaumaris from the Admiralty tide tables. The simulation period chosen was January 1st to January 28th 2006, in order for extracted phases to be directly comparable to those extracted from field measurements in Chapter 5. The model results have been analysed for 4 different locations: the most upstream location (bin 1), the centre of the mussel bed (bin 10), and two locations downstream of the mussel bed (bins 14 & 16) which correspond approximately to the sampling locations of Ynys Faelog and Conway Centre Dock. Results of the simulation over a period of 14 days are presented in Figure 7.10 for the 4 selected locations. Similar to the analysis in Chapter 5, a 48-hour running average was applied to the modelled Chlorophyll concentrations, and HAMELS was subsequently used to extract the 14-day oscillation from the model results. As can be seen from Table 7.3, the amplitude of the spring-neap oscillation is larger for sites further downstream of the mussels (Table 7.3). Although at all sites, there is some oscillation present with a spring-neap periodicity (Table 7.3). These findings support the hypothesis that as the strength of tidal advection fluctuates with the spring-neap cycle, it influences the Chlorophyll distribution in the Menai Strait. In relative terms, at neap tides, the mussels have better access to their food source, and are therefore able to deplete the Chlorophyll concentration in the downstream direction more than at spring tides.

Bin	A_0 (μg l^{-1})	A (μg l^{-1})	ϕ (°)	R^2
1	2.04	0.02	-143	0.86
10	0.99	0.23	29	0.96
14	0.98	0.31	28	0.96
16	0.96	0.33	28	0.96

Table 7.3: HAMELS analysis with a 14 day period of 48h running mean Chlorophyll concentration, simulated with the 1-D PHYBIO model. DF = 1501 for all bins.

7.4 Summary

In summary, it can be said that:

- The PHYBIO model has proven a useful investigative tool into the expected patterns in Chlorophyll in the Menai Strait through the inclusion of the key physical and biological processes.
- The model does an excellent job at simulating the physical environment with comparison to field measurements of flow showing good agreement.
- Simulations of the Chlorophyll distribution show that this is a complicated balance between tidal advection, diffusion and mussel filtration.
- The model has shown that not only the distribution changes over a semi-diurnal cycle, there are also observable differences which occur as the tide progresses through the spring-neap fortnightly cycle.
- The biological component of PHYBIO will be validated using Chlorophyll measurements from the different field campaigns previously presented (see Chapters 4 and 5). These results will be discussed in Chapter 8.

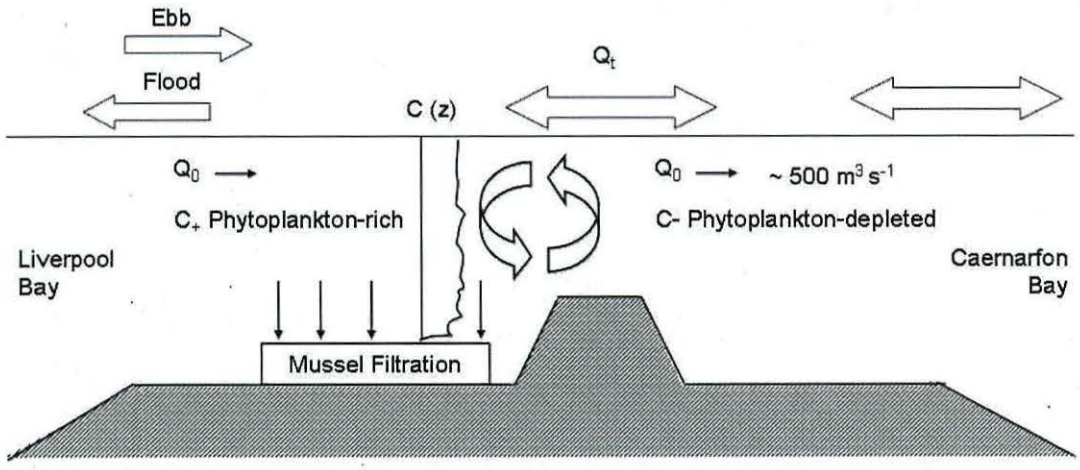

Figure 7.1: Schematic diagram of conceptual model of flow and food supply over commercial mussel beds in the Menai Strait.

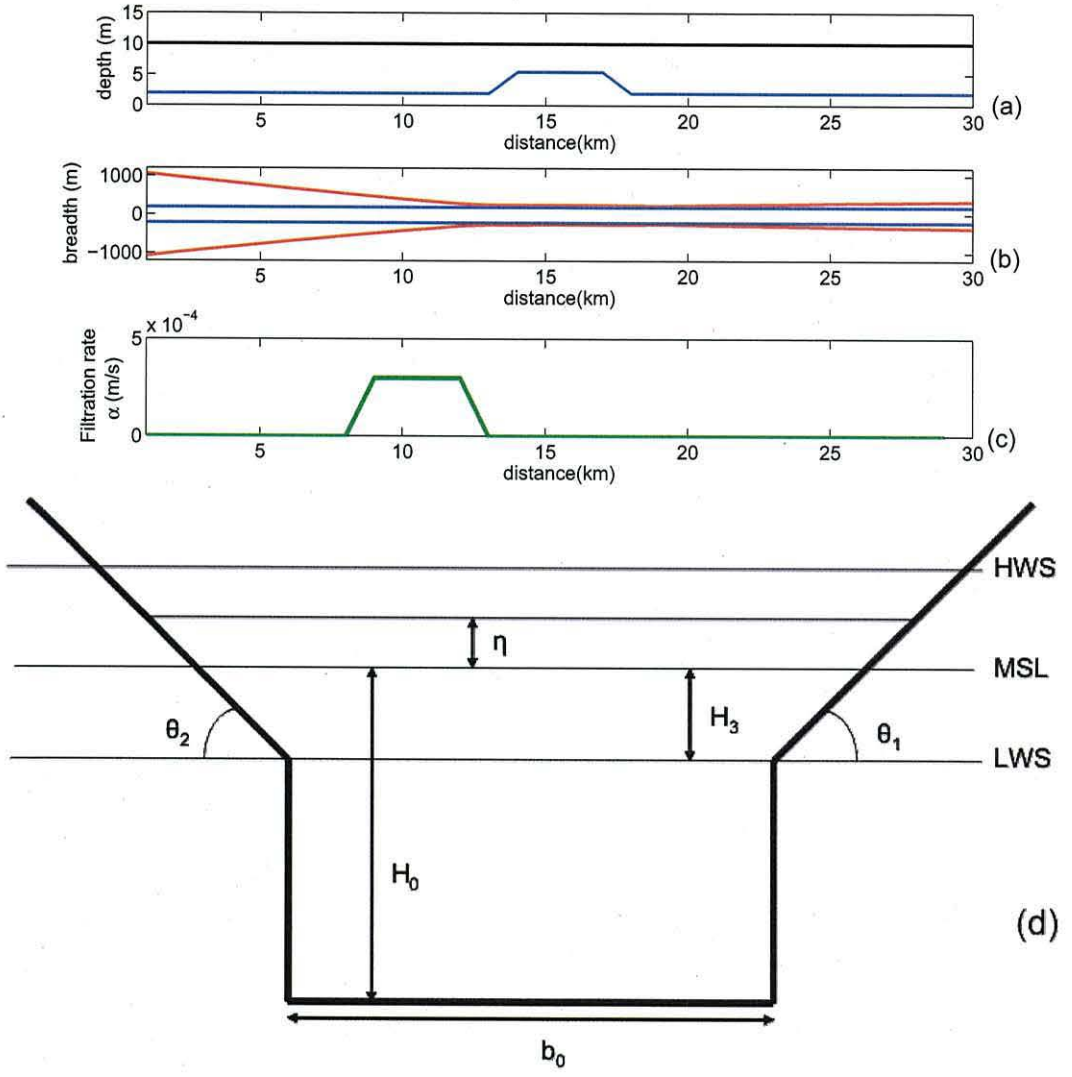

Figure 7.2: Model schematic of (a) the longitudinal section, (b) plan view showing central constriction, (c) mussel filtration function, and (d) prismatic cross-section (see also Equations 7.1 and 7.2); b_0 is the channel width at Low Water Springs (LWS), H_0 is the depth at Mean Sea Level (MSL), H_3 is the difference between MSL and LWS and θ_1 and θ_2 are the slope angles at the sides of the channel. Figure adapted from Simpson et al. (2007).

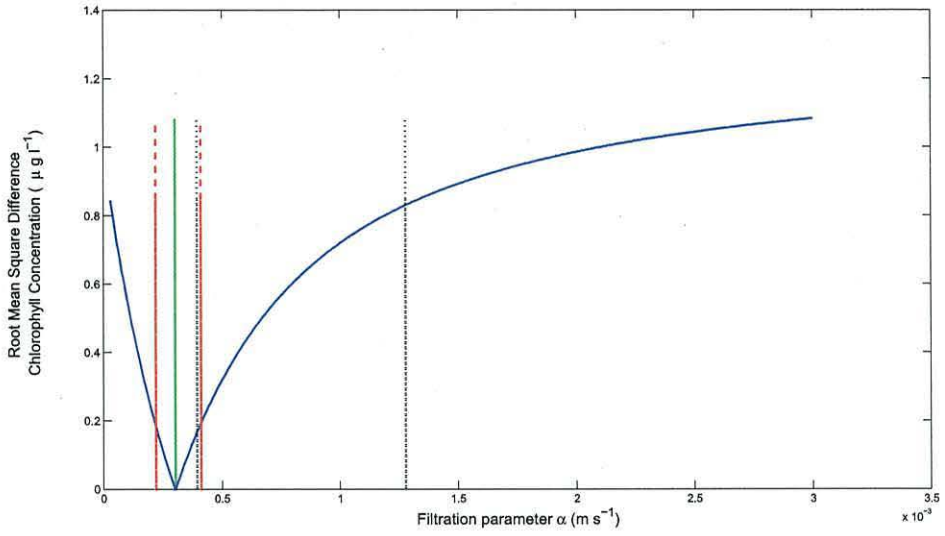

Figure 7.3: Root Mean Square Difference (μg l^{-1}) for different choices of the filtration parameter α (m s^{-1}). Dotted black lines are the minimum and maximum filtration parameter found in the literature (see Table 7.1); dashed red lines denote the interval in which the root mean square difference is within a factor of 2 change from the input concentration (2 μg l^{-1}); the green solid line shows $\alpha = 3.01 \times 10^{-4}$ m s^{-1}.

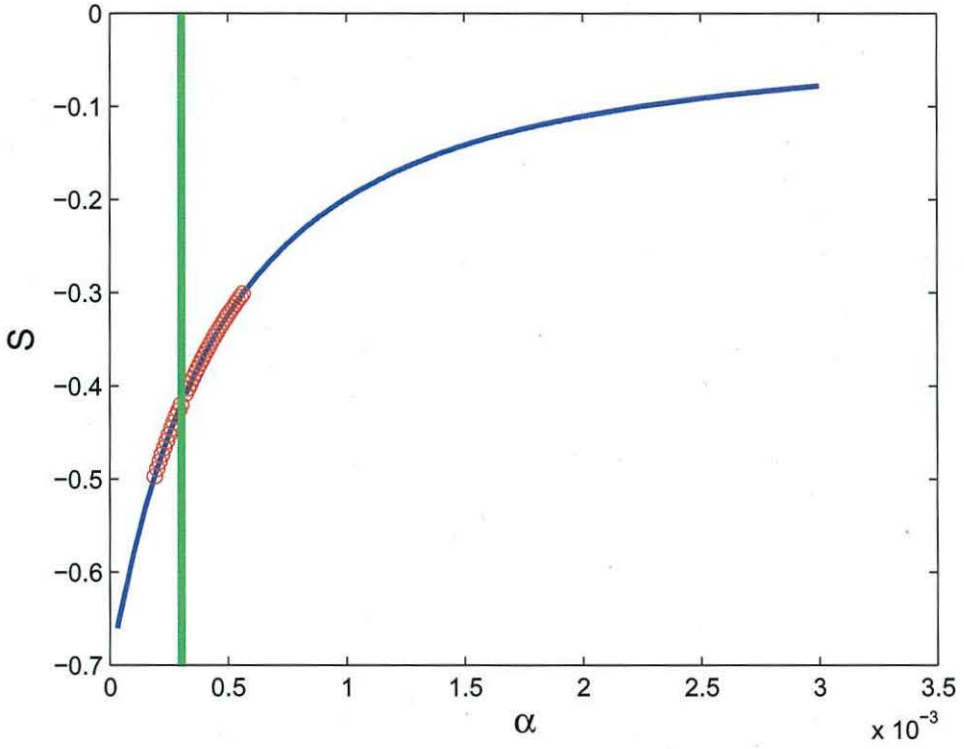

Figure 7.4: Sensitivity Parameter S (Equation 7.6) for different choices of the filtration parameter α (m s^{-1}). The solid green line shows $\alpha = 3.01 \times 10^{-4}$ m s^{-1}. Red circles show values of S within a 10% interval around 0.4.

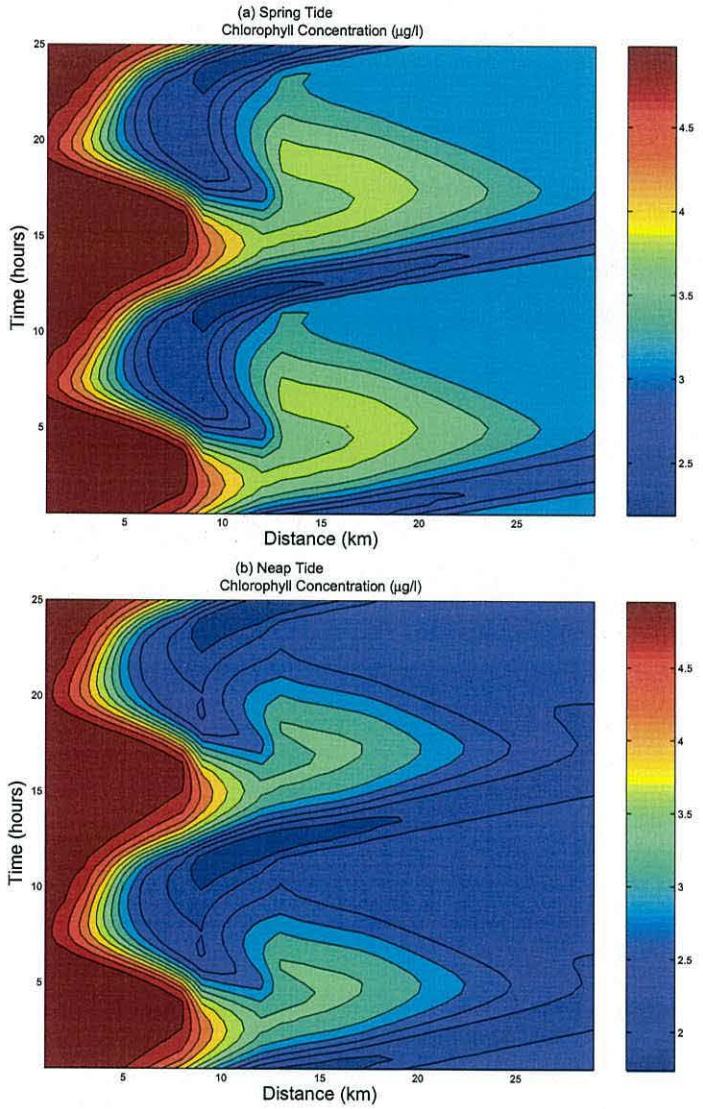

Figure 7.5: Modelled Chlorophyll distribution in the Menai Strait. (a) Spring tide - $A_{Puf}(\eta) = 3.35$ m, and (b) Neap tide - $A_{Puf}(\eta) = 2.6$ m; α=0.000301 m s^{-1}, and C_0=5μg l^{-1}. Figure adapted from Simpson et al. (2007).

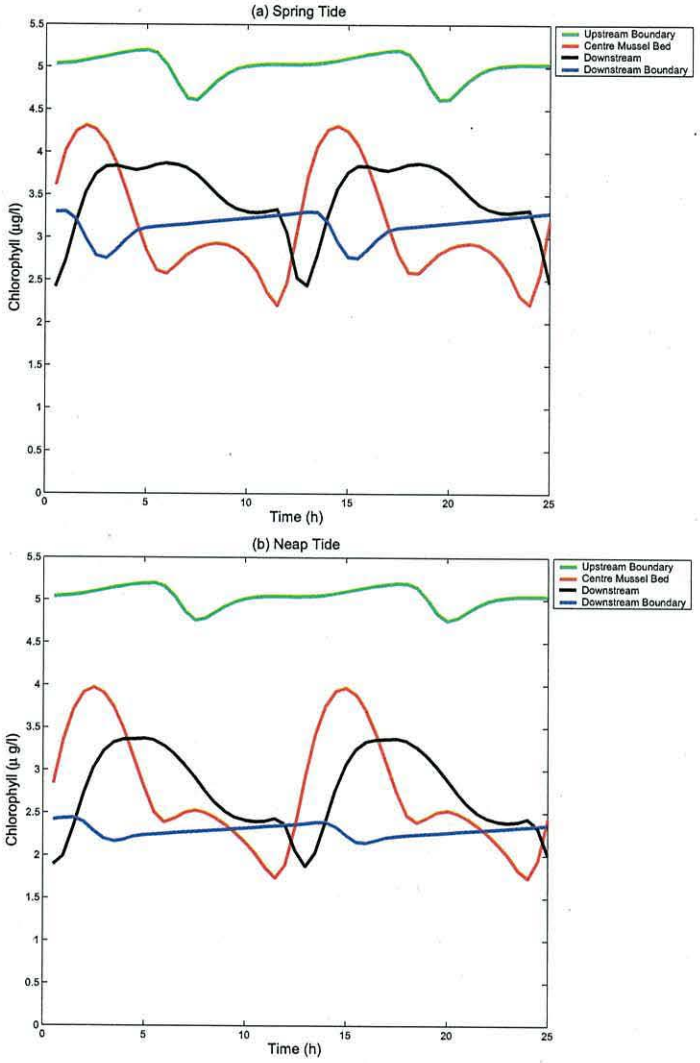

Figure 7.6: Anchor station modelled Chlorophyll in the Menai Strait: at the upstream (bin 2 - green) and downstream (bin 29 - blue) boundaries, at the centre of the mussel beds (bin 10 - red) and slightly downstream of the mussel beds (bin 16 - black). (a) Spring tide - $A_{Puf}(\eta)$ = 3.35 m, and (b) Neap tide - $A_{Puf}(\eta)$ = 2.6 m; α=0.000301 m s^{-1}, and C_0=5μg l^{-1}

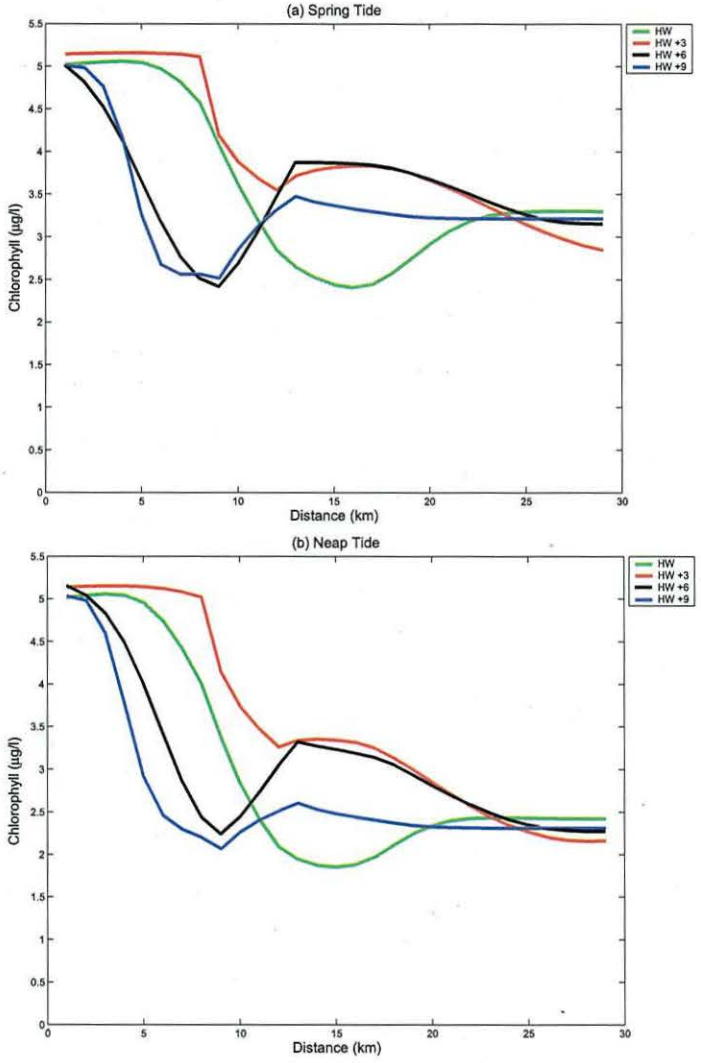

Figure 7.7: Longitudinal section of modelled Chlorophyll in the Menai Strait: at High Water (HW) (green), 3 h past HW (red), 6 h past HW (black) and 9 h past HW (blue). (a) Spring tide - $A_{Puf}(\eta) = 3.35$ m, and (b) Neap tide - $A_{Puf}(\eta) = 2.6$ m; α=0.000301 m s^{-1}, and C_0=5μg l^{-1}

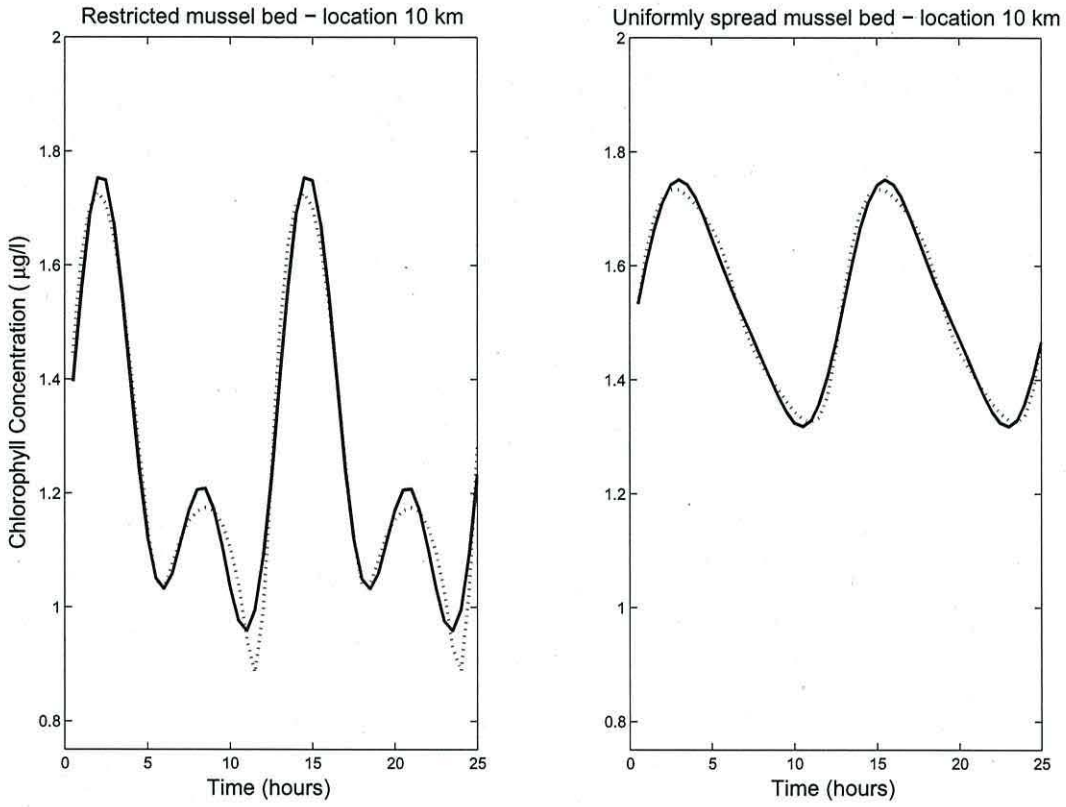

Figure 7.8: Modelled Chlorophyll Concentration ($\mu g\ l^{-1}$) at 10 km from NE boundary, showing modelled (dotted) and HAMELS fitted (solid) data for a restricted (left) mussel bed (8-12km) (α=3.01 $\times$ 10^{-4} m s^{-1}) and a uniformly distributed (right) bed (α=4.013 $\times$ 10^{-5} m s^{-1}). $A_{Puf}(\eta)$ = 3.35 m, and C_0=2μg l^{-1}

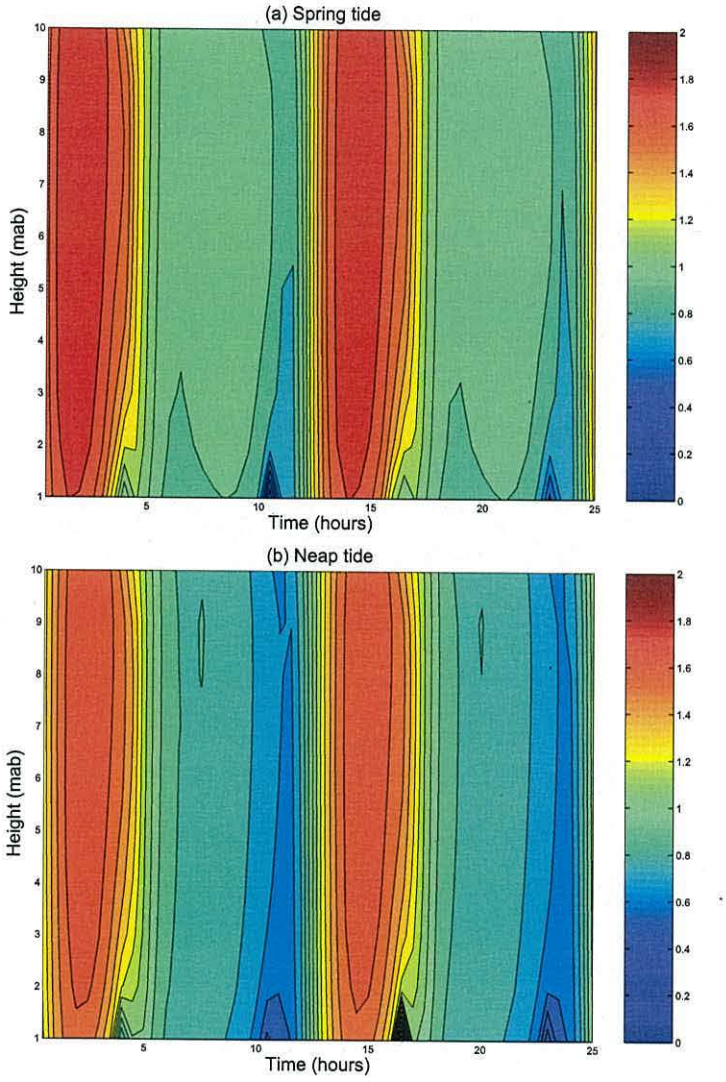

Figure 7.9: Vertical distribution of Chlorophyll over the middle of the cultivated mussel bed (bin 10). α=3.01 $\times$ 10^{-4} m s^{-1} and C_0=2μg l^{-1}. (a) Spring tide $A_{Puf}(\eta)$ = 3.35 m (b) Neap tide $A_{Puf}(\eta)$ = 2.6 m. Figure taken from Simpson et al. (2007).

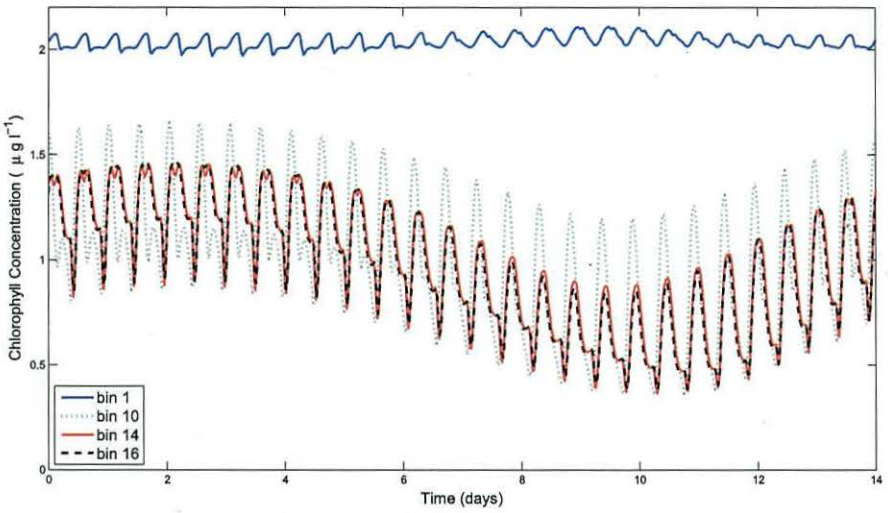

Figure 7.10: Modelled Chlorophyll Concentration ($\mu g\ l^{-1}$) at 4 locations over a 14-day period. Locations corresponding to the bin numbers quoted in the legend can be found in the text page 90

Chapter 8

Comparison of Field Observations to PHYBIO Model

8.1 Introduction

In the previous chapter, it has been shown that the PHYBIO model is a valuable tool in studying how Chlorophyll distributions in the Menai Strait are expected to change within the semi-diurnal and spring-neap cycles. Although the physical component to the model has already been validated using measurements of flow in the Menai Strait, the validity of the predicted Chlorophyll distributions has yet to be demonstrated through comparison with field observations. During 2005 and 2006, various fluorometer deployments were made in the Menai Strait extending over varying time scales and covering the spatial scale of the ecosystem. From these deployments, described in Chapters 4 and 5, it could be seen that there are strong oscillations in Chlorophyll of a semi-diurnal and quarter-diurnal period, as well as a distinct horizontal gradient in Chlorophyll. Both of these can be linked to the presence of a large quantity of mussels in the North-Eastern section of the Strait. Analysis of this oscillation using HAMELS has shown that in the observations the semi-diurnal component of the Chlorophyll concentration lags that of the elevation by $\sim 75°$. Moreover, analysis of measurements on a medium time scale have also shown there are significant oscillations in the Chlorophyll concentration in the downstream direction of the mussel beds. This chapter aims to validate the biological component of the PHYBIO model through comparison with the above mentioned measurements.

8.2 Short time series results

Figure 8.1 shows the modelled and observed amplitude of Chlorophyll, as well as the phase difference between elevation and Chlorophyll, both at the semi-diurnal (SD) frequency. The amplitudes have been scaled to the maximum concentration encountered. For the field data this has been scaled as $\frac{A_{SD}}{A_0+A_{SD}}$, therefore assuming the maximum concentration is the mean concentration (A_0) plus the semi-diurnal amplitude; while for the model results, this has been scaled to the input concentration ($C_0 = 2\ \mu g\ l^{-1}$) at the Northern boundary ($=\frac{A_{SD}}{C_0}$).

At this point it should be noted that the biological model of PHYBIO has been tuned to match the observed amplitude changes in the measurements. This tuning has been done through modifying the filtration parameter α. During model development, this parameter was set to 0.0002 m s^{-1} which showed to approximately match the observed oscillations in Chlorophyll above the mussel beds. This value was further fine-tuned using the observed amplitudes (measured in April and August 2005) of the semi-diurnal tidal constituent and those modelled, finalising the filtration parameter to 0.000301 m s^{-1}.

The filtration parameter α is the only tunable parameter within the model, and after tuning to match the observed amplitude oscillations, a sensitivity analysis of the choice of filtration parameter was also completed. A factor of 2 change in the value of α only introduces a small deviation from the observed amplitudes and phase differences of the semi-diurnal constituent; while an order of magnitude change introduces up to 25° error in the phase difference between elevation and Chlorophyll concentration and up to 30% error in the amplitude oscillation.

The fact that the scaled amplitudes match, is , therefore, a direct result of tuning the model using the filtration parameter (Figure 8.1). More significant is that the PHYBIO model also predicts a phase lag of ~80 °, agreeing well with the phase lags observed at the field location near Bangor Pier in the Menai Strait. However, as can be seen in Figure 8.1, this phase difference changes over the length of the domain. This is a likely result of the changes in the velocity phasing along the channel due to the Strait connecting to the open sea at both ends. HAMELS of the SCUFA deployment at Conway Centre Dock has shown that the phasing further down the Menai Strait is not correctly represented. Although not explicitly presented, the results show that the Chlorophyll signal leads the elevation by ~30 ° for the semi-diurnal frequency, while the model predicts a lag of ~180°.

Nevertheless, comparison of results from the PHYBIO-1D simulations with time series measurements in the Menai Strait show good agreement, and reinforce the proposed hypothesis that observed patterns are a combination of tidal advection, and mussel filtration.

8.3 Horizontal Chlorophyll gradients

Comparison with the spatial surveys conducted in the Menai Strait in April 2005 and August 2006 (Figure 8.2) shows that the model does a good job at representing the spatial distribution of Chlorophyll in the ecosystem. In order to exclude the influence of the input concentration at Puffin Island, which changes seasonally, the Chlorophyll concentration has been normalised using the same method as described in Section 4.3. The slight under-estimation of the concentration in the Southern section (Figure 8.2) could be attributed to the model not having an input source at its Southern boundary, even though in reality tidal inflow from Caernarfon Bay would occur. It could also be related to an underestimation of the local productivity, which would be more important in the Southern section of the Strait, where strong mussel filter feeding is absent. Nevertheless, it can be concluded that the prediction from the PHYBIO model is representative of the patterns in Chlorophyll observed over the channel's spatial scale.

The gradient can also be quantified using the same calculation by which the gradients in August 2005 and May 2006 were calculated (see Section 4.3). Taking the tidally averaged concentration at Bin 3 (approximately corresponding with the location of the North most mooring location) and Bin 10 (the approximate location of the Southern mooring site), taking their difference and dividing by the distance in metres, results in a horizontal gradient of 8.1×10^{-5} $\mu g\, l^{-1}$ m^{-1}. This is a difference of a factor of 5 with the measurements of May 2006, although compared to measurements of August 2005, the modelled gradient differs by an order of magnitude. Assuming that the mussel filtration rate is constant year round is, however, a strong assumption. *Mytilus edulis* can change their filtration rate with season as their metabolism is affected by temperature, and depending on whether their food source is more abundant or not (Saurel et al., 2007). It is therefore likely that the horizontal gradient in Chlorophyll created by the mussel beds will vary with the season as they change their filtration rate and food uptake.

8.4 Vertical Chlorophyll gradients

Measurements of vertical water column structure (see Section 4.4) have shown a significant vertical gradient in Chlorophyll concentration at various stages of the tide. However, no consistency can be found in the field data as to when these strong vertical gradients occur. It is expected that at peak currents a significant positive (increasing downwards) vertical gradient occurs due to resuspension of settled micro-algae, and that at slack water a negative one may be observed due to vertical depletion by mussel feeding. The vertical structure predicted by the PHYBIO-2DV model suggests that a small vertical depletion occurs at each period of slack water (Figure 8.3). The vertical extent of the depletion, however, is variable, as can be seen in Figure 8.3 by the gradient between vertical bins 10 and 2 in the model not showing depletion at each slack tide.

Comparing field and model results, shows it is therefore likely that the full extent of the vertical depletion layer is still not included in the observations. As can be seen in Figure 4.10, the depletion values do tend to be lower at times of slack water, although they are not significant events on each occasion. Moreover, it can also be seen from Figure 4.10 that at times of peak current, significant positive gradients also occur, although once again not each tidal cycle. Results from the PHYBIO model are suggestive of the fact that the dynamics of vertical Chlorophyll structure are complex and occur in a narrow region close to the mussels. In the summer of 2006, as part of a seperate project, measurements were made closer to the bed using the method of siphon mimics in order to attempt better vertical resolution to observe the formation of a concentration boundary layer. However, these results were unavailable at time of writing.

8.5 Spring-neap results

Chapter 5 presented observations made over the spring-neap cycle, and simulations were carried out over a similar period of time using the PHYBIO-1D model (previously presented in Section 7.3.4). Table 8.1 shows that when the effect of seasonality is removed by scaling the amplitude of the spring-neap oscillation (A_{SN}) to the mean concentration (A_0), the changes predicted by the PHYBIO-1D model are comparable to those observed in the field. Although the PHYBIO model overestimates the amplitude of the oscillation slightly, there is a general agreement with obervations at Ynys Faelog. In the PHYBIO-model, the Chlorophyll oscillation on a fortnightly frequency has a phase of $\sim 28°$. In field measurements, however, there is no consistency in

phase between the two sites: a phase of -44° is observed at Ynys Faelog, and one of -105 ° at Conway Centre Dock. These results suggest the possibility of some missing processes in the model. For example, resuspension by stronger tidal currents, as well as changes in the mussel feeding behaviour on these time scales should be considered for inclusion.

Location	$\frac{A_{SN}}{A_0}$ (%)
Model Bin 1	1
Model Bin 10	23
Model Bin 14	32
Model Bin 16	34
Ynys Faelog	24
Conway Centre Dock	9

Table 8.1: Scaled amplitude of spring-neap oscillation (from HAMELS) at 4 locations in the model (Bins 1, 10, 14 and 16) and from field measurements at Ynys Faelog and Conway Centre Dock.

8.6 Summary

The comparison of the biological component of PHYBIO with observations may be summarized as:

- The phase differences between elevation and Chlorophyll concentration modelled with PHYBIO-1D show good agreement with those observed in the field in April 2005, August 2005 and May 2006.
- The horizontal gradient modelled by PHYBIO-1D shows good qualitative agreement with those measured previously in the Menai Strait. Quantitatively, the horizontal change in Chlorophyll concentration is within a factor of 5 of that calculated for observations in May 2006. With respect to the August 2005 estimated horizontal gradient, the model is out by an order of magnitude. It is thought differences could be the effect of seasonal changes in the strength of mussel filtration.

- Comparison of the measured and modelled vertical water column structure suggests that the vertical resolution of the measurements is still insufficient to include the significant vertical gradient predicted at each period of slack water.

- Although both model results and field observations show strong oscillations in down-stream Chlorophyll concentration with a fortnightly period, and the magnitude of the signal shows some agreement between PHYBIO-1D and measurements, the phase of the fortnightly cycle does not show good agreement and is an area needing consideration in future.

- It can be concluded that the interaction of tidal advection, mixing and mussel filtration are the key processes underlying the observed changes in Chlorophyll concentration in the Menai Strait. Predictions of the PHYBIO model's biological component have shown good agreement with observations on shorter timescales; therefore, confirming the hypothesis that the responsible processes acting on this time scale have been included correctly in the PHYBIO model.

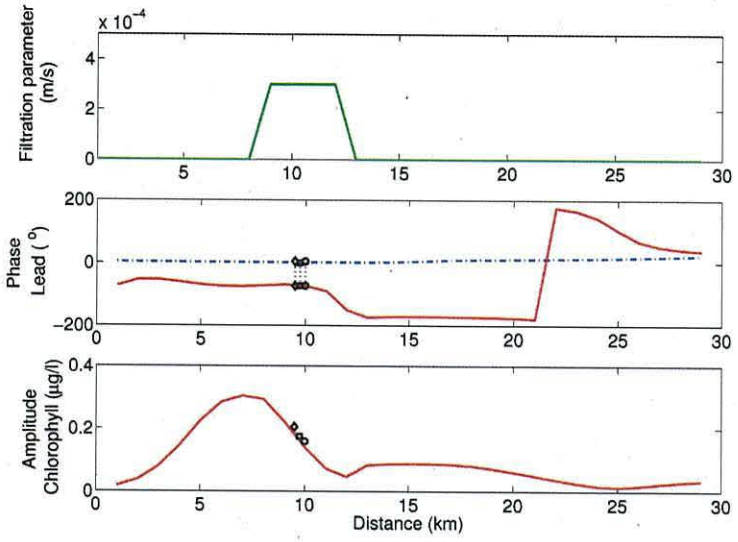

Figure 8.1: Comparison of PHYBIO model with field results obtained from anchor stations in April 2005, August 2005 and May 2006. (a) filtration parameter α (m s^{-1}), (b) amplitude of semi-diurnal oscillation in Chlorophyll (μg l^{-1}), and (c) phase of semi-diurnal oscillation (°) for elevation and Chlorophyll concentration.

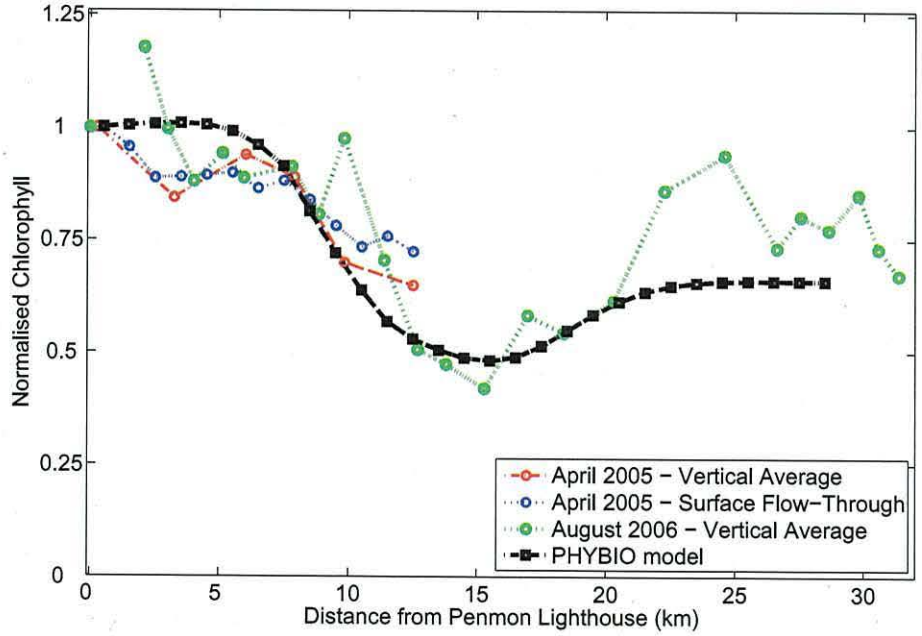

Figure 8.2: Comparison of PHYBIO model with field results obtained from spatial surveys of the Menai Strait in April 2005 and August 2006.

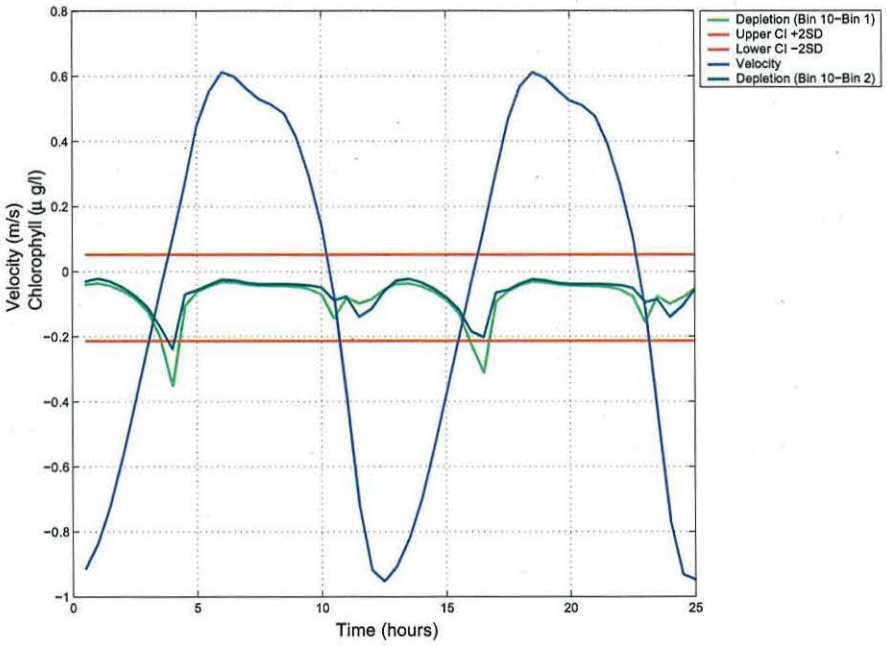

Figure 8.3: Modelled depletion values from PHYBIO 2DV model.

Chapter 9

TELEMAC-2D: Model Description and Results

Whilst the PHYBIO model approximates the Menai Strait as a 1-dimensional simulation, several researchers have already identified significant 2-dimensional patterns in circulation in the channel. Mainly for this reason, the simple parametrization included in the PHYBIO model where the mussel beds are simulated as a sink term removing Chlorophyll from the environment, was included in a more complex 2-dimensional numerical model, TELEMAC.

9.1 Introduction

The TELEMAC modelling package is one of several available packages for the numerical representation of the marine environment and its key processes. Within this project, the 2-dimensional horizontal (2-DH) numerical modelling was initially started using the freely available General Estuarine Turbulence Model (GETM); however, after careful consideration it was decided to further develop the work undertaken by Marten (2006), who successfully applied TELEMAC-2D to model flow in the Menai Strait. Within the TELEMAC-2D model, the option to model tracer advection and diffusion two-dimensionally has meant the distribution of Chlorophyll, including its removal by the mussel beds, could be modelled.

TELEMAC is a finite element model which was initially developed by the Laboratoire National d'Hydraulique (LNH), a department of Electricité de France (EDF). The model uses a combi-

nation of flow, wave, sediment and water quality modules to represent the relevant processes occurring in the natural environment. Within this package, TELEMAC-2D is a powerful hydrodynamical model much suited to maritime and river hydraulics due to its ability to take into account amongst other things the propagation of long waves, bed friction, Coriolis effects, meteorological conditions (such as atmospheric pressure and wind), turbulence, sub- and supercritical flows, density effects (due to temperature and salinity), flooding and drying of tidal areas or flood plains, the decay and creation of a tracer and particle tracking and Lagrangian drift computations (Berx, 2004). The TELEMAC-2D model solves the de Saint-Venant equations for depth-averaged free surface flow (Berx, 2004; Marten, 2006), representing the equations of continuity, of momentum along the x and y directions of the model domain, and of tracer conservation (Berx, 2004). Further details of this numerical model have been presented by EDF (1998), Hervouet (2000), Berx (2004), and Marten (2006).

Previous research on hydrodynamically modelling the Menai Strait using TELEMAC, conducted by Marten (2006), showed good agreement with field measurements for elevations, velocities, the residual flow and transport rates. Moreover, for the completion of this work a relatively high resolution flexible mesh of the Menai Strait was created, which had the necessary complexity in key areas such as the tidal channel for hydrodynamic accuracy; and the research also resulted in an accurate method for dealing with the variation in Mean Water Level in the Menai Strait (Marten, 2006).

Model simulations presented in this chapter are the result of using this existing model and simulating the advection of a passive conservative tracer (Chlorophyll, expressed in $\mu g\ l^{-1}$): its creation through a source term (i.e. phytoplankton net production) and its removal through a sink term (i.e. feeding by the commercial mussel beds) have been included. Thus all key processes thought to influence the distribution of Chlorophyll in the Menai Strait have been taken into account.

9.2 Model Description

The model domain comprises the complete length of the Menai Strait and stretches from a few miles beyond Puffin Island in the North-East to some miles offshore in Caernarfon Bay. Figures 9.1 and 9.2 show respectively the model mesh and bathymetry for the Menai Strait. From Figure 9.1 it can be seen that the model has a higher resolution in key areas such as the tidal channel,

in order to resolve the hydrodynamics accurately.

9.2.1 Boundary Conditions

Within TELEMAC-2D, the boundary conditions are defined through the implementation of a .conlim-file, where the user specifies which of the predefined cases best describes the desired conditions at the boundary point (see also Appendix 2 in Berx (2004)). In the Menai Strait, the model is forced by imposing the elevation at the two open boundaries (the North-East and South-West corners) and allowing for free velocity through these boundaries. All other boundaries in the domain are closed boundaries defined as solid walls with slip or friction. The boundary condition for the tracer at the closed boundaries is also set as a solid wall, while at the open boundaries the forcing of the tracer is described in the .conlim-file and its value given in the steering file (.cas-file). At the North-East boundary, the tracer value is kept constant in time and space, while at the South-Western boundary, the tracer gradient is zero. Figure 9.3 gives a schematic overview of the location and definition of the boundaries in the model domain.

9.2.2 Forced elevations at the boundaries

The prescribed elevations at each open boundary are constant along the boundary, but vary in time according to the tide. Marten (2006) developed a predictive equation for tidal elevation for a tide consisting of an M2-constituent, as well as a relationship describing the spring-neap cycle. Table 9.1 shows the amplitudes, phases and periodicities for the two different schematic tides at the Northern and Southern boundaries, which are used in Equation 9.1 to calculate the elevation at each time step for each location. For a simulation with only a semi-diurnal tide, the period of the M_2 tidal cycle (Table 9.1) is modified to T=45000 s, due to TELEMAC requiring an integer number of tidal cycles in a run.

$$\eta = \sum_{i=1}^{n} A_i \cos\left(\omega_i t - \phi_i\right) \tag{9.1}$$

where A is the amplitude, ω is the tidal frequency ($= \frac{360^\circ}{T_i}$) and ϕ is the phase of the specified tidal constituent (i). t is the time since the start of the model run in seconds.

Tidal Constituent		South-West	North-East
M2	A_{M2} (m)	1.3291	2.60
	ϕ_{M2} (°)	284.6	304.0
	T_{M2} (s)	44689.66	
S2	A_{S2} (m)	0.49	0.751
	ϕ_{S2} (°)	320.0	350.1
	T_{S2} (s)	43200	
M4	A_{M4} (m)	0.143	0.136
	ϕ_{M4} (°)	115.0	185.0
	T_{M4} (s)	22344.827	

Table 9.1: Amplitude (A), phase (ϕ) and period (T) for the M2, S2 and M4 tidal constituents used to calculate the prescribed tidal elevation at the open boundaries in the Menai Strait for a spring-neap cycle.

9.2.3 Description of tracer sink and sources

In the PHYBIO-model (see Chapter 7), the production and consumption of Chlorophyll is simulated through the definition of a mussel filtration parameter in the sink term (α), and a net production parameter in the source term (γ) to represent phytoplankton production and grazing by organisms other than the mussels. Within the TELEMAC2D model, the generation and consumption of the tracer has been simulated through the addition of a semi-implicit source term in the tracer equation (Equation 9.2). This equation includes only advection, as diffusion of the tracer is not included.

$$\frac{\partial T}{\partial t} + \vec{u} \cdot \vec{\nabla}(T) = S_T \tag{9.2}$$

At the forced boundary (NE), the tracer concentration is held constant in time and space at 5 μg l^{-1}, while at the SW the tracer concentration is left unforced. In the grid cells outside of the commercial lays, the sources and sink term in Equation 9.2, S_T, becomes $\gamma_* T$ representing the net production of phytoplankton. In the presence of the mussel beds, this term is modified to $(\alpha_* + \gamma_*)\ T$. The parameter α_* is similar to the mussel filtration parameter α in the 1-D

PHYBIO-model, while γ_* corresponds to the net growth parameter γ. The initial choices of $\alpha_* = -2 \times 10^{-5}$ m s^{-1} and $\gamma_* = 1 \times 10^{-6}$ m s^{-1} yielded realistic results, and it was thought unnecessary to further tune these values.

The distribution of mussels in the TELEMAC-2D domain reflects the approximate location of the commercial mussel beds in the Menai Strait, which was kindly supplied by Myti Mussels Ltd. (K. Mould, pers. comm.). Figure 9.4 shows the rough location of the mussel beds in the model domain, as well as the Chlorophyll distribution approximately 4 tidal cycles into the simulation. Although this is only an approximate representation of the commercial fishery, the more accurate inclusion of mussel distribution in the Menai Strait would involve further observational data from multi-beam sonar or other acoustical measurements, particularly when requiring the inclusion of the different densities which occur on the various lays. This lies, however, outside of the scope of the research presented here.

9.2.4 Model spin-up and stability

Previous research simulating only currents and elevations in the Strait, showed that a stable solution is obtained after an initial spin-up period of approximately 1 tidal cycle (Marten, 2006). The inclusion of a tracer, however, requires a longer initialization period, especially due to each simulation starting with a uniform distribution of Chlorophyll (tracer). Similar to the PHYBIO model, it was thought best to allow the system several tidal cycles to obtain a stable solution for the distribution of tracer in the Menai Strait. TELEMAC-2D was allowed to stabilise over a period of 8 tidal cycles, which were then followed by a simulation over 4 cycles. The initial distribution of Chlorophyll is set at 3 μg l^{-1}.

Introducing the mussel grazing or net primary productivity does not affect the stability of the model, and the choice of these parameters does not introduce numerical error. It does however affect how closely the model will represent reality.

9.3 Model Results

The majority of simulations presented here are the result of the final 2 tidal cycles of a simulation run over a total of 12 cycles with a semi-diurnal tide only (M2). Some results from the spring-neap cycle (M2+S2+M4) will also be presented.

Figure 9.5 shows the Chlorophyll distribution in μg l^{-1} as modelled with TELEMAC-2D, starting from a uniform distribution ($C_0 = 3$ μg l^{-1}) and applying the above mentioned values of α_* and γ_*. Comparison between the different panels in Figure 9.5 shows the tidal advection of the Chlorophyll gradient over the mussel beds. Soon after the time of peak flood tide ($\sim$ 139 h), the concentration gradient is at its most Northerly point, while after peak ebb flow ($\sim$ 147-149 h), the concentration gradient established by the mussel feeding has progressed furthest into the Menai Strait. Moreover, from Figure 9.5 it can be seen that the effects of mussel filtration can be observed as far South as Caernarfon.

Figure 9.6 shows the modelled Chlorophyll concentration in the Menai Strait at two different locations: one in the vicinity of the mussel beds near Bangor Pier (i.e. immediately "downstream" in the residual circulation) and the other close to Caernarfon Bay in the Southern section of the Strait. It can be seen that the amplitude oscillation near the mussel beds is slightly stronger (with the concentration range being $\sim$ 35 % larger) than that close to Fort Belan, and this oscillation also shows a stronger quarter-diurnal signal close to the mussels. This strong quarter-diurnal component is, as discussed previously, thought to be related to the change over time of the relative strength of the tidal advection and mussel filtration.

Previous research by Dr. E. Williams using the GETM model (E. Williams, pers. comm.), as well as results from TELEMAC-2D (Marten, 2006), have highlighted various locations where the flow has considerable lateral variation. One such region is the Northern edge of the Lavan Sands (see Figure 9.7). It is thought that the deeper Penmaen Swatch region affects the current pattern through topographic steering (Figure 9.7). Figure 9.7 shows the residual water transport (vectors) and tidally averaged Chlorphyll distribution (colour surface) in the Northern section of the Menai Strait. It can be seen that the residual circulation has a complex 2-D pattern, and is, furthermore, not directed to the South West in all locations of the Lavan Sands. The Chlorophyll concentration averaged over a tidal cycle shows the strong gradient established by the mussel feeding, reinforcing previous results from field observations and 1-D modelling results.

Chlorophyll concentration simulated over a fortnightly cycle (forced with tidal elevations from combined M2, S2 and M4 constituents) are shown in Figure 9.8. It can be seen that the concentration downstream shows a strong spring-neap oscillation. Using the same sequence of 48-h running average and HAMELS analysis as applied to field and PHYBIO model results previously (see Chapters 5 and 7), results show that the amplitude of the spring-neap cycle scaled to the mean concentration is approximately 34% downstream of the mussels, and approximately

3% at a location upstream (see Figure 9.2 for locations, marked as $\times$).

9.4 Comparison to previous results

Measurements of longitudinal concentration gradients of Chlorophyll in the Menai Strait, as well as results from modelling the interaction of tidal advection and mussel filtration 1-dimensionally, have already been shown to be in good agreement (see Chapter 8). Figure 9.9 shows a longitudinal transect extracted from the TELEMAC-2D model, and how it compares to field measurements and PHYBIO modelling results, taken at similar stages of the tide. As before, the concentrations have been normalised using the concentration near Penmon Lighthouse. It can be seen that the 2-D model does reasonably well at simulating the horizontal Chlorophyll gradient established by the mussel feeding (Figure 9.9). TELEMAC-2D slightly overestimates the reduction in Chlorophyll by the mussels (although if required this could be further tuned against observations), as well as predicts it to occur over a narrower section of the Strait. However, in contrast to the PHYBIO-model, TELEMAC-2D performs better at predicting the rebound in Chlorophyll concentration which occurs in the Southern section of the Strait. This despite boundary conditions at the South-West entrance to the channel being the same for both simulations.

Figure 9.10 shows a comparison of the longitudinal sections of normalised Chlorophyll at different stages of the tide for the PHYBIO and TELEMAC-2D models. The results of this comparison between the 2-D and 1-D modelling show consistent agreement between the two approaches, except for close to HW at Puffin Island, when the largest discrepancy between the predictions occurs.

On the longer time scale of the spring-neap cycle, the results of simulations with TELEMAC-2D agree well with those previously obtained from modelling with PHYBIO and they are in general agreement with field measurements downstream of the mussel beds (see Section 8.5). Downstream of the commercial lays, the oscillation in Chlorophyll on a fortnightly cycle is approximately 30% of the mean concentration.

9.5 Summary

In summary, it can be said that:

- TELEMAC-2D results of Chlorophyll distribution show good agreement with the distributions measured, as well as those modelled by the 1-D PHYBIO model.
- The accurate description of the physical processes in the Menai Strait, together with a parameterised representation of the mussel feeding and net phytoplankton growth, depicts more complicated patterns than previously observed. Especially, the possible finer scale circulation patterns over the shallow Lavan Sands and through the deeper Penmaen Swatch channel remain to be observed in the Menai Strait.
- Not only are Chlorophyll distribution measurements lacking at this scale, also accurate measurements of flow fields remain to be analysed and used for validation of the 2-D modelling.

Acknowledgements

This work would not have been possible without the kind help of Prof. A.G. Davies, Miss K. Marten, Miss J. Brown, and Dr. J. Malarkey at Bangor University and J.-M. Hervouet of Electricité de France.

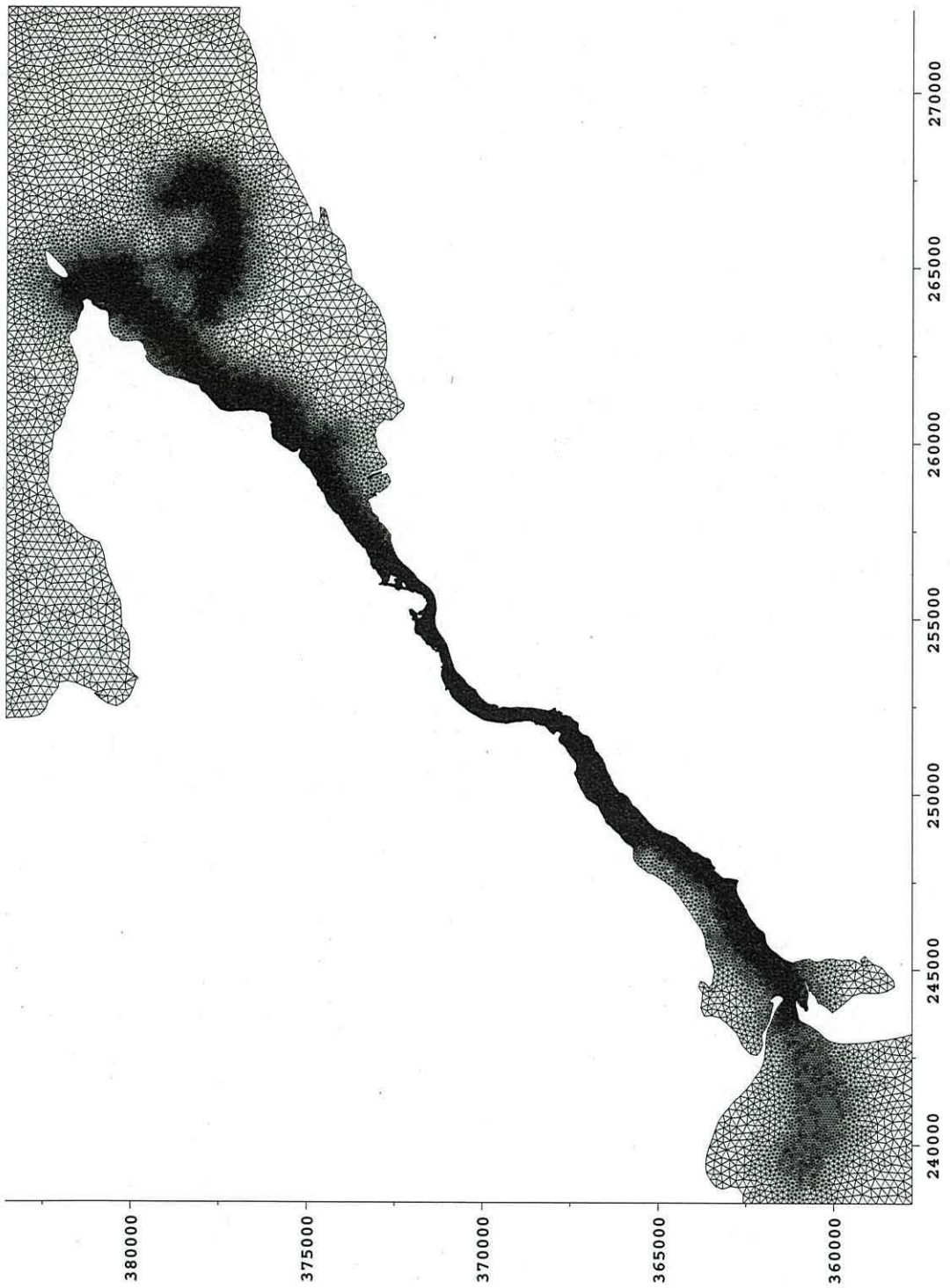

Figure 9.1: Model Mesh of the TELEMAC Model for the Menai Strait.

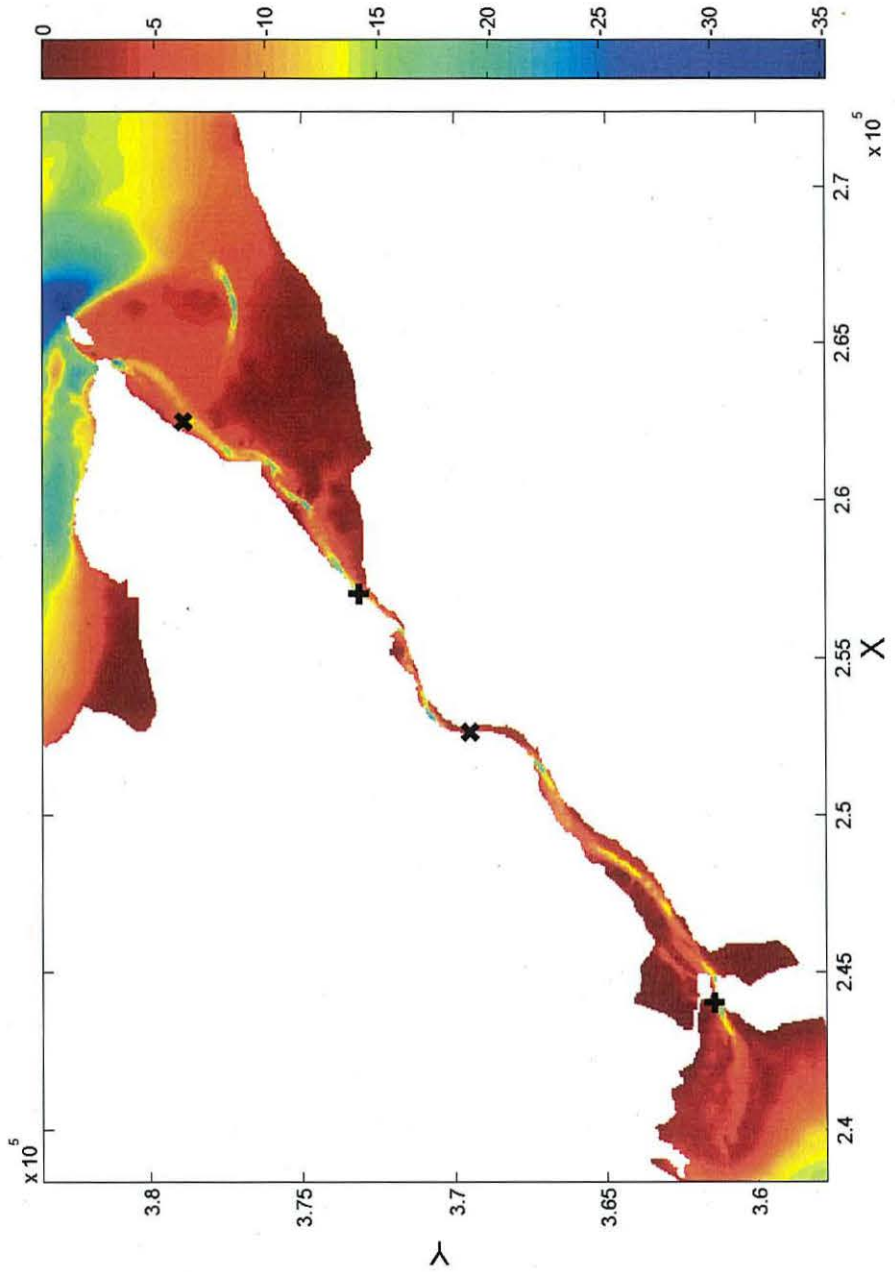

Figure 9.2: Model Bathymetry of the Menai Strait. + show locations for Figure 9.6 and × show locations for Figure 9.8.

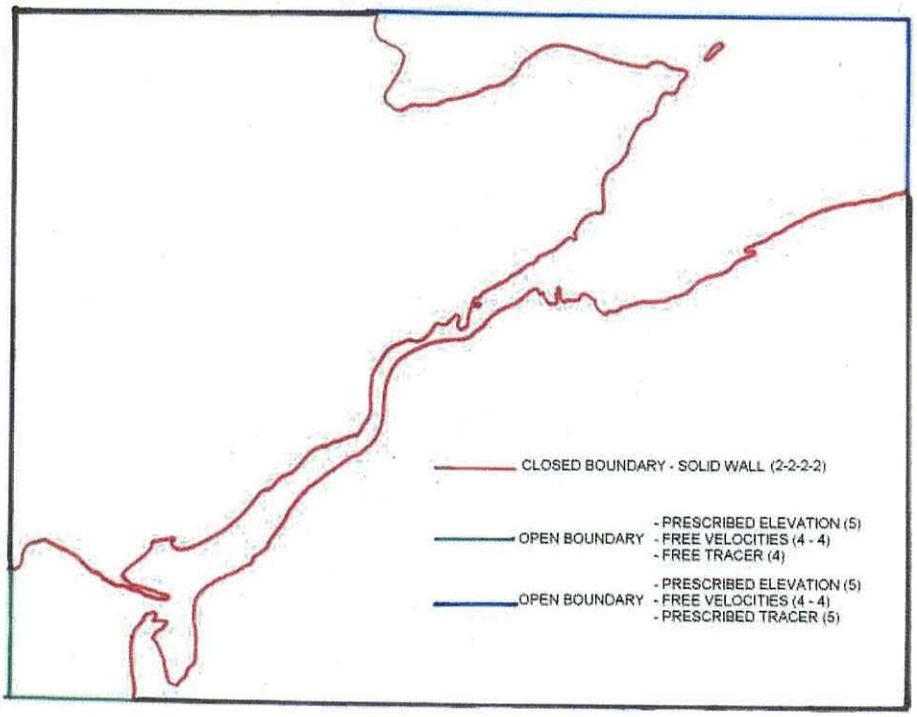

Figure 9.3: Schematic diagram of boundary conditions applied to the TELEMAC-2D model of the Menai Strait.

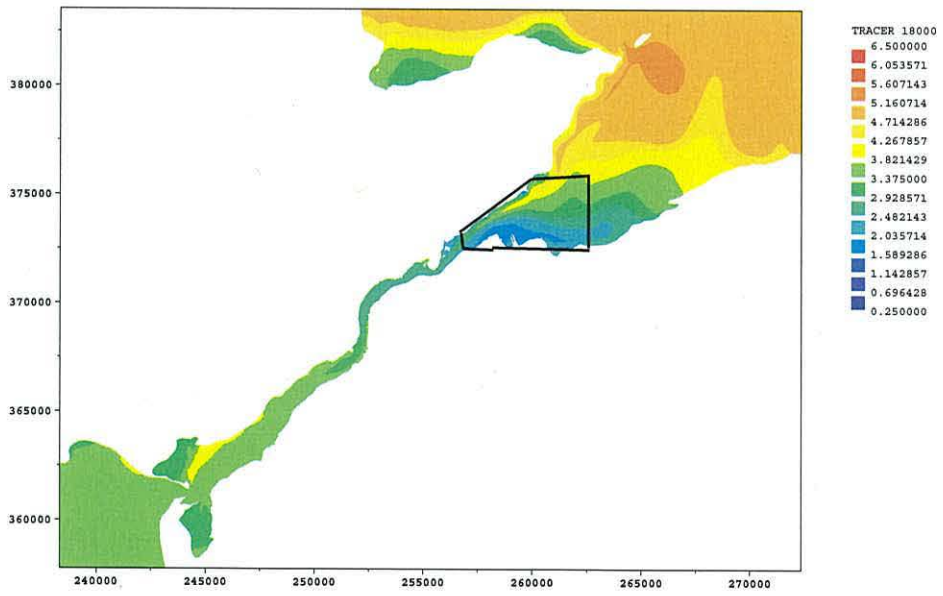

Figure 9.4: Chlorophyll distribution ($\mu g\ l^{-1}$) in the Menai Strait, as modelled during an early development run with TELEMAC-2D. The location of the mussel bed in the model domain has been highlighted by the black outline. Within this area, S_T equals $(\alpha_* + \gamma_*)T$, while in grid cells outside of this outline S_T becomes $\gamma_* T$.

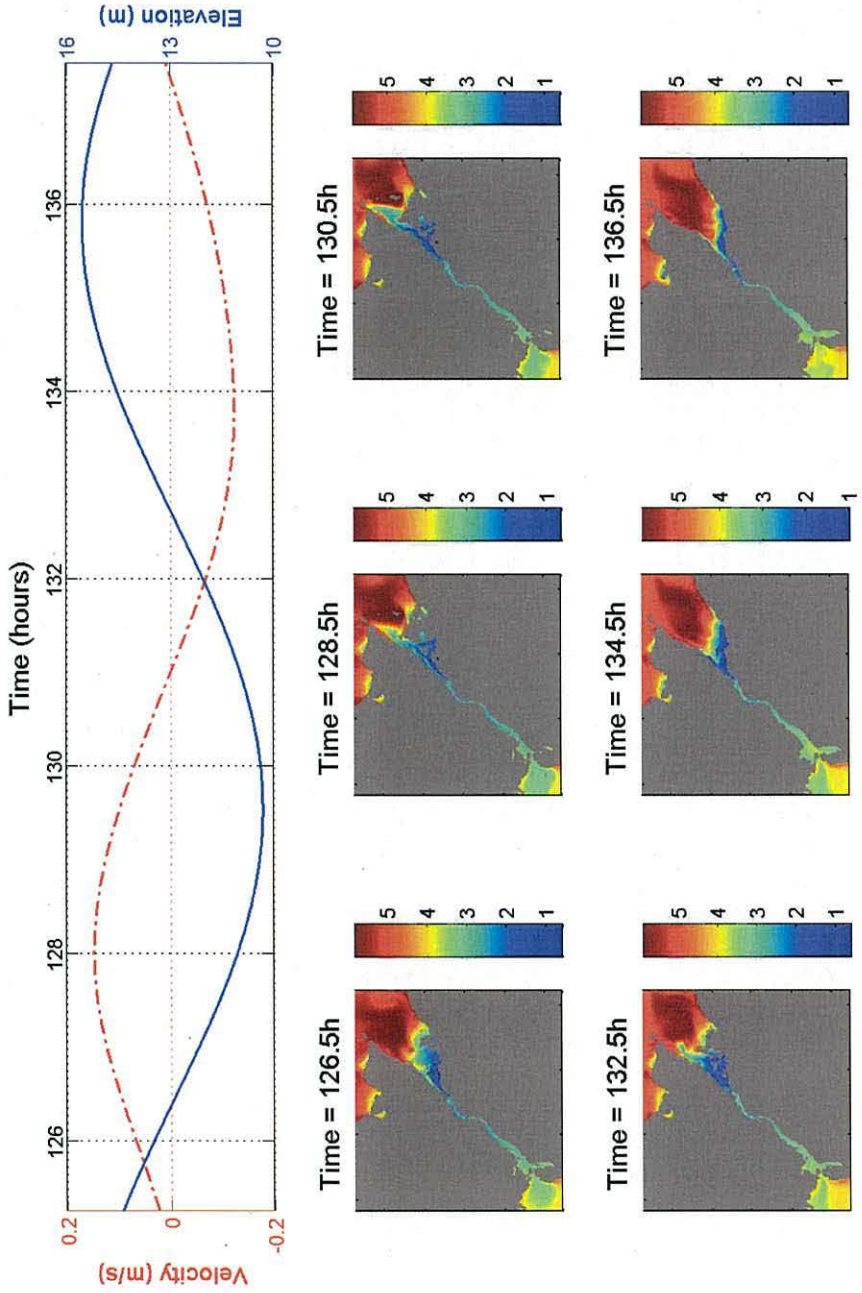

Figure 9.5: Chlorophyll distribution ($\mu g\ l^{-1}$) in the Menai Strait, as modelled with TELEMAC-2D at different time steps. Along-channel velocity and elevation at the Northern boundary, presented as an indication of tidal stage (flood in positive direction).

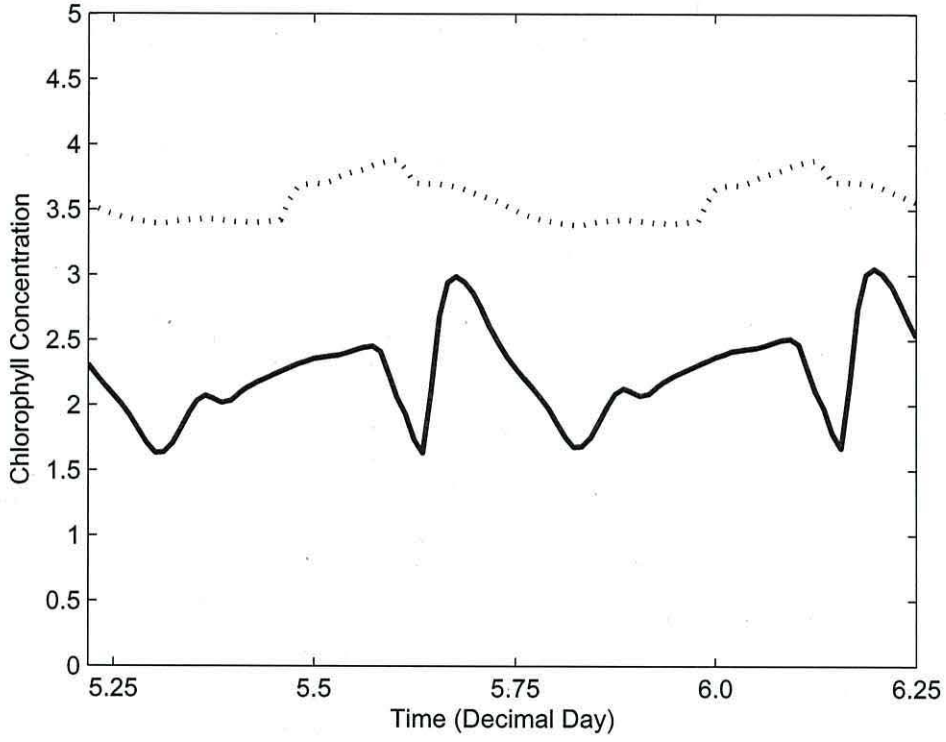

Figure 9.6: Time series of Chlorophyll (μg l^{-1}) at Caernarfon Bay and in the vicinity of Bangor Pier, as modelled with TELEMAC-2D (locations marked in Figure 9.2 as +).

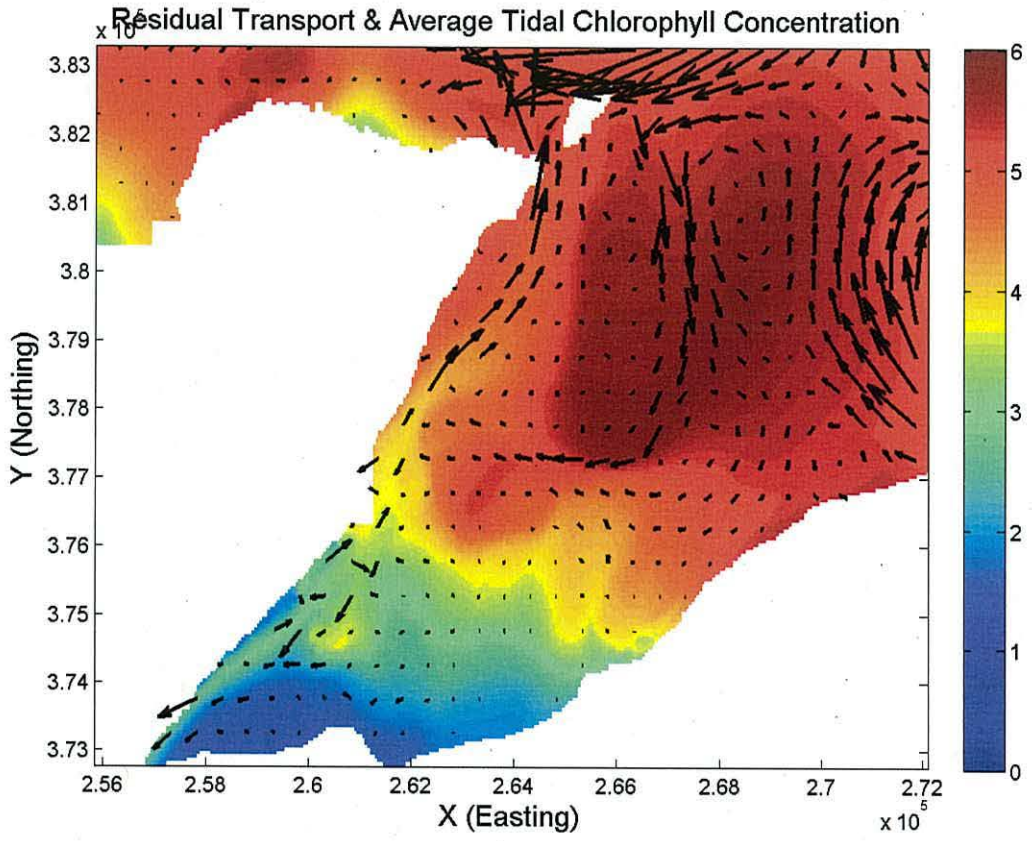

Figure 9.7: Residual transport vectors ($m^3\ s^{-1}$) and tidal mean Chlorophyll distribution ($\mu g\ l^{-1}$) in the Menai Strait, as modelled with TELEMAC-2D.

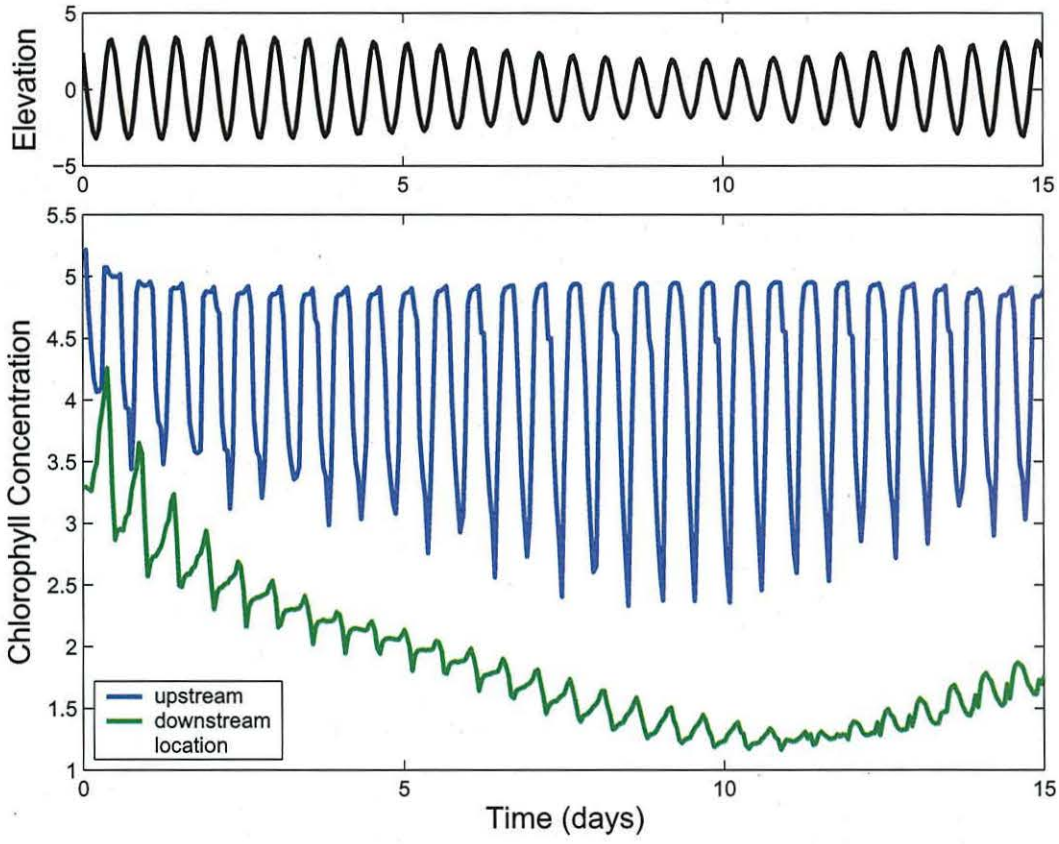

Figure 9.8: Elevation (m) and Chlorophyll concentration (μg l^{-1}) upstream (x = 262475, y = 378867) and downstream (x = 252153, y = 369490) of the mussel beds over a spring-neap cycle (locations also marked in Figure 9.2 as ×), as modelled with TELEMAC-2D.

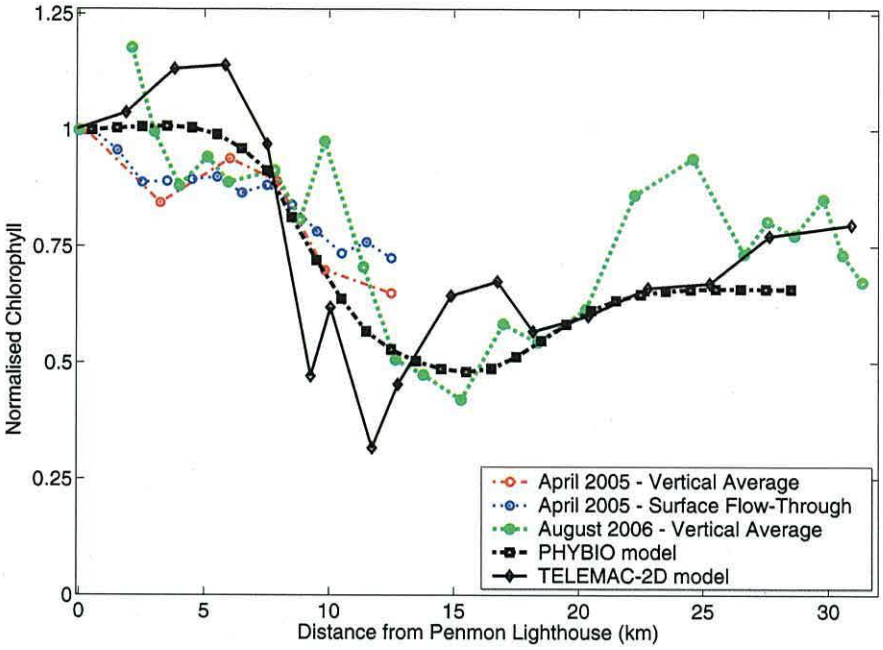

Figure 9.9: Comparison of longitudinal sections from observations, PHYBIO and TELEMAC-2D modelling of normalised Chlorophyll distribution in the Menai Strait.

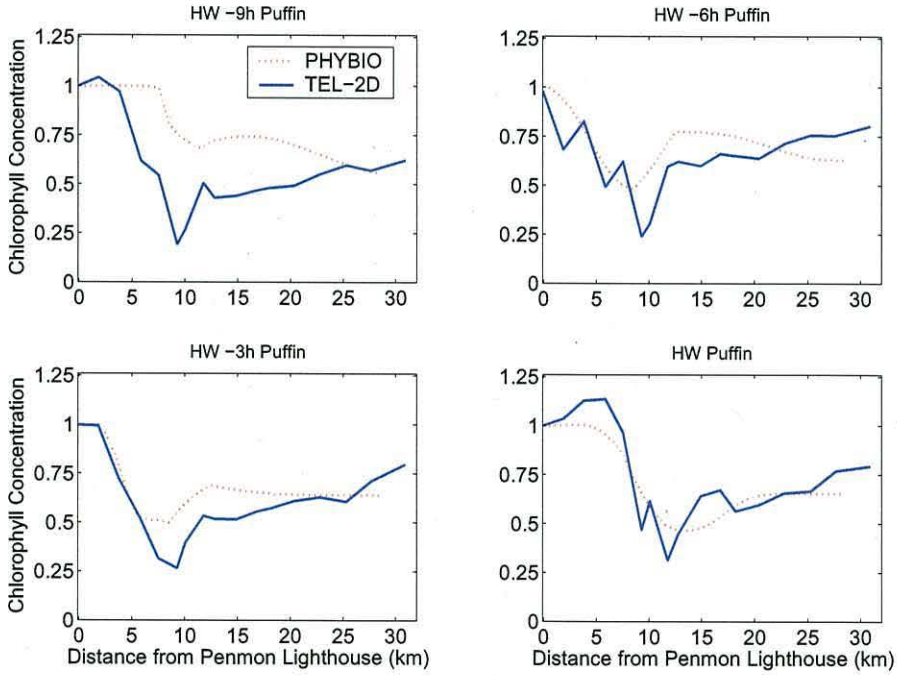

Figure 9.10: Comparison of longitudinal sections of normalised Chlorophyll from the PHYBIO and TELEMAC-2D models at different stages of the tide.

Chapter 10

Discussion

This chapter aims to discuss some of the main conclusions of the research presented in this thesis, as well as raise some issues encountered during the field measurements of Chlorophyll in the Menai Strait.

10.1 Instrumentation and methods

As shown in Chapter 3, the calibration of the different types of fluorometers can prove problematic, and even for the same instrument different calibration equations may be needed. This is mainly due to the external factors affecting fluorometer measurements, such as the species of phytoplankton, the time of year, temperature and turbidity concentration. Using fluorometers, the process of calibration should never be underestimated and during prolonged deployments, the shift of calibration with season should not be neglected. Although technology has simplified the task of measuring Chlorophyll concentrations, the most precise results will still be obtained from discrete sampling and using an accurate measurement technique such as HPLC, spectrophotometry or laboratory fluorometry. However, in order to obtain the resolution necessary to discern the different period oscillations discussed in this thesis (see Chapters 4, 5 and 6), this becomes a very laborious and time-consuming task. Nevertheless, when studying relative patterns of Chlorophyll and various time scales, the application of fluorometers has provided the best compromise possible, and has made this research innovative in its own right. Finally,

despite all the above issues with fluorometry, the results presented have shown good agreement in comparison with past research, indicating the technique to remain the best available solution to the problems posed within the scope of this project.

10.2 Interaction of mussel feeding, tidal advection & mixing

10.2.1 Time-series measurements and horizontal gradients

Results from both observations and model simulations of the Chlorophyll concentration in the Menai Strait strongly suggest that its distribution is a consequence of the interaction of the tidal currents which advect water rich in Chlorophyll into the ecosystem, and mussel filtration which removes Chlorophyll from the water column. Observations of the Chlorophyll distribution at a single location over a period of several tidal cycles have confirmed the main features of the previous observations made in the Menai Strait (Tweddle et al., 2005). There is a strong horizontal gradient in Chlorophyll concentration which can be observed in time series measurements, as well as during spatial surveys of the tidal channel. Analysis of the amplitude of the Chlorophyll oscillation measured in the vicinity of the commercial beds suggests the mussels reduce the phytoplankton concentration by half. These observations agree well with those previously made in the Menai Strait (Tweddle et al., 2005). Norén et al. (1999) also observed strong horizontal gradients over natural mussel beds in the Öresund strait which were attributed to the strong filter feeding of the bivalves.

A 1-D numerical simulation was developed, PHYBIO (Chapter 7), which includes all the major processes thought to influence the distribution of phytoplankton biomass in the Menai Strait. This new tool was designed to verify whether the correct processes defining the Chlorophyll distribution had been identified.

Analysis of field and model results show patterns in the distribution of Chlorophyll with not only a semi-diurnal, but also a quarter-diurnal and spring-neap oscillation. Moreover, time series measurements of Chlorophyll show a consistent phase lag at the semi-diurnal frequency with respect to the elevation between different seasons and different years of $\sim 75°$. This means the maximum semi-diurnal Chlorophyll concentration lags the maximum semi-diurnal elevation by approximately 2.5 hours. Results from modelling the Chlorophyll distribution using PHYBIO show good agreement with the observations, supporting the earlier hypothesis that the Chlorophyll supply to the mussel beds is driven mainly by tidal advection from Liverpool Bay,

rather than through local production. The selected filtration parameter α has been shown to be similar to filtration measurements in *Mytilus edulis* presented in the literature. However, as highlighted by Riisgård (2001), filtration rate remains a difficult to measure process. Moreover, the rate process may be affected by seasonality due to temperature dependence (Saurel et al., 2007). Strong support that other processes such as tidal resuspension of algal material are of minor importance comes from the fact that the PHYBIO model manages to predict Chlorophyll distribution accurately despite not representing them. However, possible further work could include a more in depth investigation of the effect of these processes on the Chlorophyll gradient in the channel.

Previously, Tweddle et al. (2005) had analyzed the along-channel gradient in Chlorophyll, from measurements collected in April 2002. Results summerized in Table 10.1 show that the gradients observed in August 2005 and May 2006 (see Chapter 4) are the same order of magnitude. In August 2005, however, there is a factor of 2 difference with the gradient calculated for May 2006 and for April 2002. A likely source of these minor differences are the seasonality of Chlorophyll concentrations and mussel filtration rates in the Strait, as well as the sampling strategy and locations. Not only do observations show changes in the horizontal gradient on a seasonal time scale, observations of the horizontal distribution of Chlorophyll through the R.V. Prince Madog's Flow-Through System have shown a different gradient to occur at ebb and flood stages of the tide. A possible explanation for this occurrence can be found in the stretching of the gradient when the water column is more shallow.

Data set	Horizontal Gradient	Location Water Column
April 2002	$4.4 \times 10^{-4}\ \mu g\, l^{-1}\ m^{-1}$	surface
(Tweddle et al., 2005)	$4.8 \times 10^{-4}\ \mu g\, l^{-1}\ m^{-1}$	bottom
August 2005	$8.8 \times 10^{-4}\ \mu g\, l^{-1}\ m^{-1}$	surface (SCUFA)
	$8.5 \times 10^{-4}\ \mu g\, l^{-1}\ m^{-1}$	bottom (AquaTracka)
May 2006	$3.5 \times 10^{-4}\ \mu g\, l^{-1}\ m^{-1}$	

Table 10.1: Horizontal gradients of Chlorophyll, measured in the Menai Strait

Following Tweddle et al. (2005), the flux of Carbon into the ecosystem can be estimated in a "back-of-the-envelope" style calculation. Using the mean Chlorophyll concentration measured in August 2005 and May 2006 at the NE entrance, the mean transport through the channel

($\overline{Q}$ =500 m^3 s^{-1}) and a Carbon to Chlorophyll ratio of 30 (Grant and Bacher, 1998), the calculated flux of biomass into the Menai Strait lies between 132 (August 2005) and 195 (May 2006) g C s^{-1}. This converts into approximately 11.4 to 16.8 tonnes of Carbon which is each day brought into the Strait, an estimate which agrees well with the earlier calculations of Tweddle et al. (2005). Given the population density (750 individuals m^{-2}) and extent of the mussel beds in the Menai Strait previously assumed in the PHYBIO model, an estimate of the consumption of Carbon by *M. edulis* can be made. Grant and Bacher (1998) estimated Carbon consumption by mussels to be approximately 17 mg C day^{-1} $individual^{-1}$. Applying this figure to the Menai Strait leads to an estimate of Carbon consumption by mussels as 5.1 tonnes of Carbon per day.

Observations have shown Chlorophyll concentration to reduce by half during passage over the mussel beds, therefore suggesting this is a reasonably estimate of Carbon consumption by the mussels. Even though the mussels consume such a large amount of Carbon, they do not assimilate all of it due to losses in metabolism. According to Grant and Bacher (1998), 5.2 mg C day^{-1} is assimilated per individual mussel; and when applying this to the Menai Strait, the mussel production expressed as Carbon is equal to 1.56 tonnes C day^{-1} (569.4 tonnes C $year^{-1}$). In order to calculate the total weight of mussels produced in the channel, this total carbon production can be converted to dry flesh weight: approximately 36.5% of the dry flesh of a mussel is Carbon (Smaal and Vonck, 1997), and in the average mussel approximately 1 g Ash-Free Dry Weight is equivalent to 1.2 g Dry Flesh Weight (Smaal and Vonck, 1997). Therefore, using the relationships of (Smaal and Vonck, 1997) it is calculated that approximately 1300 tonnes Ash-Free Dry Weight (AFDW) mussels are produced in the Menai Strait, which is equivalent to approximately 26 000 tonnes of fresh live (total) weight mussels (AFDW = 5% of fresh weight; Dankers and Zuidema, 1995). The mussel production cycle in the Menai Strait takes approximately 2 years, with mussels first being cultivated in the intertidal before being relayed in the subtidal to increase their size. Production of farmed mussels in Wales was reported by CEFAS (2006) to be approximately 16 000 tonnes in 2005, of which the bulk is produced in the Menai Strait (Kim Mould, pers. comm.). Hence, there is an agreement between the calculated mussel production from phytoplankton consumption and actual fishery production. However, it should also be noted that mussel production is likely to vary due to individuality of the organisms, seasonality and inter-annual variability; and the above calculations should therefore only be seen as a guide.

Smaal and Silvert (2008) recently presented a Decision Support System (DSS) to allow for an

easy tool for managers to determine shellfish capacity in their region. Using this tool in the Menai Strait, the carrying capacity calculated would be 1736 tonnes AFDW, suggesting there is still a possibility for expansion of mussel production in the system (using a volume of 0.1 km3, a residence time of 3 days, a critical concentration of 1.5 μg l^{-1} , a clearance rate of 4 l g^{-1} AFDW h^{-1} and a primary production of 12 tonnes C day^{-1}). Modifying the settings for the DSS shows that changes in the clearance rate and the filtration rate are the most significant in pushing the exploitation of the system into unacceptable management. Changes in the critical concentration (i.e. that which is needed to support phytoplankton growth, as well as feed both the cultured mussels and other organisms in the ecosystem), primary production and retention have no effect on making the Menai Strait unsuitable to shellfish aquaculture. However, they do all make significant changes to the actual shellfish AFDW which can be farmed sustainably in the channel.

In conclusion, it can be said recent observations of the Chlorophyll distribution in the Menai Strait, which have been presented here, and which in part have been published recently (Simpson et al., 2007) are in agreement with observations previously made by Tweddle et al. (2005). In conjunction with results from the PHYBIO model, these observations show convicing evidence that the measured patterns are the result of a combination of tidal advection, and mussel filtration. Furthermore, simplified calculations show that the ecosystem in terms of commercial aquaculture is not yet at its full ecological carrying capacity, leaving room for expansion of the mussel fishery. However, communications with the local businesses (Kim Mould, pers. comm.) has suggested they are not planning on any significant expansion, mainly due to space limitation in the surface area suitable for mussel farming using bottom culture.

10.2.2 Vertical gradients

No observations of the vertical depletion, expected to occur around times of slack water, have so far been made due to problems with sampling close to the mussels at closely timed intervals. Therefore, various attempts have been made at filling this gap in the observations. Initial studies by Tweddle et al. (2005) showed that the vertical distribution of Chlorophyll in the water column is in general almost uniform, except for on two occasions where statistically significant depletion of the Chlorophyll concentration was observed near the bed. However, they concluded that probable reasons for no consistent observations of mussel filtration depleting the near-bed Chlorophyll concentration were (1) the lack of measurements less than 1 metre above the bed,

and (2) the lack of temporal resolution by using a 30 minute sampling interval (Tweddle et al., 2005).

More recently collected observations of the vertical Chlorophyll distribution (see Section 4.4) show the depletion of phytoplankton in the near-bed layer on several occasions. The observations of August 2005 show good agreement with those previously made by Tweddle et al. (2005). Nevertheless, depletion is not consistently significant at every time of slack water, although the PHYBIO model suggests that this would be the case. The following could in part be responsible for the remaining gaps in our understanding of the occurrence of vertical depletion:

- The R.V. Prince Madog not necessarily being located above mussel beds. Images from the underwater camera indicated that this was the case.
- The mussel beds themselves being patchy. This not only means that the presence of mussels near the submerged mooring can not be guaranteed, it could also signify that vertical mixing in between these horizontal patches could be sufficient to replenish the near-bed layer with Chlorophyll.
- The limited vertical extent of depletions, and the bottom measurements being at least ~30 cm above the bed.
- Vertical depletion may actually not occur during each tidal cycle, either through the period of slack water being too short, or mussel feeding being insufficient to create a near-bed layer absent of Chlorophyll.

Over all, it can be said that even when these depletion events occur in the Menai Strait, their duration is insufficiently long to introduce stress in the mussels with a lasting effect on their health. Hence, with respect to cultivation of *M. edulis* commercially, the Menai Strait ecosystem is a suitable environment which is sufficiently mixed throughout the tidal cycle to supply the bottom lays with food.

10.3 Seasonality in the Menai Strait

The seasonal cycle of Chlorophyll observed in the Strait in 2005 and 2006 (see Chapter 6) is in good agreement with measurements previously made in the region by Jones (1968), Strange

(1970), Al-Hasan (1976), Harker (1997), Beadman (2003) and Bravo (pers. comm.). Moreover, values of spring bloom Chlorophyll concentrations and summer concentrations are consistent with previous studies of concentrations in Liverpool Bay (Gowen et al., 2000, 2008). This is another good indication that the Chlorophyll concentration in the Strait is determined by advection of phytoplankton from Liverpool Bay, and that additional local production in the coastal region is of limited importance.

Not only does the Chlorophyll signal express a strong seasonal cycle. It is also thought some seasonal variations in mussel filtration and metabolism may be observed in the data (see Section 4.3). Normalised horizontal gradients would be the same if mussel filtration and feeding were invariant with season. However, previous research has shown that mussel filter feeding may be influenced by several physical and biological factors. The main factors influencing mussel filtration are food particle concentration (Asmus and Asmus, 1991; Dolmer, 2000b; Riisgård, 2001), and temperature (Cranford and Hill, 1999; Saurel et al., 2007). Although Dolmer (2000b) and Widdows et al. (2002) also showed current velocity has an indirect effect on mussel filtration as turbulent mixing influences the resupply of the bottom boundary layer, and hence the near-bed Chlorophyll concentration. The importance of this in terms of modelling Chlorophyll distribution in the Menai Strait will be discussed below.

10.4 Numerical modelling of food supply to commercial mussels

Chapters 8 and 9 have shown that good results may be obtained by using simplifying assumptions to model the Chlorophyll distribution in the Menai Strait and how it is influenced by physical and biological processes. Comparison of the 1-D, 2-DV and 2-DH modelling results with field observations has shown good agreement, and it has been possible to quantify the interaction of tidal advection and mussel filtration on different time scales.

The assumptions made in the numerical representation of the effect of mussel filtration on Chlorophyll concentration (see Section 7.3.1) through a passive tracer with production and sink terms is a rather drastic simplification. Observations of horizontal gradients in the Menai Strait have shown that the filtration rate varies significantly, particularly as the mussels may exhibit a seasonal pattern. Moreover, phytoplankton is not the organism's only food source, as mussels may also feed on organic detritus and small zooplankton. However, the numerical modelling undertaken as part of this study never aimed to be a full ecosystem model. Instead of looking

into a detailed representation of mussel metabolism, phytoplankton metabolism and hydrodynamics, the numerical simulations aimed to represent all processes in their most basic form. This method allows us to investigate whether the principal processes responsible for driving the observed changes in Chlorophyll concentration have been included in the hypothesis.

A similar study by Banas et al. (2007) using the General Estuarine Turbulence Model (GETM) also showed good results in demonstrating whether benthic filter feeders (oysters) are the underlying source of the observed changes in phytoplankton distribution in Willapa Bay (USA). Thus, passive tracer modelling in 2-DH (or even 3-D) has shown an encouraging ability to explain the underlying processes of observed food concentration distributions. In a recent study by Grant et al. (2008), it was highlighted simplification may be a first step in the management process: models where primary production and other source-sink terms are neglected and bathymetry and hydrography are simplified often offer good results to base farm-scale decissions on. Smaal and Silvert (2008) have also shown that simple management tools can be developed based on these kind of numerical simulations. However, simplified models do not include the level of complexity needed for an ecosystem approach to management, i.e. to make important management decissions within the commercial fishery of marine bivalves taking into consideration the wider ecosystem. Grant et al. (2008) presented a numerical model where detailed processes of advection-diffusion, primary production and bivalve bioenergetics were included 2-dimensionally. Compared to previous models (such as those developed in the SMILE project; Ferreira et al., 2008) which for the purposes of estimating carrying capacity focus on integrated growth (over a period of a day or longer), this is one of the first models to focus on energetics processes on a time scale of hours. This approach allows to model the interaction between multiple farms as well as demonstrate their implication on an ecosystem scale. Nevertheless, Grant et al. (2008) also admit that farm-scale simulations may offer adequate information on the local effects. As more becomes known of the different ecosystem processes and specific metabolic processes in *M. edulis* (through projects such as SMILE and CANO), further developments in ecosystem-scale models are to be expected. Depending on the information required in the decision making process, however, simplified models may provide adequate information at minimal computational cost.

10.5 The Menai Strait: a unique system

The Menai Strait forms a unique regime through a combination of various physical and biological factors. The strong tidal currents and their residual transport in a South-Westerly direction import vast quantities of water and the materials suspended therein through the channel. This forms an important food source for the organisms living in the region, and in particular the location of the commercial mussel beds is optimal for utilizing this fresh supply of food particles. Moreover, the residual flow ensures mussels located furthest from the entrance to the Strait are not at a major disadvantage when it comes to food resources. In systems such as estuaries (eg. Oosterschelde (NL) or Tracadie Bay (CAN)), mussels far from the source of tidal renewal are likely to encounter less than favourable food quantities and qualities, resulting in suboptimal growth (Waite et al., 2005). For commercial culture sites, the horizontal gradients established by large quantities of bivalves can therefore negatively influence the production of the fishery. In the Menai Strait, the strong residual advection which is similar to a large river flowing through the channel (Simpson et al., 2007), ensures the flushing time of the system is relatively short (Campbell et al., 1998), thus ensuring sufficient food reaches the mussels located further into the channel too.

Furthermore, the strong tidal currents ensure vertical mixing is sufficiently strong for the majority of the tidal cycle to resupply the near-bed layer with phytoplankton. Therefore, the tidal currents break down the vertical gradients brought about through filtration by *M. edulis*. Within the Menai Strait, field observations and modelling studies have shown the effect of near-bed depletion to be limited in time and space, making its effect on mussel health even more insignificant. Compared to low energy environments such as Limfjorden (DK) (Wiles et al., 2006), the Menai Strait is therefore much more suitable for the commercial culture of mussels, as limited food supply through limited water column turnover does not influence mussel production.

Nevertheless, the Menai Strait is also a site of exploitation and exploration for other users. The measurements and observations made during this research project will prove invaluable as baseline measurements for comparing the effect of future developments in the regions. For example, should a development such as the proposed Beaumaris marina (which has always been opposed by the local mussel fishery) be given the green light, observations outlined in this thesis can be used in support of both appeals or applications. A high court ruling in May 2008, however, brought a halt to proposed plans for now, and revoked the FEPA dredging license issued by the

Welsh Assembly ("Beaumaris marina plans hit the rocks", Daily Post, May 7 2008). Similarly, should the fishery increase its mussel production, observations of Chlorophyll concentration presented here can be used to assess the impact of the expansion. Results presented in Section 10.2.1 suggest that there is some room for development.

10.6 Conclusions

The main conclusions of the research presented in this thesis are:

- The interaction of tidal advection, vertical mixing and mussel filter feeding have been shown to underly the observed changes in Chlorophyll in the Menai Strait.
- Results of HAMELS analysis of observed and modelled data have shown these interactions to establish strong oscillations in Chlorophyll concentration of a semi-diurnal and quarter-diurnal period. The quarter-diurnal signal is brought about through varying strength of tidal advection over the tidal cycle. Mussels are able to deplete the Chlorophyll concentration more when tidal advection is relatively weaker, and thus at periods of peak current, their access to the suspended particles is smaller, reducing the effect of bivalve filtration on Chlorophyll concentration.
- A strong oscillation on a fortnightly time scale can also be observed. This is the influence of the strength of residual tidal advection in the Menai Strait also changing over this time period. Hence, the relative strength of mussel filtration to horizontal advection changes; this creates noticeably lower concentrations downstream of the mussels at times when the mussels have better access to the food particles in suspension (i.e. at neap tides when advection is weaker).
- Numerical representation of these processes in a simplified form has shown to result in good agreement with the observations, suggesting the most significant processes influencing Chlorophyll distribution in the tidal channel have been included in the PHYBIO model. Not only are changes in Chlorophyll distribution shown to correspond qualitatively, there is also good quantitative agreement between numerical simulations and field measurements.

- Vertical mixing in the tidally energetic channel is sufficient to minimize the formation of near-boundary depleted Chlorophyll layers, therefore leaving the mussels relatively unaffected by shortages in food.
- Seasonal measurements of Chlorophyll show good agreement with those previously observed in the Menai Strait, as well as with those measured in Liverpool Bay. This partly reinforces the hypothesis that local production is of minor influence on the observed concentrations, and advection is the most important source of phytoplankton to the mussel beds.
- Results from the 2-DH modelling show good agreement with results from observations and 1-D modelling.
- Comparison to other studies of food supply to commercial mussel beds have shown the Menai Strait to be a unique ecosystem where the driving physical forces form part of the local mussel fishery's success.
- The calculated mussel production from phytoplankton consumption in Northern section of the channel and the actual fishery production in the Menai Strait show considerable agreement. Application of the Decission Support System developed by Smaal and Silvert (2008) suggests there is room for expansion.

10.7 Future work

Several opportunities of further research have been highlighted in this thesis. Firstly, the methodology of fluorometry still remains to be further explored. Particularly research in the application of these techniques on longer time scales, is an area deserving further attention, as the indirect measurement of phytoplankton concentrations with sufficient temporal resolution over longer time scales is much needed in locations strongly influenced by the tide.

Of relevance to the Menai Strait ecosystem, several paths of investigation remain open for future research. Specifically further investigation of the Chlorophyll distribution on a two-dimensional scale could prove useful to further quantify the food supply to the commercial mussel lays in the NE region of the tidal channel. Moreover, as highlighted in the discussion on numerical modelling (see Section 10.4), further research on the filtration rate of the mussels and its change over

time would be of interest, as well as the different contributions of phytoplankton, zooplankton and other organic particles to the Menai Strait mussel's diet. It would be particularly interesting to discover if their relative contributions change with location in the ecosystem. Applying ecosystem-style models such as those developed by Ferreira et al. (2008) and Grant et al. (2008) coud provide valuable information on ecosystem and economical carrying capacity. Cranford et al. (2008) showed strong changes in plankton population structure in flow past a mussel farm, and suggested this to be an easy method of studying the effect of mussel filtration on food concentrations. Furthermore, the SW region remains relatively under-investigated.

References

Ackerman, J., Loewen, M., Hamblin, P., 2001. Benthic-pelagic coupling over a zebra mussel reef in western Lake Erie. Limnology and Oceanography 46 (4), 892–904.

Al-Hasan, R., 1976. Seasonal variations in phytoplankton and glycollate concentrations in the Menai Straits, Anglesey. Ph.D. thesis, University of Wales, Bangor (Ocean Sciences).

Asmus, R., Asmus, H., 1991. Mussel beds: limiting or promoting phytoplankton? Journal of Experimental Marine Biology and Ecology 148, 215–232.

Baker, J., Wolff, W. (Eds.), 1987. Biological surveys of estuaries and coasts. Cambridge University Press, Cambridge.

Banas, N., Hickey, B., Newton, J., Ruesink, J., 2007. Tidal exchange, bivalve grazing, and patterns of primary production in Willapa Bay, Washington, USA. Marine Ecology Progress Series 341, 123–139.

Bayne, B., Hawkins, A., Navarro, E., Iglesias, I., 1989. Effects of seston concentration on feeding, digestion and growth in the mussel *Mytilus edulis*. Marine Ecology Progress Series 55, 47–54.

Beadman, H., 2003. The sustainability of mussel cultivation. Ph.D. thesis, University of Wales, Bangor (Ocean Sciences).

Berx, B., 2004. Morphological modelling of sandpits with TELEMAC. Master's thesis, University of Wales, Bangor (Ocean Sciences).

Biggs, C., 2006. Influence of flow direction, mussel presence and water depth on bottom drag coefficient as determined from ADCP turbulence measurements. Master's thesis, University of Wales, Bangor (Ocean Sciences).

Birkett, D., Maggs, C., 2001. Analysis of water turbidity data and macroalgal depth distributions on a transect in the Menai Strait. Tech. Rep. 468, Countryside Council for Wales.

Blight, S., Bentley, T., Lefevre, D., Robinson, C., Rodrigues, R., Rowlands, J., leB. Williams, P., 1995. Phasing of autotrophic and heterotrophic plankton metabolism in a temperate coastal ecosystem. Marine Ecology Progress Series 128, 61–75.

Bryans, A., 2003. 2D model of tidal flow in the Menai Strait. Master's thesis, University of Wales, Bangor (Ocean Sciences).

Buchan, S., Floodgate, G., Crisp, D., 1967. Studies on the seasonal variation of the suspended matter in the Menai Straits. I. The inorganic fraction. Limnology and Oceanography 12, 419–431.

Buchan, S., Floodgate, G., Crisp, D., 1973. Studies of the seasonal variation of the suspended matter of the Menai Straits. II. Mid Stream Data. Deutsche Hydrographische Zeitschrift 26, 74–83.

Buckley, F., 2004. The influence of shallow banks on residual circulation in a tidal channel. Master's thesis, University of Wales, Bangor (Ocean Sciences).

Butman, C., Frèchette, M., Geyer, W., Starczak, V., 1994. Flume experiments on food supply to the blue mussel *Mytilus edulis* l. asa function of boundary-layer flow. Limnology and Oceanography 39 (7), 1755–1768.

Caldow, R., Beadman, H., McGorty, S., Kaiser, M., Goss-Custard, J., Mould, K., Wilson, A., 2003. Effects of intertidal mussel cultivation on bird assemblages. Marine Ecological Progress Series 259, 173–183.

Campbell, A., Simpson, J., Allen, G., 1998. The Dynamical Balance of Flow in the Menai Strait. Estuarine, Coastal and Shelf Science 46, 449–455.

Castellani, C., 2001. Population dynamics and secondary production of the small copepods in the Menai Strait. Master's thesis, University of Wales, Bangor (Ocean Sciences).

CEFAS, Autumn/Winter 2006. Shellfish Production in the UK in 2005. Shellfish News 22, 32–38.

Cloern, J., 1982. Does the benthos control phytoplankton biomass in South San Fransisco Bay? Marine Ecology Progress Series 9, 191–202.

Cohen, R., Dresler, P., Phillips, E., Cory, R., 1984. The effect of the Asiatic clam, *Corbicula fluminea*, on phytoplankton of the Potomac River, Maryland. Limnology and Oceanography 29 (1), 170–180.

Cooper, M., 1976. A sublittoral transect across the Menai Strait with particular reference to currents and the fauna associated with the sponge *Halicondria panicea* (Pallas) L. Master's thesis, University of Wales, Bangor (Ocean Sciences).

Countryside Council for Wales, 1992. Glannau Menai gwarchodfa natur fr arfaethedig : dogfen drafod ddiwygiedig = Menai Strait proposed marine nature reserve : revised consultative document. Countryside Council for Wales.

Cranford, P., Hill, P., 1999. Seasonal variation in food utilization by the suspension-feeding bivalve molluscs *Mytilus edulis* and *Placopecten magellanicus*. Marine Ecology Progress Series 190, 223–239.

Cranford, P. J., Strand, Ø., Stroheimer, T., Dowd, M., Li, W., Grant, J., 2008. Phytoplankton depletion by mussel aquaculture: high resolution mapping,ecosystem modeling and potential indicators of ecological carrying capacity. In: Internation Council for the Exploration of the Seas Annual Science Conference Halifax, CM 2008/H:12.

Dankers, N., Zuidema, D., 1995. The role of the mussel (*Mytilus edulis* l.) and mussel culture in the Dutch Wadden Sea. Estuaries 18, 71–80.

Dare, P., 1980. Mussel cultivation in england and wales. Directorate of Fisheries Research Laboratory Leaflet 50, Ministry of Agriculture Fisheries and Food, Lowestoft.

Dolmer, P., 2000a. Algal concentration profiles above mussel beds. Journal of Sea Research 43, 113–119.

Dolmer, P., 2000b. Feeding activity of mussels *Mytilus edulis* related to near-bed currents and phytoplankton biomass. Journal of Sea Research 44, 221–231.

Donnet, S., 2003. Measuring the sediment transport in the Menai Strait using acoustical and optical methods. Master's thesis, University of Wales, Bangor (Ocean Sciences).

EDF, 1998. TELEMAC Modelling System: TELEMAC-2D User Manual (version 4.0). EDF-DER.

Emery, W., Thomson, R., 2001. Data Analysis Methods in Physical Oceanography. Elsevier, Amsterdam.

Fabricius, K., Dommisse, M., 2000. Depletion of suspended particulate matter over coastal reef communities dominated by zooxanthellate soft corals. Marine Ecology Progress Series 196, 157–167.

Falkowski, P., Raven, J., 1997. Aquatic Photosynthesis. Blackwell Science, Malden, Massachusettes.

Ferreira, J., Hawkins, A., Monteiro, P., Moore, H., Service, M., Pascoe, P., Ramos, L., Sequeira, A., 2008. Integrated assessment of ecosystem-scale carrying capacity in shellfish growing areas. Aquaculture 275 (1-4), 138 – 151.

Flynn, K., Marshall, H., Geider, R., 2001. A comparison of two N-irradiance interaction models of phytoplankton growth. Limnology and Oceanography 46 (7), 1794–1802.

Forbes, A., 1969. Electromagnetic monitoring of tidal currents in the Menai Straits. Master's thesis, University of Wales, Bangor (Ocean Sciences).

Fréchette, M., Bourget, E., 1985. Energy flow between the pelagic and benthic zones: factors controlling particulate organic matter available to an intertidal mussel bed. Canadian Journal of Fisheries and Aquatic Sciences 42, 1158–1165.

Fréchette, M., Butman, C., Geyer, W., 1989. The importance of boundary-layer flows in supplying phytoplankton to the benthic suspension feeder, *Mytilus edulis* l. Limnology and Oceanography 34 (1), 19–36.

Frost, N., 1997. Allozyme genetics of the introduced new zealand oyster, *Tiostrea chilensis*, in the Menai Strait. Master's thesis, University of Wales, Bangor (Ocean Sciences).

Garen, P., Robert, S., Bougrier, S., 2004. Comparison of growth of mussel, *Mytilus edulis*, on longline, pole and bottom culture sites in the Pertuis Breton, France. Aquaculture 232, 511–524.

Geider, R., MacIntyre, H., Kana, T., 1997. Dynamic model of phytoplankton growth and acclumation: responses of the balanced growth rate and the chlorophyll a:carbon ratio to light, nutrient-limitation and temperature. Marine Ecology Progress Series 148, 187–200.

Geider, R., MacIntyre, H., Kana, T., 1998. A dynamic regulatory model of phytoplanktonic acclimation to light, nutrients, and temperature. Limnology and Oceanography 43 (4), 679–694.

Gowen, R., Mills, D., Trimmer, M., Nedwell, D., 2000. Production and its fate in two coastal regions of the irish sea: the influence of anthropogenic nutrients. Marine Ecology Progress Series 208, 51–64.

Gowen, R., Tett, P., Mills, D., Shammon, T., Stewart, B., Greenwood, N., Flanagan, C., Devlin, M., Wither, A., 2008. The irish sea: Is it eutrophic? Estuarine, Coastal and Shelf Science 76, 239–254.

Grant, J., Bacher, C., 1998. Comparative models of mussel bioenergetics and their validation at field culture sites. Journal of Experimental Marine Biology and Ecology 219, 21–44.

Grant, J., Bacher, C., Cranford, P. J., Guyondet, T., Carreau, M., 2008. A spatially explicit ecosystem model of seston depletion in dense mussel culture. Journal of Marine Systems 73 (1-2), 155 – 168.

Grant, J., Curran, K., Guyondet, T., Tita, G., Bacher, C., Koutitonsky, V., Dowd, M., 2007. A box model of carrying capacity for suspended mussel aquaculture in lagune de la Grande-Entrée, Iles-de-la-Madeleine, Qu/'ebec. Ecological Modelling 200, 193–206.

Green, M., Hewitt, J., Thrush, S., 1998. Seabed drag coefficient over natural beds of horse mussels (*Atrina zelandica*). Journal of Marine Research 56, 613–637.

Haefner, J. W., 2005. Modelling Biological Systems, 2nd Edition. Springer.

Harker, G., 1997. A comparison between optical properties measured in the field and the laboratory, and the development of an optical model. Ph.D. thesis, University of Wales, Bangor (Ocean Sciences).

Harvey, J., 1967. Hydrographical studies in the Irish Sea and adjacent waters. Ph.D. thesis, University of Wales, Bangor (Ocean Sciences).

Hayward, P., Nelson-Smith, T., Shields, C., 1996. Collins Pocket Guide Sea Shore of Britain and Europe. Harper Collins Publishers Ltd, London.

Hervouet, J.-M., 2000. TELEMAC Modelling System: an overview. Hydrological Processes 14, 2209–2210.

Howlett, E., 2006. Short-term variations of suspended sediment in the Menai Strait during may and june 2006. Master's thesis, University of Wales, Bangor (Ocean Sciences).

Hussell, R., 1993. Impact of water-based recreation on bird disturbance within the Menai Strait proposed Marine Nature Reserve. Master's thesis, University of Wales, Bangor (Agricultural and Forest Sciences).

Jones, M., 1968. Phytoplankton studies in the Menai Strait. Master's thesis, University of Wales, Bangor (Ocean Sciences).

Jones, M., 1984. Megaripple stability in the S.W. Menai Strait. Master's thesis, University of Wales, Bangor (Ocean Sciences).

Jørgensen, C., 1990. Bivalve filter feeding: hydrodynamics, bioenergetics, physiology and ecology. Olsen and Olsen, Fredersborg (Denmark).

Karayücel, S., Karayücel, I., 2000. The effect of environmental factors, depth and position on the growth and mortality of raft-cultured blue mussels (*Mytilys edulis* l.). Aquaculture Research 31, 893–899.

Kjørboe, T., Møhlenberg, F., 1981. Particle selection in suspension-feeding bivalves. Marine Ecology Progress Series 5, 291–296.

Knap, A., Michaels, A., Close, A., Ducklow, H., Dickson, A. (Eds.), 1996. Protocols for the Joint Ocean Flux Study (JGOFS) Core Measurements. Vol. 19. UNESCO, Ch. 14, pp. 119–122.

Krause, G., Weis, E., 1991. Chlorophyll fluorescence and photosynthesis: the basics. Annual Review of Plant Physiology and Plant Molcular Biology 42, 313–349.

Lassen, J., Kortegård, M., Riisgård, H., Friedrichs, M., Graf, G., Larsen, P., 2006. Down-mixing of phytoplankton above filter-feeding mussels – interplay between water flow and biomixing. Marine Ecology Progress Series 314, 77–88.

Lehane, C., Davenport, J., 2006. A 15-month study of zooplankton ingestion by farmed mussels (*Mytilus edulis*) in Bantry Bay, Southwest Ireland. Estuarine Coastal and Shelf Science 67, 645–652.

Marten, K., 2006. Validated numerical simulation of the flow in the Menai Strait: a Telemac model. Master's thesis, University of Wales, Bangor (Ocean Sciences).

Maxwell, K., Johnson, G., 2000. Chlorophyll fluorescence - a practical guide. Journal of Experimental Botany 51, 659–668.

Monismith, S., Koseff, J., Thompson, J., O'Riordan, C., Nepf, H., 1990. A study of model bivalve siphonal currents. Limnology and Oceanography 35 (3), 680–396.

Musyoki, B., 1987. Community structure of the sessile epifauna of *Fucus serratus* L. in the Menai Strait, North Wales. Master's thesis, University of Wales, Bangor (Ocean Sciences).

Newton, A., 1986. Studies on phytoplankton succession. Master's thesis, University of Wales, Bangor (Ocean Sciences).

Norén, F., Haamer, J., Lindahl, O., 1999. Changes in the plankton community passing a *Mytilus edulis* mussel bed. Marine Ecology Progress Series 191, 187–194.

Nyandwi, N., 1988. Tidal flow and suspended sediment transport over a spring-neap-spring cycle on an intertidal sandbank in the southwestern Menai Strait, North Wales, UK. Master's thesis, University of Wales, Bangor (Ocean Sciences).

Officer, C., Smayda, T., Mann, R., 1982. Benthic filter feeding: a natural eutrophication control. Marine Ecology Progress Series 9, 203–210.

Ogilvie, S., Ross, A., , Schiel, D., 2000. Phytoplankton biomass associated with mussel farms in Beatrix Bay, New Zealand. Aquaculture 181, 71–80.

Ogilvie, S., Ross, A., James, M., Schiel, D., 2003. In situ enclosure experiments on the influence of cultured mussels (*Perna canaliculus*) on phytoplankton at times of high and low ambient nitrogen. Journal of Experimental Marine Biology and Ecology 295, 23–39.

O'Riordan, C., Monismith, S., Koseff, J., 1993. A study of concentration boundary-layer formation over a bed of model bivalves. Limnology and Oceanography 38 (8), 1712–1729.

O'Riordan, C., Monismith, S., Koseff, J., 1995. The effect of bivalve excurrent jet dynamics on mass transfer in a benthic boundary layer. Limnology and Oceanography 40 (2), 330–344.

Parsons, T., Maita, Y., Lalli, C., 1984. A manual of chemical and biological methods for seawater analysis. Pergamon Press, Oxford.

Ratcliff, J., 2001. The Pea Crab *Pinnotheres pisum* Pennant: its ecology, and effects on populations of the Edible Mussel, *Mytilus edulis*, in the Menai Strait, Wales. Master's thesis, University of Wales, Bangor (Ocean Sciences).

Riisgård, H., 2001. On measurement of filtration rates in bivalves – the stony road to reliable data: review and interpretation. Marine Ecology Progress Series 221, 275–291.

Riisgård, H., Poulsen, L., Larsen, P., 1996. Phytoplankton reduction in near-bottom water caused by filter-feeding *Nereis diversicolor* – implications for worm growth and population grazing impact. Marine Ecology Progress Series 141, 47–54.

Rippeth, T., Williams, E., Simpson, J., 2002. Reynolds stress and turbulent energy production in a tidal channel. Journal of Physical Oceanography 32, 1242–1251.

Robinson, D., 1981. The ecology of sublittoral opisthobranchs in the Menai Strait with special reference to *Eubranchus tricolor*. Master's thesis, University of Wales, Bangor (Ocean Sciences).

Russell, S., 2005. Revisiting eight intertidal rocky shore permanent transects along the Menai Strait Special Area of Conservation, North Wales. Master's thesis, University of Wales, Bangor (Ocean Sciences).

Rymell, M., 1995. An observational and modelling study of dispersion in the Menai Strait. Master's thesis, University of Wales, Bangor (Ocean Sciences).

Saurel, C., Gascoigne, J., Palmer, M., Kaiser, M., 2007. In situ mussel feeding behavior in relation to multiple environmental factors: Regulation through food concentration and tidal conditions. Limnology and Oceanography 52 (5), 1919–1929.

Sherwin, T., 2000. Menai Strait Tide Tables. Centre for Applied Oceanography, University of Wales, Bangor.

Shuttleworth, P., 1979. The residual flow in the Menai Strait by electromagnetic cable calibration. Master's thesis, University of Wales, Bangor (Ocean Sciences).

Simpson, J., Berx, B., Gascoigne, J., Saurel, C., 2007. The interaction of tidal advection, diffusion and mussel filtration in a tidal channel. Journal of Marine Systems 68, 556–568.

Simpson, J., Forbes, A., Gould, W., 1971. Electromagnetic observations of water flow in the Menai Strait. Geophysical Journal of the Royal Astronomical Society 24, 245–253.

Smaal, A., 2004. European mussel cultivation along the atlantic coast: production status, problems and perspectives. Hydrobiologia 484, 89–98.

Smaal, A., Vonck, A., 1997. Seasonal variation in c, n and p budgets and tissue composition of the mussel *Mytilus edulis*. Marine Ecology Progress Series 153, 167–179.

Smaal, A. C., Silvert, W., 2008. A simple model for estimation of shellfish carrying capacity. In: Internation Council for the Exploration of the Seas Annual Science Conference Halifax, CM 2008/H:03.

Spencer, B., 2002. Molluscan Shellfish Farming. Blackwell Publishing, Oxford (UK).

Stacey, M., Monismith, S., Burau, J., 1999. Measurements of Reynolds stress profiles in unstratified tidal flow. Journal of Geophysical Research 104 (C5), 10933–10949.

Strange, M., 1970. Phytoplankton of Anglesey waters. Ph.D. thesis, University of Wales, Bangor (Ocean Sciences).

Taylor, A., Geider, R., Gilbert, F., 1997. Seasonal and latitudinal dependencies of phytoplankton carbon-to-chlorophyll a ratios: results of a modelling study. Marine Ecology Progress Series 152, 51–66.

Troëng, S., 1994. Environmental monitoring in the Menai Strait. Master's thesis, University of Wales, Bangor (Ocean Sciences).

Turner Designs, 2004. SCUFA Self-Contained Underwater Fluorescence Apparatus User's Manual (revision 2.3). Turner Designs, Inc.

Tweddle, J., 2002. Biophysical interactions between phytoplankton, mussel beds and flow in the Menai Strait. Master's thesis, University of Wales, Bangor (Ocean Sciences).

Tweddle, J., Simpson, J., Janzen, C., 2005. Physical controls of food supply to benthic filter feeders in the Menai Strait,UK. Marine Ecological Progress Series 289, 79–88.

UNESCO, 1981a. Backgroud papers and supporting data on the practical salinity scale, 1978. Vol. 37 of Technical Papers in Marine Science. UNESCO Division of Marine Science, Paris.

UNESCO, 1981b. The Practical Salinity Scale 1978 and the International Equation of State of Seawater 1980. Vol. 36 of Technical Papers in Marine Science. UNESCO Division of Marine Science, Paris.

UNESCO, 1983. Algorithms for computation of fundamental properties of seawater. Vol. 44 of Technical Papers in Marine Science. UNESCO Division of Marine Science, Paris.

van Duren, L., Herman, P., Sandee, A., Heip, C., 2006. Effects of mussel filtering activity on boundary layer structure. Journal of Sea Research 55, 3–14.

Waite, L., Grant, J., Davidson, J., 2005. Bay-scale spatial growth variation of mussels *Mytilus edulis* in suspended culture, Prince Edward Island, Canada. Marine Ecology Progress Series 297, 157–167.

Widdows, J., Lucas, J., Brinsley, M., Salkeld, P., Staff, F., 2002. Investigation of the effects of current velocity on mussel feeding and mussel bed stability using an annular flume. Helgoland Marine Research 56, 3–12.

Wildish, D., Kristmanson, D., 1984. Importance to mussels of the benthic boundary layer. Canadian Journal of Fishery and Aquatic Sciences 41, 1618–1625.

Wiles, P., 2007. The application of acoustic doppler techniques to the measurement of turbulence over mussel beds. Ph.D. thesis, University of Wales, Bangor (Ocean Sciences).

Wiles, P., van Duren, L., Häse, C., Larsen, J., Simpson, J., 2006. Stratification and mixing in the limfjorden in relation to mussel culture. Journal of Marine Systems 60, 129–143.

Williams, E., 2000. Characteristics of the flow in the Menai Strait. Master's thesis, University of Wales, Bangor (Ocean Sciences).

Williams, E., Simpson, J., 2004. Uncertainties in Estimates of Reynolds Stress and TKE Production Rate Using the ADCP Variance Method. Journal of Atmospheric and Oceanic Technology 21, 347–357.

Yahel, G., Post, A., Fabricius, K., Marie, D., Vaulot, D., Genin, A., 1998. Phytoplankton distribution and grazing near coral reefs. Limnology and Oceanography 43 (4), 551–563.

YSI, 2006. 6-Series Multiparameter Water Quality Sondes User Manual (revision D). YSI, Inc.

Zeldis, J., Robinson, K., Ross, A., Hayden, B., 2004. First observations of predation by New Zealand Greenshell mussels (*Perna canaliculus*) on zooplankton. Journal of Experimental Marine Biology and Ecology 311, 287–299.

Appendix A

Research Cruises aboard the R.V. Prince Madog

A.1 April 2005

Anchor Station Bangor Pier

- **Duration:** 22 April 2005 13.32 GMT – 26 April 2005 08.02 GMT
- **Location:** 53 ° 14.619' N 04 ° 07.360' W
- **Instrumentation:**
  - 181 CTD+LISST+SCUFA casts (from anchored ship)
  - Camera frame with SCUFA deployed on bed (from anchored ship)
  - ADCP (53 ° 14.592' N 04 ° 07.513' W)
- MSc-students brought on and off

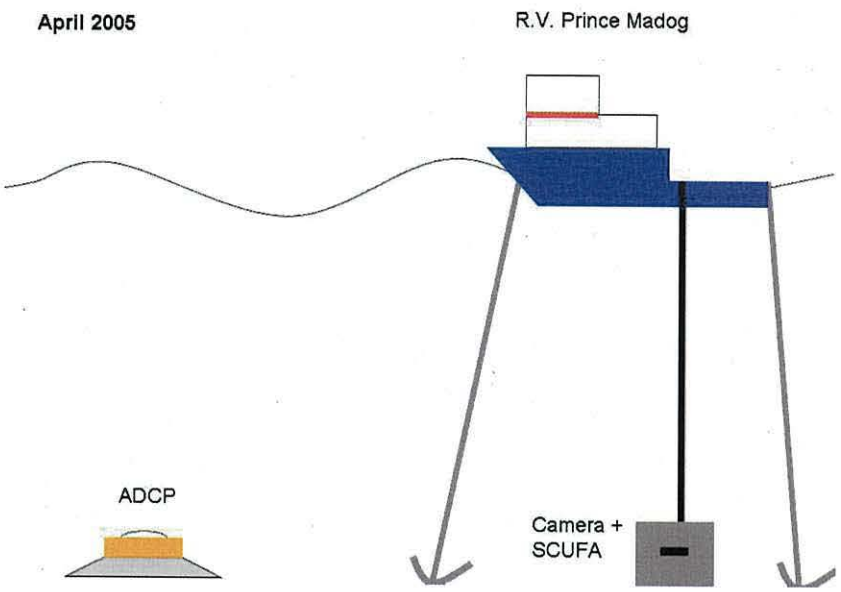

Figure A.1: Schematic overview of sampling strategy during April 2005 research cruise.

A.2 August 2005

Longitudinal sections See Appendix B

Anchor Station Bangor Pier

- **Duration:** 12 August 2005 08.03 GMT – 14 August 2005 09.58 GMT
- **Location:** 53 ° 14.633' N 04 ° 07.224' W
- **Instrumentation:**
  - 101 CTD+LISST+SCUFA casts (from anchored ship)
  - Camera frame (from anchored ship)
  - Mooring (Figure A.3) (from anchored ship)
  - ADCP (located at 53 ° 14.347' N 04 ° 07.725' W)

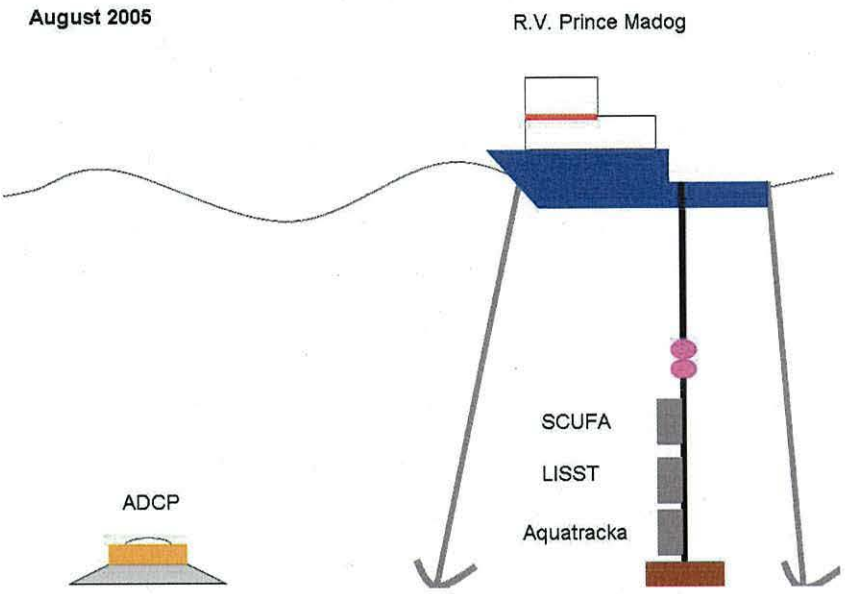

Figure A.2: Sampling strategy during August 2005 research cruise. Figure A.3 gives a more detailed view of the optical instrumentation mooring.

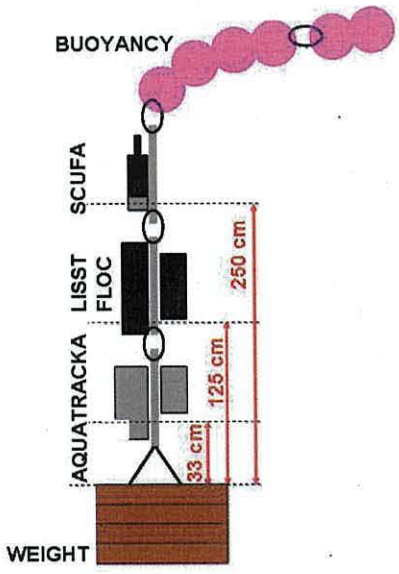

Figure A.3: Mooring design August 2005 research cruise.

A.3 May 2006

Longitudinal sections Not included in this thesis

Anchor Station

- **Puffin (P)**
  - **Duration:** 03 May 2006 07.00 GMT – 04 May 2006 08.00 GMT
  - **Location:** 53 ° 17.346' N 04 ° 03.129' W
- **Gallows Point (GP)**
  - **Duration:** 04 May 2006 13.04 GMT – 05 May 2006 15.00 GMT
  - **Location:** 53 ° 14.755' N 04 ° 06.955' W
- **Instrumentation:**
  - 51 (P) & 53 (GP) CTD+LISST+SCUFA casts (from anchored ship)
  - Camera frame (from anchored ship)
  - Stand-alone moooring (Figure A.5)
    * ADCP + LISST-FLOC + LISST-B + SCUFA SN615 + SN639 (faulty)
    * Location 53 ° 14.933' N 04 ° 06.753' W
- MSc-students brought on and off

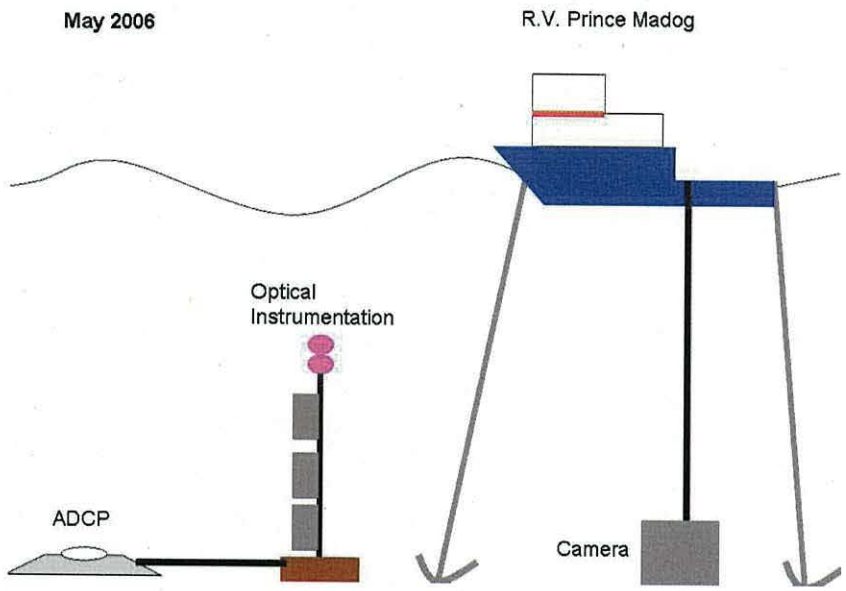

Figure A.4: Sampling strategy during May 2006 research cruise. Figure A.5 gives a more detailed view of the stand-alone mooring.

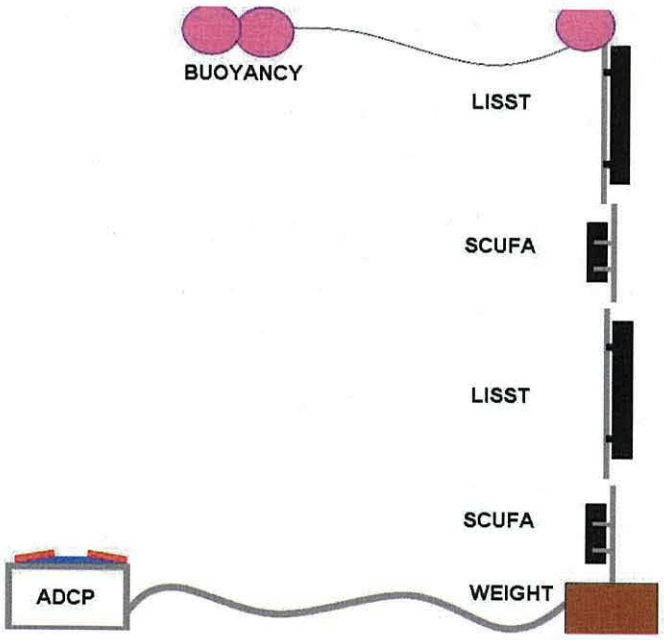

Figure A.5: Mooring design May 2006 research cruise.

Appendix B

Spatial surveys of the Menai Strait

B.1 R.V. Prince Madog

- **Section length:** T6 – T1 (see Table B.1)

Station	Latitude (°)	Longitude (°)	
T6	53.307183	-4.036667	Penmon Lighthouse
T5	53.284033	-4.064800	~ Trecastell Point
T4	53.260683	-4.086500	Beaumaris
T3	53.250417	-4.103317	Gallows Point
T2	53.241117	-4.130316	Bangor Pier
T1	53.225050	-4.157233	Menai Bridge

Table B.1: Approximate locations for stations on longitudinal sections made aboard the R.V. Prince Madog. Also given are nearby features for each station to give an idea of their approximate location within the Menai Strait.

- **Duration:**
  - 11 August 2005 07.19 GMT – 09.32 GMT
  - 11 August 2005 10.21 GMT – 12.18 GMT
  - 11 August 2005 12.57 GMT – 14.12 GMT (T5 to T1 only)

  - 11 August 2005 14.54 GMT – 16.05 GMT (T5 to T1 only)
  - 14 August 2005 12.26 GMT – 13.58 GMT
  - 15 August 2005 07.58 GMT – 09.22 GMT

- **Instrumentation:**
  - CTD+LISST+SCUFA casts
  - Flow-through measurements (surface water)

B.2 Mya

- **Section length:** MSB01 – MSB25 (see Table B.2)
- **Duration:** 03 August 2006 15.42 GMT – 17.44 GMT
- **Instrumentation (hand-profiles):**
  - Seabird SBE-19 CTD
  - Turbidometer
  - SCUFA Fluorometer

Station	Latitude (°)	Longitude (°)	Time (GMT) (HH.MM)
MSB01	53.310566	-4.036783	15.42
MSB02	53.301400	-4.038583	15.48
MSB03	53.292217	-4.050667	15.53
MSB04	53.286383	-4.059833	15.56
MSB05	53.279350	-4.069150	16.00
MSB06	53.270250	-4.077633	16.04
MSB07	53.262167	-4.081950	16.08
MSB08	53.251367	-4.102300	16.16
MSB09	53.246500	-4.115467	16.20
MSB10	53.241817	-4.127683	16.23
MSB11	53.232800	-4.144983	16.32
MSB12	53.223950	-4.157317	16.39
MSB13	53.219117	-4.171967	16.45
MSB14	53.214617	-4.194733	16.50
MSB15	53.203800	-4.211617	16.55
MSB16	53.187500	-4.214617	17.00
MSB17	53.176317	-4.235783	17.06
MSB18	53.166283	-4.259333	17.10
MSB19	53.146950	-4.276367	17.17
MSB20	53.135917	-4.300050	17.22
MSB21	53.131033	-4.310917	17.26
MSB22	53.125883	-4.324517	17.30
MSB23	53.122350	-4.341817	17.35
MSB24	53.118983	-4.352150	17.39
MSB25	53.117650	-4.365600	17.44

Table B.2: Stations, locations and times for longitudinal sections made aboard the research vessel Mya.

Appendix C

R.V. Prince Madog Time Series: ADCP and CTD depth profiles

C.1 ADCP velocity profiles

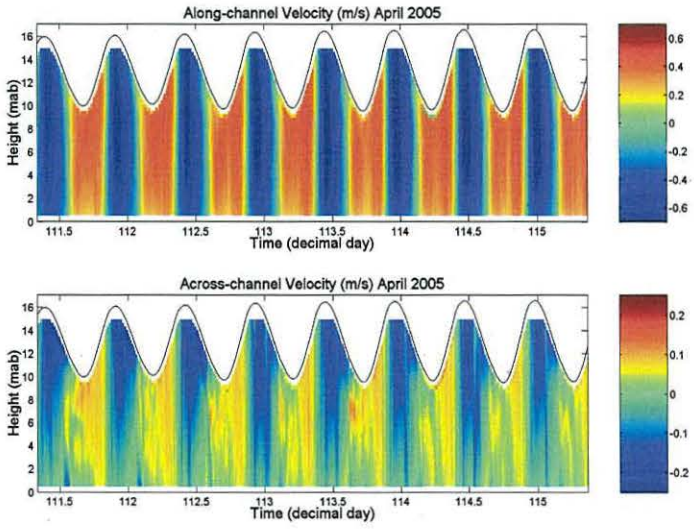

Figure C.1: Depth profiles of along-channel (top) and across-channel (bottom) velocity (m s^{-1}), measured by ADCP in April 2005.

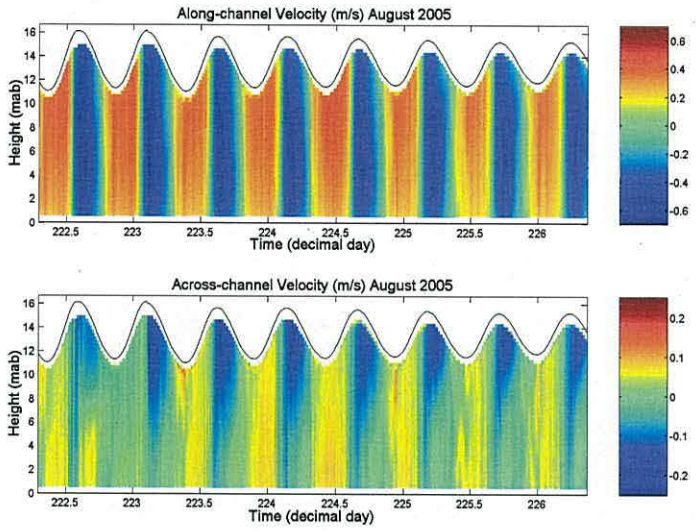

Figure C.2: Depth profiles of along-channel (top) and across-channel (bottom) velocity (m s^{-1}), measured by ADCP in August 2005.

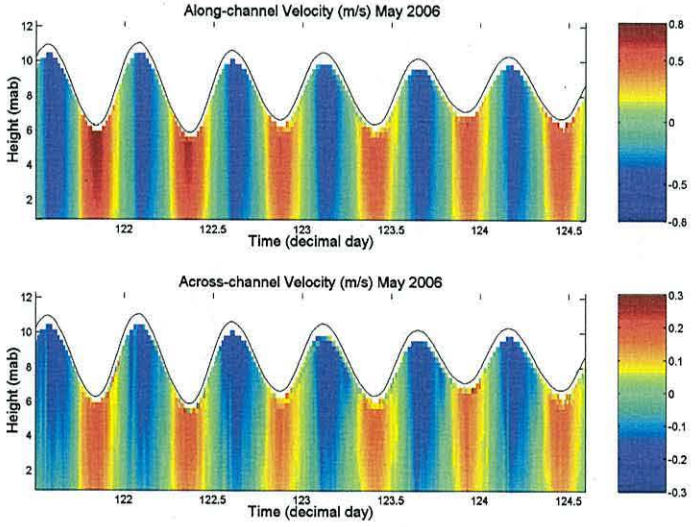

Figure C.3: Depth profiles of along-channel (top) and across-channel (bottom) velocity (m s^{-1}), measured by ADCP in May 2006.

C.2 CTD water properties profiles

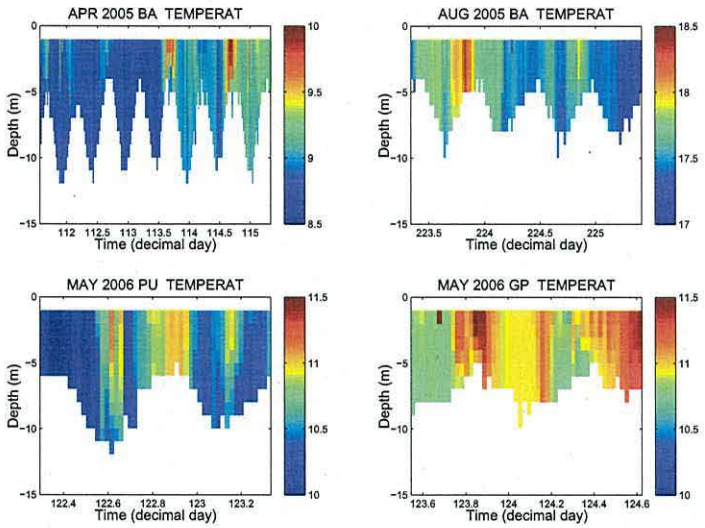

Figure C.4: Depth profiles of temperature (° C) measured using the CTD profiler aboard the R.V. Prince Madog.

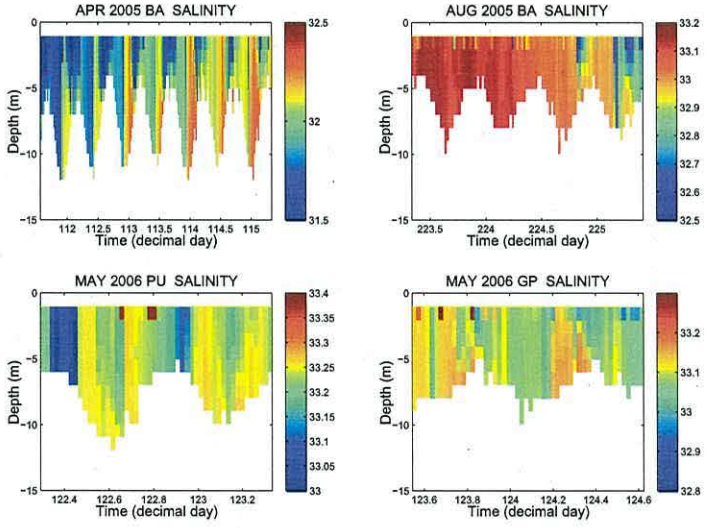

Figure C.5: Depth profiles of salinity (PSU) measured using the CTD profiler aboard the R.V. Prince Madog.

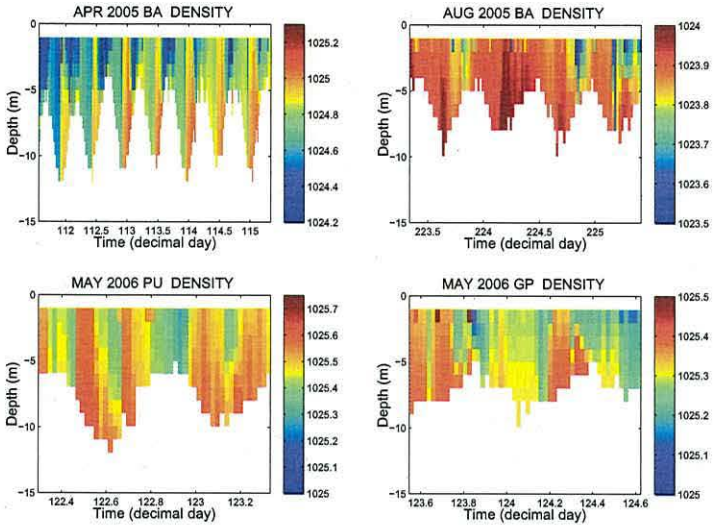

Figure C.6: Depth profiles of density (kg m^{-3}) measured using the CTD profiler aboard the R.V. Prince Madog.

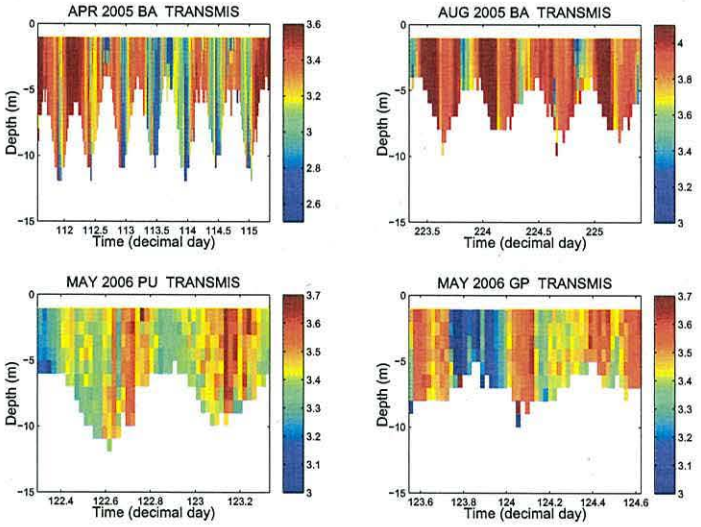

Figure C.7: Depth profiles of Transmissometer Transmittance (V) measured using the CTD profiler aboard the R.V. Prince Madog.

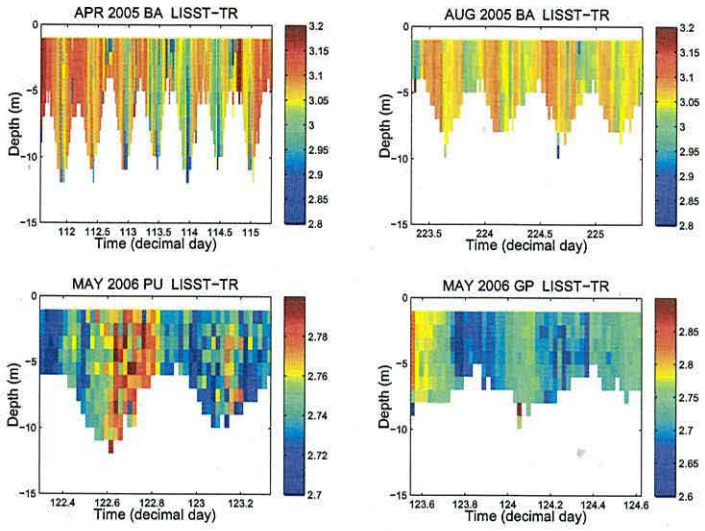

Figure C.8: Depth profiles of LISST Transmittance (V) measured using the CTD profiler aboard the R.V. Prince Madog.

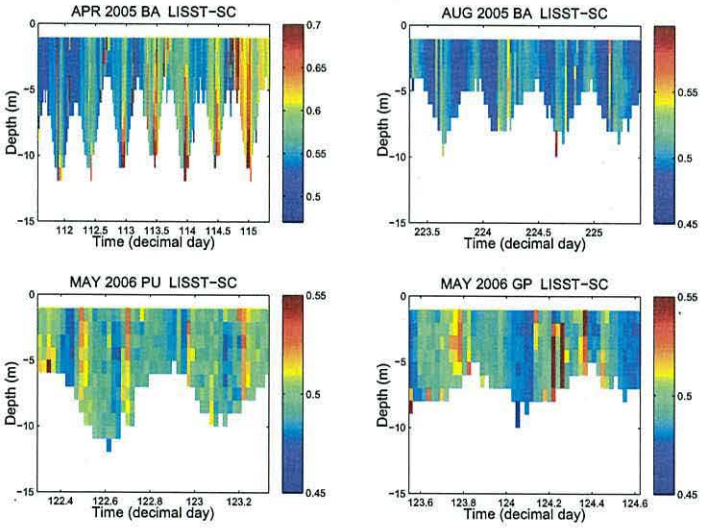

Figure C.9: Depth profiles of LISST Scattering (V) measured using the CTD profiler aboard the R.V. Prince Madog.

Appendix D

PHYBIO model MATLAB ® code

```
k= 0.0025;
g=9.81;
w2=2*pi/(12.42*3600);
AP=input('Puffin amplitude[springs=3.35]=?');

AC=AP*0.61;PhC=0.4;

%set topography
n=30;dx=1000;
qi=1:n;qx=1:n-1;
q1=13; q2=n-q1;4
H3=3.4-qi*1.3/n;
bLW=ones(1,n)*400;
qb=1:q1-1;
q3=n-q1-5;
qc=1:q3;

cots1=ones(1,q1-1).*(1-0.9*(qb+1)/q1)*150;
cots2=ones(1,6)*10;
cots3=ones(1,q3).*(5+qc/q3*30);
cots=[cots1 cots2 cots3];
bHW=bLW+4*H3.*cots;

H1=4.5;
```

```
H0=ones(1,n)*8;

hm=floor(n/2);
H0(hm)=H1;
H0(hm+1)=H1;
H0(hm+2)=H1;
H0(hm-1)=H1;

H0bar=(H0(1:n-1)+H0(2:n))/2;
bbar=(bLW(1:n-1)+bLW(2:n))/2;
H3bar=(H3(1:n-1)+H3(2:n))/2;
cotbar=(cots(1:n-1)+cots(2:n))/2;

%Specify vertical mixing Kz (m2/s)
mz=10;dz=8/mz;
qz=1:mz;
Uprof= (1.15-0.425*(1-qz/mz).*(1-qz/mz))';
Ushape=Uprof;
Kprof=((qz/mz).*(1-qz/mz))';
Kprof=Kprof(1:mz-1);
Kshape=Kprof;

Umax=1;
h=8;
Kmax=0.0205*Umax*h/4;
dt=0.25*dz^2/Kmax

%production-grazing: lamda-mu
lamu=0.000002;

%set up mussel bed filtration function F(x)
alpha=0.000301; %filtration parameter
pm=4;%bed size factor(no of bins in mussel bed)
mx1=8;%mussel bed begins at x=mx1
qv=mx1+floor(pm/2);%chooses the location for taking the profile
 %as mid-way the mussel bed
```

```
F1=zeros(1,mx1);
F2=alpha*ones(1,pm);
F3=zeros(1,n-mx1-pm-1);
F=[F1 F2 F3];
Lx=[0 n];Ly=[10 10];

m=1800/dt;
%Initial elevations an velocities
EtaP0=0; EtaC0=AP*cos(PhC);
Etadif=EtaC0-EtaP0;

Eta=EtaP0+(qi-1)*Etadif/n;
fin=100;
fin=fin*2;

Eta=zeros(1,n);
u1=zeros(1,n-1);
th=0;
Q=zeros(1,n-1);

%Initial Chl condition
C0=2;
C=[C0*ones(1,n-1)];
Cpr=C0*ones(1,mz)';

Qst=[]; Ust=[];Etast=[]; Cst=[];Cprst=[];
lm=0;

while lm<fin
    l=0;
    while l<m
        t=(lm*m+l)*dt;
        Etabar=(Eta(1:n-1)+Eta(2:n))/2;
        Abar=bbar.*(H0bar+Etabar)+(H3bar+Etabar).^2.*cotbar;
        bbeta=bbar+2*(H3bar+Etabar).*cotbar;
        beta=bLW+2*(H3+Eta).*cots;
        Hm=Abar./bbeta;
```

```
%linearised momentum equation
u2=u1-(g*diff(Eta)/dx+k*abs(u1).*u1./Hm)*dt;
%add non-linear term
du=diff(u1);
du1=[0 du];
du2=[du 0];
dubar=(du1+du2)/(2*dx);
udu=u1.*dubar;
u2=u2-udu;
% end momentum equation

% Continuity
Etared1=Eta(2:n-1);
bred=beta(2:n-1);

Etared2=Etared1-diff(Abar.*u2)./(bred*dx)*dt;
EtaP=AP*cos(w2*t);  EtaC=AC*cos(w2*t+PhC);
Eta=[EtaP Etared2 EtaC];

% Chl advection

%advection by mean flow
dcon=diff(C);
dcon2=[(C(1)-C0) dcon];
dcon3=[dcon 0];
y1=u2>0;
y2=u2<=0;
gradC=(y1.*dcon2+y2.*dcon3)/dx;
C=C-u2.*gradC*dt-F.*C*dt./Hm;
%+growth-grazing
C=C+lamu*C*dt;

%set velocity profile and Kz over the mussel bed
Umod=abs(u2(qv));
h=H0bar(qv)+Etabar(qv);
Kz=0.0205*h*Umod*Kshape;
```

```
        U=u2(qv)*Ushape;
        dz=h/mz;
        %Advection by the mean flow
        Cpr=Cpr-gradC(qv)*U*dt;

        %---------------------------------
        %vertical diffusion at mussel bed
        DD=diff(Kz.*diff(Cpr))/(dz^2)*dt;
        delC=[0; DD; 0];
        Cpr=Cpr+delC;
        Cpr(mz)=C(mz-1);
        Cpr(1)=Kz(1)*Cpr(2)./(Kz(1)+alpha*dz);
        %---------------------------------
        u1=u2;
        l=l+1;
    end
    tim=t/3600;
    Q=u1.*Abar;
    Qst=[Qst Q'];Cst=[Cst C'];
    Ust=[Ust u1'];Etast=[Etast Eta'];
    Cprst=[Cprst Cpr];
    th=t/3600;
    lm=lm+1;
end
```

Acknowledgments

Many people have managed to be a source of inspiration, influence or help during the course of this project, and although it is difficult to name each and everyone after 3 years have passed, it is only fair I should try. I just hope my memory doesn't fail me now. A few words of warning should first be given: firstly, my gratitude to each is equal and does not influence their position in this "chapter". Secondly, the fact that some will be mentioned more than once, shouldn't be a disappointment to others: it just seems some people had their fingers in all the pies. Finally, I placed these at the end, because I believed that my acknowledgments and the people they are directed at deserved their own chapter. Even though I worked hard and consider my PhD a personal achievement, I know it would never have ended this well without all the kind help and support along the way.

Firstly, I would like to say thank you to my supervisor, Prof. John Simpson, without whose kind help and support I would have been unable to start, continue, or finish this research project. I am very grateful for the opportunity of publishing my research, and your guidance throughout. Although you took the lead on writing the paper, it was a wonderful experience to do the analyses and contribute to the presentation; as well as learn to deal with the submission and review process, which thanks to being the corresponding author I could experience first hand.

I would also like to thank Dr. Tom Rippeth, the members of the Turbulence and Mixing research group, and the members of my research committee for being a second port of call for help and support throughout my project.

This project would not have ended successfully without the kind help of my sponsors: the European Social Fund and locally, Myti Mussels Ltd. Kim, Janice and Alan, thank you very much for all your kind help with the field work and supplying me with information on the mussel fishery.

In my time here, I have had many offices, and I would like to thank all who have put up with me and my sighing and shouting at computers, and who have kindly distracted me with friendly banter and advice on all life's issues: Nicola and Graeme in Room 213, Neil and Eirwen in Room 211, and finally all those in Room 204: Matthew, Phil, Pete, Biz, Katherine, Shiho, João, Mike and Kerry. I'm also grateful to the post-docs who took over Room 211: Ole and Mattias, for their strong coffee and pleasant Scandinavian humour. For all their help with MATLAB ® , a special thank you goes to the three Golden Boys, and for the kind lending of his executive chair, which made writing a lot more comfortable, I am very grateful to Mike.

In parallel to this research, a BBSRC-funded project (Grant No. D18866) was also studying the local mussel beds. I am grateful to Dr. Eirwen Williams, Dr. Jo Gascoigne, Ms. Camille Saurel, and Prof. Michel Kaiser, for their kind help and collaboration. I am particularly grateful to Jo for her excellent organisation skills at bringing together the research cruises aboard the R.V. Prince Madog and to both Jo and Camille for help with analysing the endless filters afterwards in the lab.

I would also like to thank Mr. Ray Wilton, Ms. Anne Hammerstein and Mr. Ben Powell for their endless technical support, patience and not getting upset with me when something I touched once again broke.

Many of the results were collected during research cruises aboard the R.V. Prince Madog, and I would therefore like to thank the captain and crew of the R.V. Prince Madog, as well as the various years of MSc. classes who helped out, particularly for midnight entertainment playing "drinking" games without alcohol whilst admiring the lights of the Gazelle Hotel and Tap & Spile Pub, and for letting me

bounce around the back deck in the late hours of the night and the early hours of the morning.

For their help with the deployments of the long-term monitoring stations, I am grateful to Mr. Gwynne Parry-Jones, Mr. Graham Worley, Dr. Dave Bowers, Mr. Jon Brookes and the Conway Centre, Dr. Kate Smith, Dr. Bill Sanderson and the Countryside Council for Wales. I would also like to thank OSIL for their technical support, and finally also for their participation in "covert operations" a big thank you to Ole, Greg and Lieve.

I would also like to thank Mr. David Goldsmith and RS Aqua, as well as Ms. Chelsea Donovan and Turner Designs for help and technical support with the deployment and use of the SCUFA and 10-AU fluorometers.

Throughout my research, I have spent many hours in the lab, and this would never have ended well, or have even been bearable without the kind help and support of Ms. Viv Ellis, Ms. Joan Griffiths, Mr. Ian Pritchard, and Mr. Gwyn Hughes. I am also grateful to Rathburn for manufacturing acetone. To all the other users of the Craig Mair Lab: thank you for allowing me to sing off key and for not touching my acetone (once again apologies for the threats of death and pixies, although they did prove effective).

The effort of modelling the Menai Strait with Telemac was completed successfully thanks to the kind help of Ms. Kerry Marten, Prof. Alan Davies, Ms. Jennifer Brown, Mr. Jean-Michel Hervouet (EDF), and Dr. Jonathan Malarkey. I would also like to thank Dr. Eirwen Williams and Mr. Graham Worley for their help with the initial simulations done in GETM.

I would also like to thank Mr. Claudio Bravo for the kind contribution of his HPLC measurements of Chlorophyll Concentration in the Menai Strait in 2004 – 2005 to the chapter on seasonal cycles in the channel.

For help with learning to write LaTeX, ensuring my thesis looked presentable, and proof-reading: thanks goes to Mr. Dominic van der A. I am also grateful to Mrs. Mik Berx for reading for spelling and grammar mistakes.

I am also grateful to Fisheries Research Services, not only for employing me, but also for their wonderful flexi-time system which has been very useful whilst laying the finishing touches on this thesis. Also thanks to Dr. Alejandro Gallego, Ms. Sarah Hughes and everyone in the "Bearpit" for all your kind support.

To conclude on a more personal level, I would like to especially thank the following people.
Thanks goes to the Craig Mair coffee room and everyone who attends, for non-work related banter and distracting conversations.
Also for pleasant distraction throughout the research and write-up stages, I would like to say thank you to the swimmers, climbers and surfers, who offered me tempting alternatives to being stuck behind my desk.
I would never have completed this project without the quiet peaceful atmosphere and the new friends I discovered during writing "holidays" at the School of Engineering and Physical Sciences at the University of Aberdeen.
Lastly, for their never-ending belief in me, I would like to say thank you to my family and friends. For all your support and love: "Dankjewel" Mama, Papa & Simon, Stinne & Ingrid, Berx'en en Debeys'en. Also thanks to Ruth, Michael, Kathryn, Cerys, Chloe, Greg, Jenny, Gaz, Sophie, Lieve, Ole, Si, Adam, Sara, and Sarah for your friendship and support in the last few years. Finally, Guy & Dave: thanks for making sure lately that I was fed and took some time to relax, thanks for letting me Wii all over your front room and being great friends. To you both and to Lorna, I would also like to say: thank you for your continuous encouragement in the last few months, and making the light at the end of the tunnel come back on; most times I thought you just flicked the switch, but at times I must admit you probably had to replace the light bulb.

Despite my lack of guts to dedicate this thesis to Mike D, MCA, Adrock and Mix Master Mike, their inspiration and support can not go unmentioned. Music has always been important to me and several bands have helped during the completion of this project. As this is the third thesis written to their life work, none have deserved a special mention more than the Beastie Boys.

I would like to end my thesis with the last paragraph being the following words in Dutch:
"De laatste persoon die nog speciaal hoort te worden vermeld, is iemand die pas op het einde zijn intrede maakte, maar toch een grote steun, hulp en motivatie was. Dominic, bedankt om mee die laatste, zware loodjes te dragen.

"Op de toppen van je kunnen, Bedenk je soms opeens:
Je doet het niet voor hun, Je doet het niet voor mij
En zelfs niet voor jezelf, Je bent de zin voorbij"

Donker hart – Bløf

Gelukkig kon ik dan op je rekenen: jouw aanmoediging toen ik het net weer even niet zag zitten, jouw overtuiging dat ik het einde wel kon halen, en jouw geloof in mij. Na 158 dagen (en enkele meer maar die was ik vergeten te tellen), komt het jaar "Thesis" eindelijk ten einde: in die tijd ben je een bron van oneindig veel begrip en liefde geweest, en daar ben ik je onmeunig dankbaar voor."